



Particle radiation environment in the heliosphere: Status, limitations, and recommendations

Jingnan Guo ^{a,b,*}, Bingbing Wang ^c, Kathryn Whitman ^d, Christina Plainaki ^e,
 Lingling Zhao ^{c,f}, Hazel M. Bain ^{g,h}, Christina Cohen ⁱ, Silvia Dalla ^j, Mateja Dumbovic ^k,
 Miho Janvier ^{l,m}, Insoo Jun ⁱ, Janet Luhmann ⁿ, Olga E. Malandraki ^o, M. Leila Mays ^p,
 Jamie S. Rankin ^q, Linghua Wang ^r, Yihua Zheng ^s

^a Deep Space Exploration Laboratory/School of Earth and Space Sciences, University of Science and Technology of China, Hefei 230026, China

^b Collaborative Innovation Center of Astronautical Science and Technology, Harbin 150001, China

^c Center for Space Plasma and Aeronomics Research, University of Alabama in Huntsville, Huntsville, AL 35899, USA

^d University of Houston, 4800 Calhoun Road, Houston, TX 77204, USA

^e Italian Space Agency, 00133 Rome, Italy

^f Department of Space Science, University of Alabama in Huntsville, Huntsville, AL 35899, USA

^g Cooperative Institute for Research in Environmental Sciences, University of Colorado Boulder, Boulder, CO 80309, USA

^h National Oceanic and Atmospheric Administration, Space Weather Prediction Center, Boulder, CO 80305, USA

ⁱ California Institute of Technology, Pasadena, CA 91125, USA

^j Jeremiah Horrocks Institute, University of Central Lancashire, Preston PR1 2HE, UK

^k Hvar Observatory, Faculty of Geodesy, University of Zagreb, 10000 Zagreb, Croatia

^l European Space Agency, European Space Research and Technology Centre, 2200 AG Noordwijk, Netherlands

^m Université Paris-Saclay, CNRS, Institut d'Astrophysique Spatiale, 91405 Orsay, France

ⁿ Space Sciences Laboratory, University of California, Berkeley, Berkeley, CA 94720, USA

^o Institute for Astronomy, Astrophysics, Space Applications and Remote Sensing, National Observatory of Athens, 118 10 Athens, Greece

^p NASA Goddard Space Flight Center, Greenbelt, MD 20771, USA

^q Department of Astrophysical Sciences, Princeton University, Princeton, NJ 08540, USA

^r School of Earth and Space Sciences, Peking University, 100871 Beijing, China

^s Space Weather Laboratory, NASA Goddard Space Flight Center, Greenbelt, MD 20771, USA

Received 31 January 2023; received in revised form 25 March 2024; accepted 27 March 2024

Abstract

Space weather is a multidisciplinary research area connecting scientists from across heliophysics domains seeking a coherent understanding of our space environment that can also serve modern life and society's needs. COSPAR's ISWAT (International Space Weather Action Teams) "clusters" focus attention on different areas of space weather study while ensuring the coupled system is broadly addressed via regular communications and interactions. The ISWAT H3 cluster "Radiation environment in heliosphere" (<https://www.iswat-cospar.org/h3>) has been working to provide a scientific platform to understand, characterize, and predict the energetic particle radiation in the heliosphere with the practical goal of mitigating radiation risks associated with aerospace activities, the satellite industry, and human space explorations. In particular, present approaches help us understand the physical phenomena at large, optimizing the output of multiviewpoint observations and pushing current models to their limits. In this article, we review the scientific aspects of

* Corresponding author.

E-mail addresses: jnguo@ustc.edu.cn (J. Guo), bw0121@uah.edu (B. Wang), kathryn.whitman@nasa.gov (K. Whitman), christina.plainaki@asi.it (C. Plainaki), lz0009@uah.edu (L. Zhao), hazel.bain@noaa.gov (H.M. Bain), cohen@srl.caltech.edu (C. Cohen), SDalla@uclan.ac.uk (S. Dalla), mdumbovic@geof.hr (M. Dumbovic), miho.janvier@universite-paris-saclay.fr (M. Janvier), insoo.jun@jpl.nasa.gov (I. Jun), jgluhman@ssl.berkeley.edu (J. Luhmann), omaland@noa.gr (O.E. Malandraki), m.leila.mays@nasa.gov (M. Leila Mays), jsrankin@princeton.edu (J.S. Rankin), wanglhwang@pku.edu.cn (L. Wang), yihua.zheng@nasa.gov (Y. Zheng).

the radiation environment in the heliosphere, covering four different radiation types: solar energetic particles, ground-level enhancement (a type of solar energetic particle event with energies high enough to trigger signals in ground-level detectors), galactic cosmic rays, and anomalous cosmic rays. We focus on related advances in the research community in the past 10–20 years and what we still lack in terms of understanding and predictive capabilities. Finally, we also consider some recommendations related to the improvement of both observational and modeling capabilities in the field of the space radiation environment.

© 2024 COSPAR. Published by Elsevier B.V. This is an open access article under the CC BY-NC-ND license (<http://creativecommons.org/licenses/by-nc-nd/4.0/>).

Keywords: Space weather; Space radiation; Solar energetic particles; Galactic cosmic rays; Ground-level enhancement; Anomalous cosmic rays

1. Introduction and motivation

Space weather studies generally address the conditions on the Sun and in the heliosphere and how they impact the interplanetary and planetary space environment, influence the performance and reliability of space-borne and ground-based technological systems, and endanger human life or health, as illustrated in Fig. 1 (also see the US National Space Weather Plan for the up-to-date definition of space weather at <http://www.nswp.gov/>).

In recent years, space weather has appropriately become a multidisciplinary research area connecting scientists from across all heliophysics domains, from solar physics to aeronomy. The international members of this community work together under the umbrella of the COSPAR Panel on Space Weather, the International Space Weather Action Teams (ISWAT; <https://iswat-cospar.org/>), which were established recently. Each Action Team is an international group of interested researchers charged with addressing a

specific and focused space weather-related task. Action Teams are, in turn, organized into various “clusters” grouped by domain, phenomena, or impact, and work in coordinated efforts to improve the scientific understanding of space weather phenomena and our society’s resilience to the effects of space weather. The goal of the ISWAT H3 cluster (<https://iswat-cospar.org/h3>) is to understand, characterize, and predict the fluxes of the major sources of energetic particle radiation in the heliosphere, including solar energetic particles (SEPs), galactic cosmic rays (GCRs), and anomalous cosmic rays (ACRs).

1.1. Introduction to the heliospheric radiation environment

SEPs are protons, heavier ions, and electrons that are accelerated by solar flares and shocks driven by coronal mass ejections (CMEs; see Cohen et al., 2021), and have energies from a few kiloelectronvolts up to several gigaelectronvolts (Fig. 2). In some very large SEP events, the pres-

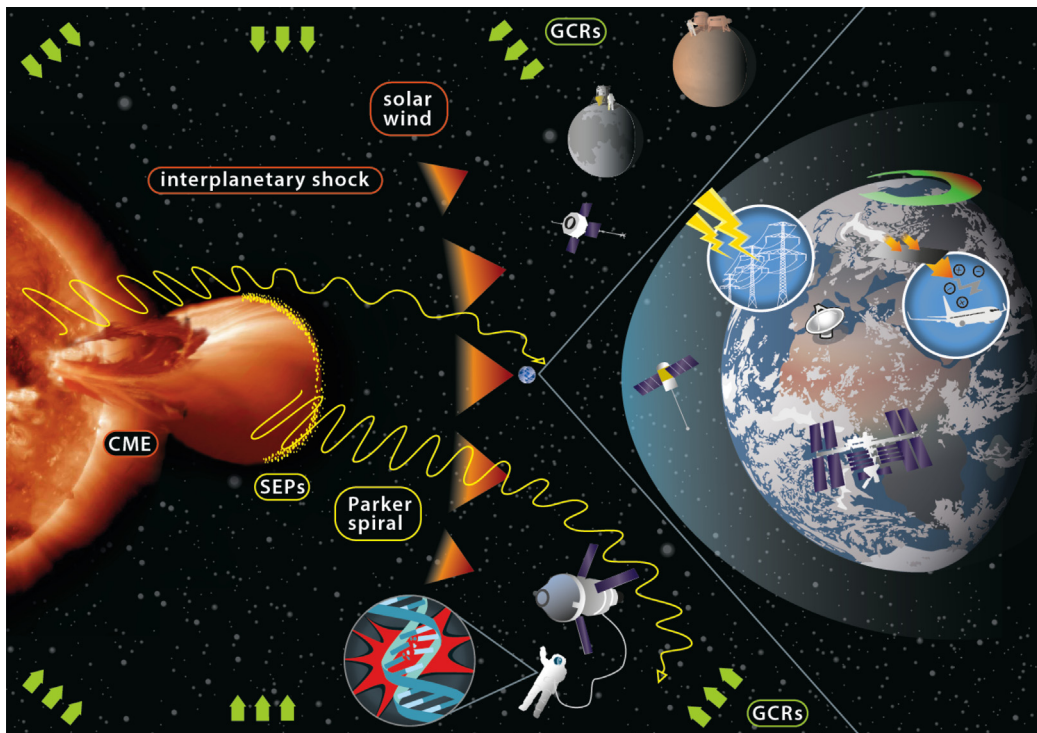


Fig. 1. Cartoon illustration of space weather phenomena and impacts. More discussions can be found in the main text.

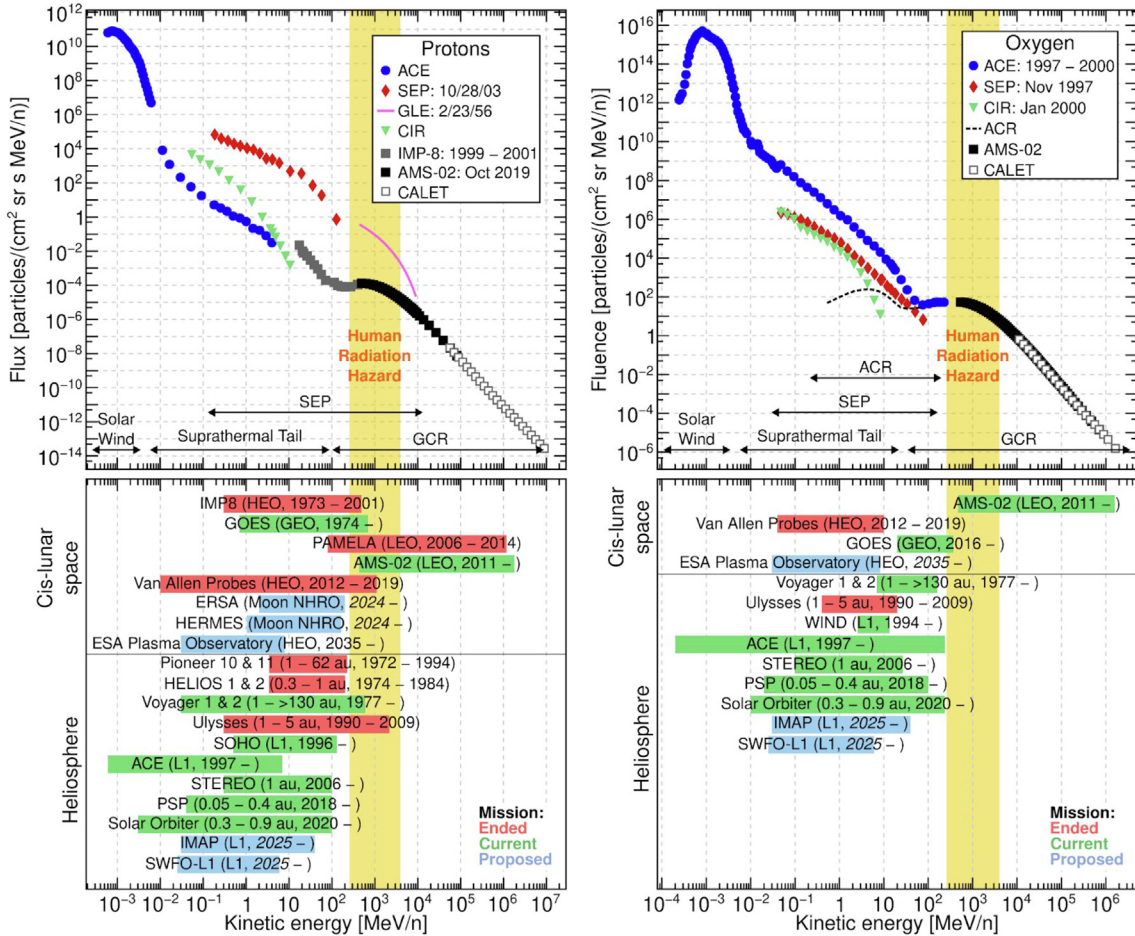


Fig. 2. Proton (top left) and oxygen (top right) fluence spectra showing the energy ranges of various particle populations in the heliosphere. The coverages of in situ particle detectors (bottom panels) are also shown. The vertical yellow band highlights the energy range most relevant for human radiation exposure behind shielding in the deep space environment. CIR, corotating interaction region. (From Corti et al. (2023).)

ence of protons of energies up to tens of gigaelectronvolts can contribute to Earth's surface particle fluxes and can be detected through ground-based neutron monitors (NMs), in so-called ground-level enhancement (GLE) events. SEP events occur sporadically, leading to intense but temporary increases in radiation levels in the heliosphere that can commence with little warning (a few minutes) following observed solar activity. Their occurrence rate follows the 11-year solar activity cycle, with more events occurring during the solar maximum and also during the declining phase of the cycle, especially those leading to GLEs (e.g., Shea and Smart, 1993). Being electrically charged, SEPs gyrate around and follow the interplanetary magnetic field lines (with the nominal condition described as Parker spirals) such that the largest particle fluxes tend to be related to flares and CME-driven shocks that had a direct magnetic connection to the observer (e.g., Klein and Dalla, 2017). However, SEPs can be distributed more widely in the heliosphere, indicating that additional transport processes, often modeled as diffusion, occur near the Sun and/or in the solar wind (e.g., Desai and Giacalone, 2016). The physics of these processes is poorly understood at present, as are the processes accelerating SEPs. In partic-

ular, the roles of reconnection in solar flares versus acceleration by CME-driven shocks, which become spatially extended sources themselves, continue to be debated. In addition, theories of particle acceleration by shocks may require the presence of a “seed population,” i.e., suprathermal particles, at the Sun and/or in the interplanetary medium that are difficult to quantify (e.g., Cohen et al., 2021). Thus, the successful prediction of the contribution of SEPs to the radiation environment in the heliosphere is challenging because there is much uncertainty in the fundamental processes involved, and little forewarning of when a SEP event will occur. For instance, we do not know when an active region will erupt or what flare size it will create or how big a CME will be or if any of that will accelerate particles and to what energies. More detailed discussions concerning the current understanding and limitations as well as forecasting capability related to SEPs and GLE events can be found in Sections 2 and 3, respectively.

GCRs are particles with high energies (from tens of megaelectronvolts up to 10⁸ GeV, with their fluxes peaking at around gigaelectronvolts per nucleon) most likely accelerated by supernova-driven shocks that enter the heliosphere from the interstellar medium (Blasi, 2013). Once

in the heliosphere, they are subject to solar modulation processes that are dominated by the large-scale structure of the heliospheric magnetic field and its variation during the solar activity cycle (e.g., Potgieter, 2013). This gives rise to 11-year solar cycle (and 22-year solar magnetic cycle)-variations in the GCR intensity that are anticorrelated with solar activity. GCRs are nearly isotropic in the interplanetary space. However, a small diurnal anisotropy has been observed, and it may also change following the solar magnetic cycle (e.g., Modzelewska et al., 2019). The long-term solar cycle variations in the GCR flux are reasonably well characterized in comparison with the case for SEPs. However, some observations, such as the lag of the GCR variation after the solar activity cycle, still cannot be fully explained, and detailed quantification of the modulation is still needed. Meanwhile, short-term depressions of the GCR flux that result from transient disturbances in the solar wind (such as interplanetary shocks and interplanetary CMEs (ICMEs), or stream interaction regions (SIRs)) are poorly understood and difficult to predict (e.g., Richardson and Cane, 2011; Richardson, 2018). When one is assessing radiation risk, GCRs pose a bigger challenge than SEPs for long-term space explorations such as a mission to Mars (Cucinotta et al., 2013; Guo et al., 2021) as they contribute cumulatively throughout the mission and particles with energy above hundreds of megaelectronvolts per nucleon are very difficult to shield against (see the energy range of GCRs shown in Fig. 2). More detailed discussions on the current understanding and open questions related to GCRs can be found in Section 4.

ACRs are a population of predominantly singly ionized ions that generally include the elements H, He, C, N, O, Ne, and Ar located in the low-energy part of the GCR spectrum. They are believed to result from interstellar neutral atoms that have entered the heliosphere and are ionized by photonionization, electron impact ionization, or charge exchange to become pickup ions (Fisk et al., 1974). These pickup ions are then convected into the outer heliosphere, where they are accelerated at or near the heliospheric termination shock and can reach energies of about 1–100 MeV per nucleon (McComas and Schwadron, 2006). However, the acceleration mechanism of ACRs is still debated. Since ACRs are transported in the same heliospheric environment as GCRs, they also experience the solar modulation effect (Fu et al., 2021). Presently, the differences in the ACR modulation and the GCR modulation by the solar activity are not fully understood. They are probably related to the different source origin and rigidity dependence of these two populations. More detailed discussions on the current understanding and open questions concerning ACRs can be found in Section 5.

1.2. Space radiation risks

Space radiation is a major concern for the safety of robotic and human exploration both in the near-Earth environment and toward deep space and other planets,

such as Mars. Near Earth, the National Oceanic and Atmospheric Administration (NOAA) uses a five-level system, the solar radiation storm scale, i.e., the S scale¹, to indicate the severity of a solar radiation storm and the anticipated impacts on satellites, high-frequency communications, and astronauts as well as flight crew and passengers on high-flying aircraft at high latitudes. This scale ranges from S1 to S5, corresponding to minor, moderate, strong, severe, and extreme levels of radiation. Fig. 3 illustrates various levels of radiation storms and camera signals triggered by energetic particles. The severity is determined by examination of the greater than 10 MeV proton flux observed by the Geostationary Operational Environmental Satellite (GOES) spacecraft particle sensors: the threshold to be exceeded is 10 , 10^2 , 10^3 , 10^4 , and 10^5 pfu (1 pfu is equal one particle per square centimeter per second per steradian for S1, S2, S3, S4, and S5 storms, respectively. The severity of these storms is anticorrelated with their occurrence frequency.

With differing degrees of impact, space radiation over a wide energy range and particle types can affect modern technological systems in various ways. For example, sudden enhancement of energetic protons can penetrate into the atmosphere and ionize the D layer of the ionosphere. This process prevents the high-frequency radio waves from reaching the much higher E, F1, and F2 layers, where these radio signals are normally refracted and bounce back to Earth, thus causing degraded high-frequency radio communications. SEPs may also produce high-latitude atmospheric chemistry changes, including ozone depletion (Maliniemi et al., 2022). Both SEPs and GCRs can affect satellite, spacecraft, and their instruments in various ways and cause temporary or permanent damage (Stassinopoulos and Raymond, 1988). Total ionizing dose effects can lead to long-term radiation damage. “Single-event effects” refers to the deposition of charge in spacecraft circuits that can cause, for example, upset, latch-up, or burnout. Internal charging or internal electrostatic discharge is a phenomenon where energetic particles deposit their charges in materials inside the spacecraft structure, ultimately causing electrical breakdown. Another phenomenon, called *surface charging*, occurs when the incoming electrons with energies below about 100 keV accumulate on spacecraft surfaces and produce surface discharges leading to arcing and electromagnetic interference. With the above-mentioned effects, energetic protons can degrade solar panel efficiency, onboard electronic circuitry can malfunction, and the protons can create noise in star-tracking systems.

Space radiation also poses a radiation hazard for human space exploration endeavors. By showing the energy range of SEPs, GCRs, and ACRs as measured by current and upcoming in situ particle detectors, Fig. 2 highlights a current and prospective future gap in energetic particle mea-

¹ <https://www.swpc.noaa.gov/noaa-scales-explanation>

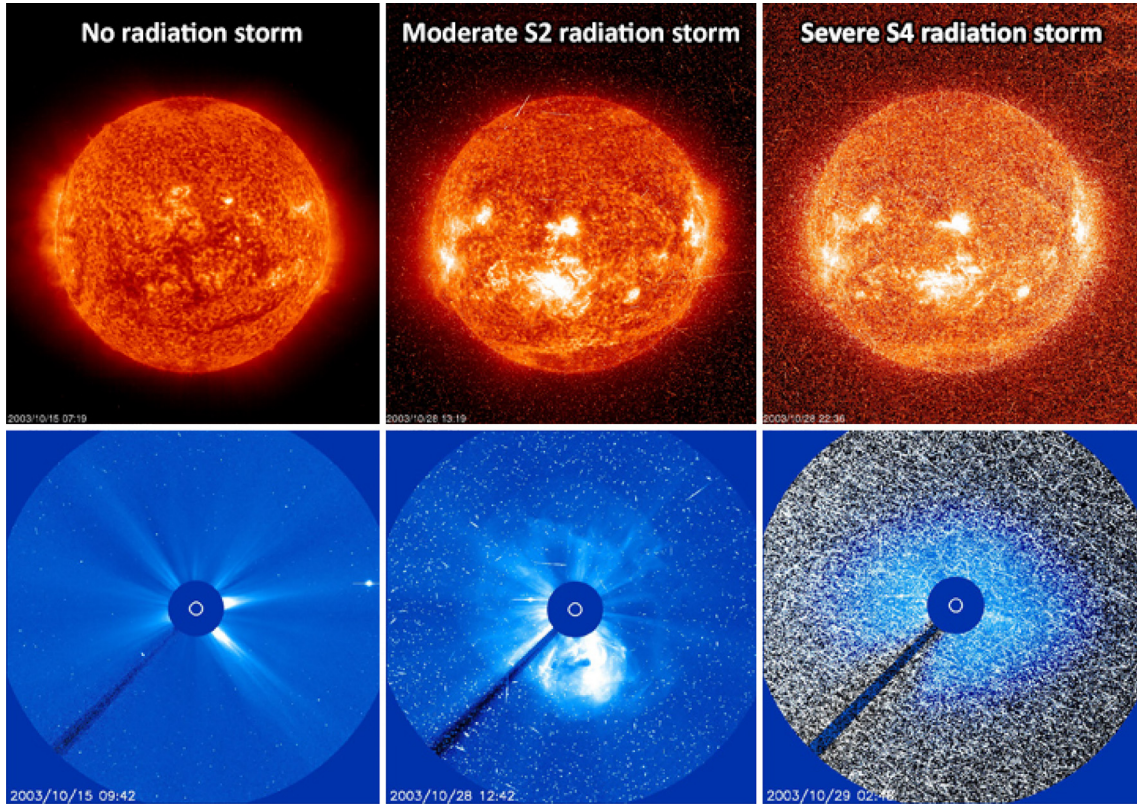


Fig. 3. Normal (S0, left column), moderate (S2, middle column), and severe (S4, right column) radiation storms illustrated with use of signals triggered by the Solar and Heliospheric Observatory (SOHO). Image taken from <https://www.spaceweatherlive.com/en/help/what-is-a-solar-radiation-storm.html>.

surements in the critical energy range concerning human radiation risks (Corti et al., 2023). As shown, GCRs in the energy range from 250 MeV per nucleon to 4 GeV per nucleon (Slaba and Blattig, 2014; Dobyynde et al., 2021) and SEP protons with energy above 100 MeV (Mertens and Slaba, 2019) are the most significant contributors to radiation dose in humans behind shielding. For a potential human mission to Mars, which will generally require a long mission duration (about 3 years), both modeled results and measurements show that NASA's exposure limits are approached or exceeded (Cucinotta et al., 2017; Guo et al., 2021). Long-term exposure to the GCR radiation environment does not immediately endanger the life of astronauts, but it increases the probability of late-term consequences (e.g., Cucinotta and Durante, 2006; Kennedy, 2014), such as development of cancer and cataracts or damage to the central nervous system and/or cardiovascular system and hereditary effects (Iancu et al., 2018). Alternatively, intense SEP events, apart from contributing to the above-mentioned stochastic effects, may also be associated with deterministic effects as they may deliver short-term, intense doses that cause radiation poisoning or even death.

Even for aviation activities, radiation poses potential risks (Sihver et al., 2015). During the most energetic SEP events, i.e., those that result in a GLE event at Earth, the radiation environment at aviation altitudes can be significantly enhanced, particularly for flight routes over the geo-

magnetic polar regions (Copeland et al., 2008; Meier et al., 2020; Dobyynde et al., 2024). In recent years, the International Civil Aviation Organization has requested new space weather advisories specifically tailored to the needs of the aviation industry, including a requirement for advisories notifying operators and airlines of SEP events that increase the effective dose rates at commercial flight levels above preset threshold levels (e.g., Bain et al., 2023a). Therefore, improved scientific understanding, modeling, and forecasting of these events will be required for crews both at aviation altitudes and in space (e.g., Hands et al., 2022; Bain et al., 2023).

1.3. The importance of studying space radiation

From the brief discussions in the previous sections, we see that it is important to study energetic particle radiation in the heliosphere driven by the space weather forecasting requirements and also by scientific interest in understanding particle energization and transport processes. We stress the following important aspects for studying the space radiation environment (which is also discussed in detail in Sections 2,3,4,5):

- To constrain physical mechanisms of SEP acceleration at the Sun.
- To understand SEP transport processes in the heliosphere.

- To understand the large-scale heliospheric environment through which GCRs and ACRs propagate.
- To forecast and nowcast SEP occurrence, fluence, energy range, and ionization effects that may pose radiation risks to the aviation and space industries.
- To understand and predict the variability of GCR radiation (both its long-term and its short-term modulations) for better mitigating long-term radiation risks.

1.4. Context and structure of this article

In this article, we review the scientific aspects of the radiation environment in the heliosphere with a focus on advances in the past 10 years concerning our current scientific understanding and predictive capabilities. We also discuss the limitations in our knowledge and open questions in the field, and offer considerations related to the planning of future space observations.

Sections 2,3,4,5 provide an overview of our current understanding of energetic particles in the heliosphere, including SEPs, GLE events, GCRs, and ACRs. As GLE events are SEP events with fluxes at relativistic proton energies high enough to generate secondary particles that trigger signals in ground-based particle detectors, they are discussed separately as different methods are often required to study the interaction of GLE particles with planetary magnetospheres and atmospheres.

In Section 6, we stress our knowledge gaps in observing, modeling, physical understanding of, and forecasting capabilities for space particle radiation, and we offer suggestions for narrowing these gaps and moving the field forward in the next 5–10 years.

2. Solar energetic particles

2.1. Introduction

SEP events are transient enhancements (with a duration ranging from hours to days) in ions (mainly protons) and electrons in the space environment associated with solar activity. SEPs have been observed in Earth's space environment since the early years of the space age (e.g., Arnol'dy et al., 1968), either via intentional detection with various forms of dosimeters and particle telescopes or as background in other forms of data-including images. Improvements in detector technology subsequently led to species identification (including ion composition), charge states, and anisotropies (directionality).

The detection of SEPs in recent decades has revealed that they span a very broad energy range from the suprathermal energy range (a few tens of kiloelectronvolts per nucleon) up to a few gigaelectronvolts per nucleon for ions, or up to a few megaelectronvolts for electrons. Most SEP protons have energy in between the solar wind plasma energies and the higher energies (greater than 100 MeV)

where the ACR and GCR populations (see Sections 4 and 5) dominate the heliospheric fluxes. Fig. 2 illustrates the energy range of the SEPs and GCRs, and typical relative fluxes, within the heliospheric particle energy spectrum.

The bottom panels in Fig. 2 show that SEP fluxes are currently monitored in space by instruments onboard the following spacecraft near Earth: GEOS-1 to GEOS-17 since 1974, at geosynchronous orbit altitude and also serving for real-time forecasting (Sauer, 1989; Rodriguez et al., 2014; Kress et al., 2020), the Solar and Heliospheric Observatory (SOHO) since 1996, at the Lagrangian point L1 (Domingo et al., 1995), the Advanced Composition Explorer (ACE) since 1997, at L1 (Stone et al., 1998), the Global Geospace Science Wind satellite since 1994, at L1, and the Alpha Magnetic Spectrometer (AMS-02), which is mounted on the International Space Station, since 2011, at low Earth orbit (LEO) altitude (Kounine, 2012). At LEO altitude, strong magnetic shielding of SEPs by Earth's magnetosphere can modulate SEP fluxes, causing them to be different from those measured at geosynchronous orbit altitude by GOES satellites or at L1. Fig. 4 shows the 5-min resolution proton fluxes measured by the GOES series of spacecraft from 1974 until 2020 over more than four solar cycles. To account for the different instrument responses, GOES data have been calibrated with eighth Interplanetary Monitoring Platform (IMP-8; in service from 1973 to 2001) data and rebinned into different energies (Sandberg et al., 2014; Crosby et al., 2015). Fig. 4 illustrates the episodic nature of the occurrence of the SEP populations (spikes in particle flux in the middle panel) and the solar activity cycle dependence of SEP events (top panel), superposed on a background tied to the slowly varying GCR fluxes (bottom panel; Section 4) anticorrelated with long-term solar activities.

Both flares and the resulting heliospheric disturbances associated with CMEs are considered sources for accelerating particles (Reames, 2013; Reames, 2015; Cliver, 2016). However, the relative role of flare or CME association with particle energization is still debated. The exact transport effects of SEPs in the heliosphere and how they can modify SEP properties are unclear. Understanding the physical mechanisms responsible for the energization of SEPs and their transport through the heliosphere is the key to better forecasts of the heliospheric radiation environment.

2.2. Recent progress and current understanding

In recent decades, important progress has been made on the interconnection, within the space weather chain, of the various episodes of a SEP event related to the generation, acceleration, and propagation of solar particles (see, e.g., Desai and Giacalone, 2016; Klein and Dalla, 2017; Cohen et al., 2021). However, both our knowledge of the exact physical mechanisms occurring within the various regions of the solar atmosphere and/or in the interplane-

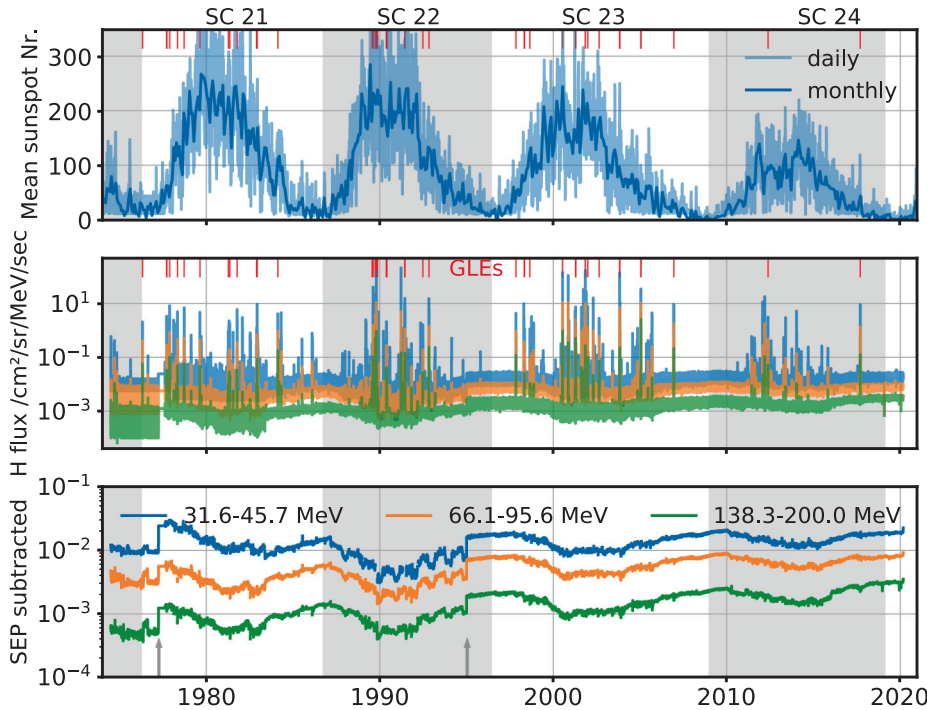


Fig. 4. Top: Daily and monthly averaged value of sunspot numbers over different solar cycles. Middle: Five-minute-resolution proton fluxes binned into three different energies (31.6–45.7 MeV, 66.1–95.6 MeV, and 138.3–200 MeV, as plotted in different colors) as calibrated from GOES-series measurements by the European Space Agency's Solar Energetic Particle Environment Modelling (SEPEM) service for data before 2016 (Crosby et al., 2015) and by application of the GOES recalibrated effective energies (Sandberg et al., 2014) for data from 2016 to 2020. Bottom: Daily-averaged GCR flux with SEPs removed. The gray arrows mark two noticeable discontinuities of the background flux resulting from a change in GCR effective energy across different instruments (while the calibration ensures that the SEP effective energy is consistent over time). To differentiate adjacent solar cycles, even cycles are shaded in gray in all three panels. Times of historical GLEs are marked by vertical red lines in the top two panels. The monthly sunspot data in the top panel were downloaded from the World Data Center SILSO, Royal Observatory of Belgium, Brussels (<http://www.sidc.be/silso/monthlyssnplot>). The SEPEM V2.0 data in the lower panels were obtained from the European Space Agency's SEPEM application server (<http://sepem.eu>). SC, solar cycle.

tary space and our capacity to predict relativistic SEP events are still limited (Anastasiadis et al., 2019; Cliver et al., 2022).

2.2.1. SEP acceleration sources

It was widely accepted that flares are often associated with relatively weak, electron-rich, and ^3He -rich events with impulsive (sudden) onsets and a duration of less than 1 day, while CME-driven shocks are more responsible for the spatially (up to circumsolar) and temporally (up to several days) extended enhancements known as *gradual events* (Reames, 1999; Reames, 2013; Reames, 2015; Desai and Giacalone, 2016). As shown in Fig. 5, the conceptual picture of SEP acceleration includes (1) the “flare source,” where energization is associated with the flare processes via, for example, wave-particle interactions and magnetic reconnection and (2) the “shock source,” where theoretical work suggested ambient plasma compression and collisionless shock can energize particles via shock drift acceleration at quasiperpendicular shocks or diffusive shock acceleration at quasiparallel shocks. Shock acceleration may occur in the solar corona close to the original eruption site or in the interplanetary space as the CME shock propagates outward. Interested readers can find more details on the acceleration processes in a review by Klein and Dalla (2017).

The suprathermal particles in the corona and solar wind (e.g., Mason and Gloeckler, 2012; Wang et al., 2015) can provide seed populations for the acceleration/generation of SEPs. The composition of SEPs carries key information on the seed populations and particle acceleration process in these events. Gradual SEP events generally exhibit large proton-to-electron ratios, as well as ion compositions and charge states similar to those of the corona and solar wind. This indicates that their seed populations can directly originate from the corona and solar wind, while their formation processes likely lead to the preferential acceleration of protons (Cohen et al., 2021).

Impulsive electron-rich/ ^3He -rich SEPs are typically characterized by small proton-to-electron ratios (Wang et al., 2012), strong enhancements of ^3He , significant enhancements of heavy nuclei such as Fe, extreme enhancements of ultraheavy nuclei up to more than 200 amu, and high heavy-ion ionization states (Mason, 2007). Thus, this commoner type of SEP would favor the preferential acceleration of electrons and heavy ions such as ^3He and Fe (e.g., Liu et al., 2006; Mason, 2007).

However, the traditional view that impulsive/ ^3He -rich/small SEPs are associated with flares, while gradual SEP events are related to CMEs has been challenged (e.g., Mason et al., 1999; Cohen et al., 1999; Wiedenbeck et al.,

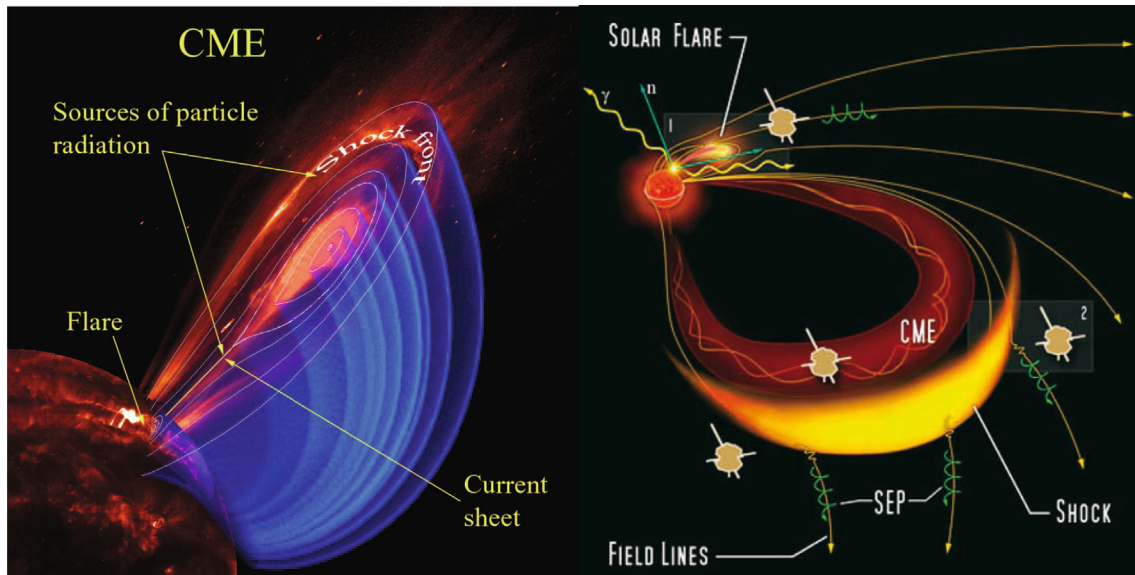


Fig. 5. Left: A generic flare and CME system related to the production of energetic particles close to the Sun (image from National Research Council (2006), as adapted from Kohl et al. (2006); copyright 2006, Springer). Right: SEPs associated with the interplanetary shock and the SEP propagation from the acceleration sites along interplanetary magnetic field lines (image from Lin et al., 2006).

2012) and the relative contribution of flare-related mechanisms and CME-driven shocks to particle energization remains an open question (Cane et al., 2003; Cane et al., 2006). The difficulty in disentangling the role of the two types of process is because a SEP event is often associated with the onset of both a solar flare and a CME. Both flare-related and CME-driven shock acceleration may contribute to the energized SEPs during the same event, and their relative role is likely to depend on particle energy (Dierckxsens et al., 2015). In addition, the transport conditions of SEPs in interplanetary space further blur the cause-effect associations (e.g., Klein and Dalla, 2017). A number of studies have concluded that at low proton energies (up to approximately tens of megaelectronvolts), energization at CME-driven shocks plays a key role in particle acceleration in the corona and interplanetary space (e.g., Desai and Giacalone, 2016). The sources of acceleration at relativistic particle energies, for example, during GLEs, might include flare processes, CME-driven shock acceleration, or both (e.g., Masson et al., 2009; Aschwanden, 2012). High-sensitivity observations show that solar energetic electron events have only a weak association with solar flares (Wang et al., 2012).

One important way to better understand the energization close to the Sun and the process of injection into interplanetary space is to use remote-sensing solar images and radio burst observations provided by ground-based and spacecraft-based solar telescopes. For instance, X-ray and γ -ray emissions can be produced by accelerated particles during solar flares (via bremsstrahlung emission or nuclear collisions), and their observations provide direct information on particle acceleration at the solar corona (Cliver et al., 1989). Therefore, they give complementary diagnos-

tic information regarding the escaping SEPs seen by in situ spacecraft. Meanwhile, radio emission at different wavelengths provides important information on the source and injection; for example, shock propagation can be closely related to type II radio emission and escaping nonthermal electrons are associated with type III bursts. Thus, radio emissions can give direct proof of the release of SEPs into interplanetary space (Kouloumvakos et al., 2015). Moreover, coronal observations of the flare or CME eruption processes and shock dynamics, via, for example, coronagraph images, and their association with the properties of SEPs give important information on the acceleration and injection process of SEPs (Kahler, 1994; Tylka et al., 2005; Dierckxsens et al., 2015).

2.2.2. Transport in the heliosphere

When the energized particles reach interplanetary space, they travel preferentially along the magnetic field, and observers with the best magnetic connectivity normally see the earliest onset of SEPs. However, turbulence in the interplanetary magnetic field plays an important role: it produces particle scattering and may cause transport across the average magnetic field, so observers not magnetically connected to the acceleration site may also observe the SEPs. Traditionally, only particle scattering has been taken into account, described as pitch-angle scattering. In the past decade, however, the possibility that turbulence may produce perpendicular transport of SEPs via magnetic field line meandering has also been studied (Laitinen et al., 2016; van den Berg et al., 2020). Drifts associated with the gradient and curvature of the Parker spiral field of interplanetary space (Dalla et al., 2013; Dalla et al., 2020; Marsh et al., 2013) may also contribute to particle trans-

port across the average magnetic field. The relative roles of different factors for cross-field transport are still not fully understood and may differ for different event scenarios.

The heliospheric current sheet (HCS), fast-slow solar wind SIRs, the magnetic structures of CMEs, and even shocks themselves may also influence the transport of SEPs in the heliosphere. For more descriptions and discussions of heliospheric disturbance structures, see Sections 4 and Temmer et al. (2023). During large gradual SEP events, gradients of particle fluxes (often observed as a jump in the intensity time profile) have been observed in association with the passing by of these disturbances (e.g., Guo et al., 2018), and this is likely because perpendicular diffusion of SEPs could be damped at magnetic discontinuities within these structures (Strauss et al., 2016). Additionally, Waterfall et al. (2022) showed that transport along the HCS is likely to play an important role in the transport of relativistic protons. Consequently, predicting SEPs assuming that they travel primarily along the nominal interplanetary magnetic field lines to reach a certain observer is further challenged in the presence of heliospheric disturbances.

Direct observation of particle scattering in the interplanetary space is impossible, although anisotropy and pitch-angle information (which needs to combine the particle direction and the vector magnetic field measurement) can provide considerable insight into the transport physics. For example, counterstreaming SEP fluxes may indicate “reservoirs” produced by local magnetic trapping, while the pitch-angle distribution indicates the role of scattering during transport to the detection site. Studies in recent years using multiviewpoint observations combined with directionality measurements by the Solar Terrestrial Relations Observatory (STEREO; since 2007) telescopes have made considerable progress in better understanding the transport physics (e.g., Dresing et al., 2014; Gómez-Herrero et al., 2015; Strauss and Fichtner, 2015). However, these observations are mostly based at a solar distance of 1 AU, with limited spatial resolution. The observed anisotropy is a combined result of the connectivity to the particle acceleration/injection site and different transport processes occurring over the long propagation path from the Sun to the observer. More measurements of this feature closer to the Sun with advanced detection techniques allowing better angular resolution, such as by Solar Orbiter’s Energetic Particle Detector (Rodríguez-Pacheco et al., 2020) and the Integrated Science Investigations of the Sun (IS \odot IS) instrument suite on the Parker Solar Probe (PSP; since 2018; McComas et al., 2016), can help constrain SEP event sources, provide information on early transport processes, and advance modeling efforts.

The in situ SEP onset information is also important for understanding the release and transport processes (e.g., Rouillard et al., 2012). Although particle scattering has been widely recognized to play an important role in SEP transport, velocity dispersion analysis has been commonly used to diagnose the first-arriving SEPs on the basis of

either single-viewpoint observations or multiviewpoint observations for the same event (e.g., Krucker et al., 1999; Xu et al., 2020; Kollhoff et al., 2021; Wimmer-Schweingruber et al., 2023). Velocity dispersion analysis assumes that these first-arriving particles with different energies are injected at the same time t_{rel} and travel nearly scatter-free along the same path L to the observer (with arrival time $t_{\text{arr}}(E)$) such that the release time and the path length can be derived by one fitting $t_{\text{rel}} = t_{\text{arr}}(E) - L/v(E)$. For some events, the release time and propagation length predicted by velocity dispersion analysis are consistent with the expected physical process, indicating that these particles experienced mostly scatter-free conditions during the transport, while for many other events, the fitted values are not sensible, suggesting that cross-field transport should be taken into account and/or there may have been different release times for particles with different energies (Laitinen et al., 2015).

2.2.3. SEP spatial distribution

The spatial distribution of SEPs in the heliosphere, in the radial, longitudinal, and latitudinal directions, depends on the energy of the particles, the transport conditions, the connectivity to the source, and the duration of the particle injection. Previously, the SEP spatial distribution was examined by statistical studies using observations near Earth (e.g., Lin et al., 1995; Cane et al., 2003; Reames, 2013) and also by multispacecraft missions such as Helios (from 1974 to 1984) (e.g., Wibberenz and Cane, 2006; Lario et al., 2006). For single-event studies, if multiple spacecraft can be in service at various well-separated locations, multiviewpoint studies can provide simultaneous in situ measurements at radial and longitudinal separations and reveal the injection and transport processes of SEPs. Studies in the last decade using the STEREO twin spacecraft have obtained insight into the longitudinal distribution of SEPs (Rouillard et al., 2012; Dresing et al., 2014; Lario et al., 2013; Lario et al., 2016; Richardson et al., 2014; Xie et al., 2019). It has been shown that the SEP peak intensity is dependent on the longitudinal separation between the observer and the source region, and their relationship can be fitted by, for example, a Gaussian expression with slight east–west asymmetry. However, it does not always make sense to fit three Gaussian parameters based on, in most cases, only three observers (two STEREO viewers and one from Earth). Future multispacecraft studies (using more heliospheric locations) are needed to reveal the longitudinal extent of SEPs. Moreover, the relative role of extended source injection and cross-field transport for the longitudinal distribution for SEPs is often case dependent and not fully understood. We have limited observations on the latitudinal distribution of SEPs, which has been sampled by the Ulysses spacecraft. Data from this mission showed that SEPs have relatively easy access to high latitudes, although their onsets are significantly delayed (Dalla et al., 2003).

The radial dependence of peak intensities is suggested to follow $R^{-\alpha}$, where α may range from less than 1 to greater than 5 as derived by different studies using different datasets (which cover different particle energies and heliospheric distances), whereby different conclusions are obtained. For instance, Lario et al. (2006) suggest that the shorter the mean free path of the particles, the larger the decrease of both peak intensities and fluences with radial distance; i.e., the smaller the energy of the particles, the larger the decrease of both peak intensities and fluences with radial distance. In contrast, Fu et al. (2022) showed that the higher the energy of protons, the larger the decrease of the peak intensity with greater radial distance.

More observations by ongoing Solar Orbiter (since 2020; Müller et al., 2020), PSP (since 2018; Fox et al., 2016), and BepiColombo (launched in 2018 and delivering two spacecraft to Mercury; Milillo et al., 2020) missions as well as future interplanetary missions will be essential to understand the spatial distribution of SEPs.

2.2.4. SEP energy distribution

The energy distribution of SEPs is another important and combined outcome of both the acceleration process and transport effects. The energy range over which SEPs are observed at 1 AU varies considerably between different events. In the largest events, the presence of protons of energies up to a few gigaelectronvolts can be detected through NMs at Earth's surface, in so-called GLE events (marked in Fig. 4; see Section 3), while most SEPs have energies up to tens of megaelectronvolts. SEP spectra can be described by a single power law distribution or a double power law (band function), or a power law with an exponential decay at high energies. The decay of the flux at high energies was considered a consequence of a finite lifetime and a finite size of the shock (Ellison and Ramaty, 1985), and the spectral break is thus considered to be a direct consequence of the acceleration process in the source region (Mason et al., 2012). However, some other studies suggest that a double power spectrum can result from a single power-law spectrum at the source that gradually forms as particles propagate out from the Sun (Li and Lee, 2015).

More spectral observations with different radial distances from the Sun would be helpful to better understand the SEP spectral evolution in relation to the acceleration/transport effects.

In synergy, the remote, in situ, and multiviewpoint observations with both energy and direction resolutions could allow the tracing of sequences of phenomena from the flare or coronal eruption at the Sun to radio signatures of near-Sun shock formation and to the energy-resolved SEP intensity time profile observations at different points in space for different directions (e.g., Kollhoff et al., 2021; Klein et al., 2022); see Fig. 6 displaying a synergistic analysis of a CME eruption shown in remote-sensing images and multi-view SEP measurements by in-situ detectors. With the new observations near Earth and from PSP and Solar Orbiter as well as various planetary missions, we expect

to make important progress in understanding the exact physics of SEP energization and transport during this new solar cycle (solar cycle 25).

2.3. Nowcasting and forecasting capability

SEP forecasts can be made only with information that is accessible before or at the start of a SEP event, and the related measurements may include solar magnetograms, optical imaging, extreme ultraviolet (EUV) imaging, soft X-ray measurements, coronagraph imaging of CMEs from single or multiple vantage points, ground-based and space-based radio observations in the wavelengths pertinent for type II, III, and IV radio bursts, in situ energetic proton and electron observations, and in situ measurements of solar wind density, temperature, and magnetic field. In real time and at geosynchronous orbit altitude, energetic particle measurements are available from the NOAA's GOES spacecraft (Sauer, 1989; Rodriguez et al., 2014; Kress et al., 2020). These measurements have been used in operational real-time forecasting for several decades (see Fig. 4) and provide a long-term dataset for model validation purposes. At the time of writing, real-time SEP observations are provided by the Space Environment In-Situ Suite (SEISS) on GOES-16 and GEOS-17, the first of the GOES-R series spacecraft, measuring protons with energies from 1 MeV to 500 MeV or greater in 14 energy channels. Real-time information on the solar event responsible for particle acceleration is crucial to develop predictive capabilities of the particle radiation environment. Besides, soft-X-ray data from GOES-16 are also available in real time. The GOES-16 Solar Ultraviolet Imager (SUVI) monitors the full solar disk in the EUV wavelength range. Obtaining real-time CME data is a critical development needed for improvement of SEP forecasting capability (Whitman et al., 2023). It can take 4–6 h, sometimes much longer, for white-light coronagraph data from the SOHO Large Angle and Spectrometric Coronagraph (LASCO; currently more than 25 years old and the sole coronagraph near Earth) used to image and fit CME ejecta to be available for a forecaster or model (Temmer et al., 2023). Planned for launch in 2024, the next GOES mission will include an operational compact coronagraph, followed in 2025 by a similar instrument on NOAA's Space Weather Follow-On Lagrange 1 (SWFO-L1). Coronagraph latency from SWFO-L1 is expected to be 15–30 min.

A recent forecast verification study (Bain et al., 2021) from the NOAA Space Weather Prediction Center (SWPC) highlights the center's performance and skill with regard to forecasting SEP events (defined in that study as the period when the GOES 10 MeV or greater integral proton channel exceeds 10 pfu, i.e., an S1 storm) during solar cycle 23 and solar cycle 24. In particular, the study evaluates forecasters' skill in assigning a probabilistic forecast for an S1 storm in the next 1, 2, and 3 days and, separately, in issuing a shorter-term (minutes to hours) deterministic warning for an imminent event. The forecast products used in that

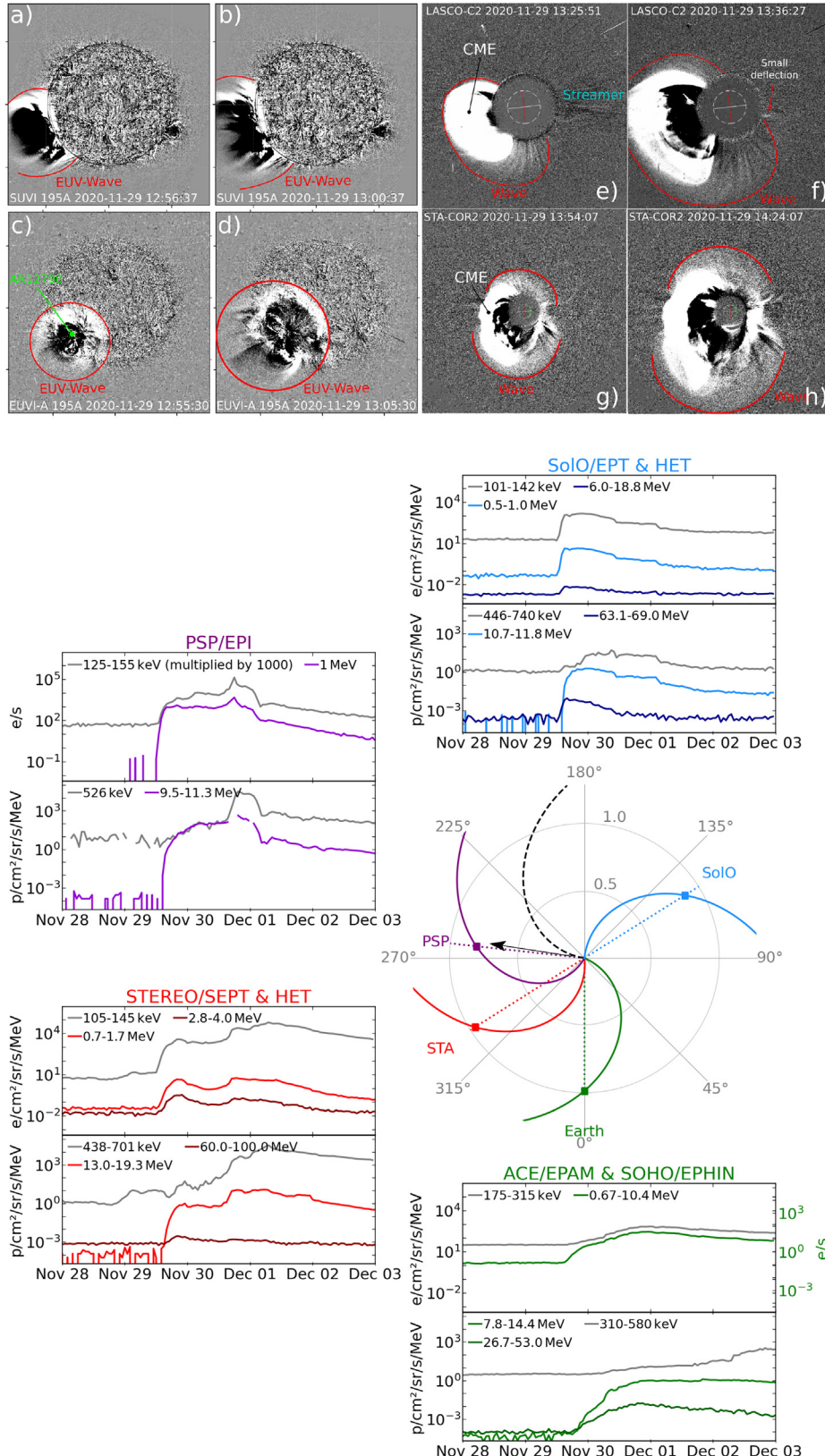


Fig. 6. Remote, in situ, and multiviewpoint observations of a widespread SEP event on 2020 November 29 (from Kollhoff et al. (2021), reproduced with permission from the European Southern Observatory). Top: Remote sensing observations of the EUV wave, the CME, and the white-light shock wave from two different viewpoints: Earth and STEREO-A. Bottom: Overview of the energetic particle measurements by PSP, Solar Orbiter (SolO), STEREO-A, and near-Earth spacecraft. EPAM, Electron, Proton, and Alpha-Particle Monitor; EPHIN, Electron Proton Helium Instrument; EPI, Energetic Particle Instrument; EPT, Electron Proton Telescope; HET, High-Energy Telescope; SEPT, Solar Electron and Proton Telescope.

study were retrieved from the NOAA archive and were based on the observations and tools that were available to forecasters in real time. The study provides a baseline for our current ability to forecast SEP events and highlights a few key points. SWPC probabilistic forecasts have improved from solar cycle 23 to solar cycle 24, with true skill scores increasing for day 1 (from 0.47 to 0.61), day 2 (from 0.16 to 0.34), and day 3 (from 0.06 to 0.13) forecasts. For solar cycle 24, SWPC 10 MeV or greater proton warnings have a probability of detection of 0.91 and a false alarm ratio of 0.24, with a median lead time of 88 min, which is better than many models currently available in the research domain. This was an improvement over solar cycle 23. SWPC also issues warning products for higher-energy, 100 MeV or greater protons. In solar cycle 24, the 100 MeV or greater proton warnings had a probability of detection of 0.53 and a false alarm ratio of 0.38, with a median lead time of 10 min. Results such as these highlight the difficulty of issuing a forecast with significant lead time while trying to limit the number of false alarms. It is also challenging to determine in advance how intense and energetic an event will be, as evidenced by the decreasing performance from 10 MeV or greater to 100 MeV or greater warning products.

Robust and accurate SEP models are needed to support forecasting endeavors. Recent years have seen the development of sophisticated modeling tools aiming to describe particle acceleration and propagation. A recent study by Whitman et al. (2023) reviewed current SEP modeling capabilities. They summarized 36 different SEP models, ranging from physics-based to empirical to machine learning approaches. For each model, they note the models' inputs/outputs, their limitations, and caveats as well as the degree of validation that had been conducted. Furthermore, they endeavored to assess the degree of readiness for these models, i.e., a measure of the maturity of the field, with regard to moving research models into operation.

They found that the different models used a wide variety of observational inputs, including ground-based and space-based remote sensing observations covering a wide range of wavelengths from X-rays to EUV to optical to radio and in situ space-based observations of solar wind and magnetic field conditions, as well as a wide range of particle energies (kiloelectronvolts to tens of megaelectronvolts) for mainly electrons and protons. In some cases, promising model approaches were demonstrated, but no real-time data are available to implement the model as a forecasting capability.

With respect to forecasting coverage, the models, taken as an ensemble, provide a wide variety of outputs that hold value for forecasters aiming to predict the near-term space radiation environment. Model outputs include all clear, probability, peak flux, fluence, and time profile predictions. Physics-based models also typically provide additional particle distribution information that, while not generally relevant to real-time forecasting, holds value for furthering the understanding of the physics of particle acceleration

and transport. Most of the models reviewed in the study, however, are not transitioned into an operational setting or require long run times and large computational resources that prevent them from being used in a forecasting context.

Currently, empirical models, which relate real-time observables to SEP forecasts, are heavily relied upon by forecast centers owing to their ability to rapidly produce results in a real-time environment. Of the 36 models discussed by Whitman et al. (2023), 12 models are running in a real-time setting serving space weather forecasters and end users through the SEP Scoreboard² or the European Space Agency's Space Weather Service Network³, at NOAA SWPC, or within other government and private institutions. Examples include the proton prediction model (Balch, 1999; Balch, 2008; Kahler et al., 2007; Kahler et al., 2017) used by the NOAA SWPC and the proton prediction system (Smart and Shea, 1989; Smart and Shea, 1992) used by the Air Force Research Laboratory. Newer empirical models such as UMASEP (University of Malaga solar particle event predictor; Núñez, 2022), RELeASE (relativistic electron alert system for exploration; Posner, 2007), and SEPSTER (SEP predictions based on STEREO observations; Richardson, 2018) are under evaluation as part of the Community Coordinated Modeling Center SEP Scoreboard; see (Whitman et al., 2023) for more details. There is broad interest in the SEP modeling community to transition models to an operational setting, which will require significant, dedicated effort from both model developers and space weather services. This worthwhile goal will need support from the various institutions that hold a stake in space weather forecasting.

However, looking forward, physics-based SEP models will be required to improve our understanding of flare and CME occurrence and resulting particle acceleration and eventually to support proton forecasting in real time. From the point of view of space weather radiation, most modeling work has focused on SEPs originating from CME-driven shocks accelerating particles in the corona and interplanetary space (e.g., Aran et al., 2006; Bain et al., 2016; Wijnen et al., 2022). However, coupled flare/CME-SEP modeling is a complex problem that should include the modeling of the flare/shock development and properties, SEP acceleration at the flare-reconnecting sites and/or the CME-driven shocks, and the transport of SEPs in the heliosphere through the temporal- and spatial-varying interplanetary magnetic field.

The previously published validation results summarized in Whitman et al. (2023) differ widely from model to model, ranging from extensive validation of a statistically significant sample of events to no validation at all. In the past, validation was not emphasized within the research community and was performed nonuniformly. However, recent

² <https://sep.ccmc.gsfc.nasa.gov/>

³ <https://swe.ssa.esa.int>

Key Process	Key Physics	Existing Key observations	Limitations and Open questions
Energization	Shock acceleration (Shock drift acceleration, Diffusive shock acceleration)	EUV Shock waves, Coronagraphs of CMEs, Radio emission, IP shock strength & orientation, SEP composition & spectral properties	<ul style="list-style-type: none"> • What is the key physics at scales and locations that cannot yet be observed? • How to distinguish CME-associated SEPs from flare-accelerated ones? • Where exactly does the flare acceleration takes place? How are particles released? • What is the exact role of current sheet & turbulence during reconnection? • What is the shock condition? How does the shock distribute in space and evolve in time? How does the shock condition affect the acceleration process? • What determines the starting and ending energy of the accelerated SEPs? • How to explain observed energy-dependence of composition in some cases? • How the variability of the SEP events (size, composition, spectral features) is correlated to the acceleration process?
	Reconnection acceleration (current sheet, turbulence, magnetic islands)	Remote-sensing images (flare, jets, flux-rope, coronal dimming), Multi-wavelength obs (EUV, X-ray, γ-ray, Radio emission), SEP composition (enhanced 3He, Ultra heavy ions)	
Transport	Field aligned	Magnetic connectivity, Pitch angle, Anisotropy (with limited resolution), onset time, spectral information and spatial distribution by multi-view observers (not yet sufficient)	<ul style="list-style-type: none"> • What is the actual field connectivity (especially with SW disturbances)? • How the field evolves dynamically in space and time? • What is the relative role of extended source and cross-field transport? • What is the relative role of particle scattering and field meandering? • How are the SEP properties modified during the propagation? • How to explain observations opposite to the existing acceleration/transport theories?
	Cross field		
Conditions	Plasma + Structures	Solar observation (magnetic field of the photosphere, Coronal holes) In-situ SW disturbance, Near-Sun and in-situ observations of CMEs	<ul style="list-style-type: none"> • How to identify the properties of the SEP source at the back-side of the Sun? • What is the IMF and SW condition at close solar distances? • What are the strength, orientation & structure of disturbances missing the observer?
	Seed population	Composition, Relative abundance, Energy spectra	<ul style="list-style-type: none"> • What are the composition & spectrum of super-thermal particles? • What is the seed population variability? What are their properties close to the Sun? • What is the spatial distribution (longitudinal, radial) of seed particles?

Fig. 7. Limitations and open questions related to the key physics of SEP studies.

efforts, such as the SHINE/ISWAT/ESWW SEP Model Validation Challenge⁴, aim to develop standards and tools for use by the SEP modeling community, and the US-based space weather enterprise has developed a formalized process⁵ for the transitioning of models from research to operation that emphasizes the role of validation in the progression from one stage to the next. Additionally, [Bain et al. \(2021\)](#) provide an important baseline for desired model performance.

In summary, a huge number of observations is required to characterize the space environments where particles are accelerated and transported, only some of which are available in real time. Besides, much more validation is required to assess the performance of these models in their ability to replicate the space environment.

2.4. Limitations and open questions

The research on SEPs still has many parts of the puzzle that remain unsolved. [Anastasiadis et al. \(2019\)](#) recently listed some key open issues, together with the expectations from new missions and forecasting schemes. Here we discuss limitations and open questions in SEP physics by grouping them into the following three categories: energization, transport, and conditions (in which the former two processes occur). Each category involves the key physics and observations as discussed in the previous sections

and also summarized in the table in [Fig. 7](#). As limited by existing key observations, there are still open questions related to different processes of the SEP problem.

Regarding understanding the process of acceleration of SEPs, we still face the following limitations:

- We are still missing the key physics at scales and locations that cannot yet be observed, such as observations for particle acceleration in the low corona (seed particle populations, injection processes, turbulence, current sheet, or shock properties).
- For acceleration attributed to flare reconnection processes, we still do not know where exactly the acceleration occurs and how particles are released through the opening of magnetic field lines.
- Because of the variability of CMEs, shocks, and SEPs and their complex correlations, we cannot always distinguish the flare-associated or CME-associated SEPs.
- We cannot yet fully capture the evolution/distribution of the particle source, such as the CME-driven shock temporal evolution, and the shock's spatial structure that may give rise to different energization processes in its different parts.
- We cannot yet fully explain the observed energy dependence of SEP composition.
- We still need to understand what the key process is for quantifying the starting and ending energy of the acceleration.
- We do not fully understand the large variability of the events (size, composition, and spectral features) and how it is correlated to the acceleration process.

⁴ <https://ccmc.gsfc.nasa.gov/challenges/sep/>

⁵ <https://www.whitehouse.gov/wp-content/uploads/2022/03/03-2022-Space-Weather-R2O2R-Framework.pdf>

Regarding understanding the transport of SEPs, we still face the following limitations:

- We cannot yet accurately describe the magnetic connection between the particle sources and the observer since the actual magnetic field connectivity (especially with solar wind disturbances) should not always be described by nominal Parker spirals.
- We do not yet understand how the magnetic field evolves dynamically in space and time (turbulence and field meandering) and how this affects SEP propagation.
- We cannot yet fully distinguish the relative role of extended source and cross-field transport for widespread events.
- We cannot yet fully characterize the way in which coronal and interplanetary transport processes modify the properties of the injected population.
- We cannot yet clarify the roles of particle scattering and field meandering in SEP transport over the full range of SEP species and energies.
- We cannot yet explain observations that show features opposite those of the two-class acceleration/transport theory, such as widely distributed ^3He -rich events or impulsive SEPs, come from a very poorly connected source.

When it comes to the conditions through which the acceleration/transport processes occur, we still have various open questions, as below:

- There are very few observations of the solar magnetic field at the far side of the Sun (seen from the Earth). This makes it difficult to identify the properties of the SEP source when it is located at the far side of the Sun.
- Despite the recent PSP and Solar Orbiter missions, there are still limited observations of the interplanetary conditions close to the Sun, which strongly influence the early phase of the SEP transport.
- It is difficult to quantify the strength, orientation, and structure of disturbances (ICMEs and SIRs) that do not pass the observer but have a large impact on the propagation of SEPs.
- Regarding the seed particle population close to the Sun, we still lack observations of its composition and spectrum and their variability; we still do not know if the seed particles are constant sources or episodic sources.
- For the seed particle population in interplanetary space, we do not fully understand its distribution in longitude and radial distance.

In addition, from the operational and SEP forecasting point of view, we follow Section 2.3 to briefly summarize a few major limitations below:

- The limitation on key observations, as discussed above, is as a major challenge for advancing SEP models.

- Most physics-based models require long run times and large computational resources, which currently prevent them from being used in a forecasting context, although they are essential for advancing our understanding of the SEP physics.
- It is difficult to use/compare models designed to reach related but different outputs. Therefore, model validation with uniform standards is still required to assess the ability of the model to replicate the space environment.
- In many cases, real-time data are still lacking to implement the model as a forecasting tool.
- SEP modeling research based on scientific interest still needs support from stakeholders within the space weather forecasting authorities to be transitioned into operations.

Last but not least, with the aim of better predicting the deep-space heliospheric radiation environment for planetary missions, it is also crucial to have multiviewpoint real-time forecasting capabilities. Effort has been made on this aspect based on the energetic particle flux time profiles from the twin STEREO spacecraft and ACE at Earth's L1 point, in combination with SOHO outer-corona images in white light and inner-corona EUV images from the Solar Dynamics Observatory⁶. However, STEREO-B has been out of service since October 2016. The implementation of other spacecraft at different locations for real-time monitoring would greatly benefit the purpose of 360° forecasting of the heliospheric radiation environment. Recently, the European Space Agency approved the Vigil mission, which is a spacecraft deployed at the L5 point of the Sun-Earth system to enable remote sensing of the Sun and interplanetary space and in situ measurements of solar wind plasma and high-energy solar particle events (Vourlidas, 2015). Meanwhile, Chinese scientists have proposed the Solar Ring mission, which includes three spacecraft at positions somewhat shifted from the L3, L4, and L5 points to observe the Sun and perform in situ observations (Wang et al., 2023). With the ongoing and future missions, we expect to see significant advances in SEP physics and forecasts in the next decade.

3. Ground-level enhancement

3.1. Introduction

GLE events occur when SEP-induced atmospheric secondary particles are registered at ground-based detectors, such as ionization chambers or muon monitors and NMIs (see, e.g., Shea and Smart, 1993; Miroshnichenko et al., 2013). GLEs are therefore related to the most energetic class of SEP events, associated with solar flares and/or CMEs, requiring acceleration processes that produce pro-

⁶ <http://stereo.ssl.berkeley.edu/multistatus.php>

tons with energies high enough to provide a ground-level signature of the event. It has been found that the threshold energy for SEPs, upon their entry in Earth's atmosphere, to cause GLE is about 430 MeV per nucleon at sea level (Plainaki et al., 2014) and about 300 MeV per nucleon for high-altitude polar stations at the South Pole (Mishev and Poluianov, 2021). After entering the atmosphere, the primary SEPs can produce showers of secondary particles with sufficient intensity to exceed the GCR background. Those primary SEPs are mainly protons and, to a smaller extent, heavier ions, although some events have also been associated with the emission of solar neutrons (see, e.g., Muraki et al., 2008).

From February 1942 until October 2021, 73 GLE events were registered. The first four GLE events were recorded by ionization chambers (Forbush, 1946). The GLE events registered from 23 February 1956 onward, starting from GLE5, were recorded by the worldwide network of NMs, which are energy-integrating detectors with cutoff rigidities depending on the actual location and altitude at which they are installed (see, e.g., Miroshnichenko, 2018). The times of GLE events are marked in Fig. 4, which shows their occur-

rence is dependent on the solar activity cycle but not solely during the solar cycle maximum years. Fig. 8 shows the recent GLE events of solar cycles 23 and 24 (the last one is from solar cycle 25), as they were registered at the Oulu NM station on the basis of 5-min data.

NMs allow the determination, to first order, of the primary SEP spectrum during a GLE event. Most NM data are part of international databases now available to the entire scientific community; for example, the International GLE Database (Usoskin et al., 2020; Väisänen et al., 2021) and the Neutron Monitor Database (Mavromichalaki et al., 2010). Numerous GLE-modeling efforts performed jointly with rigorous data analyses (see, e.g., Miroshnichenko et al., 2013), also at interdisciplinary level, have led to the detailed identification of the properties of most of the observed GLE events and to the estimation of the spectral characteristics in the circumterrestrial space of the related relativistic SEPs (Belov et al., 2005; Bombardieri et al., 2008; Plainaki et al., 2007; Plainaki et al., 2014; Mishev and Usoskin, 2016; Mishev et al., 2018). Fig. 9 shows reconstructed SEP spectra based on NMs with different cutoff rigidity (Usoskin et al., 2020).

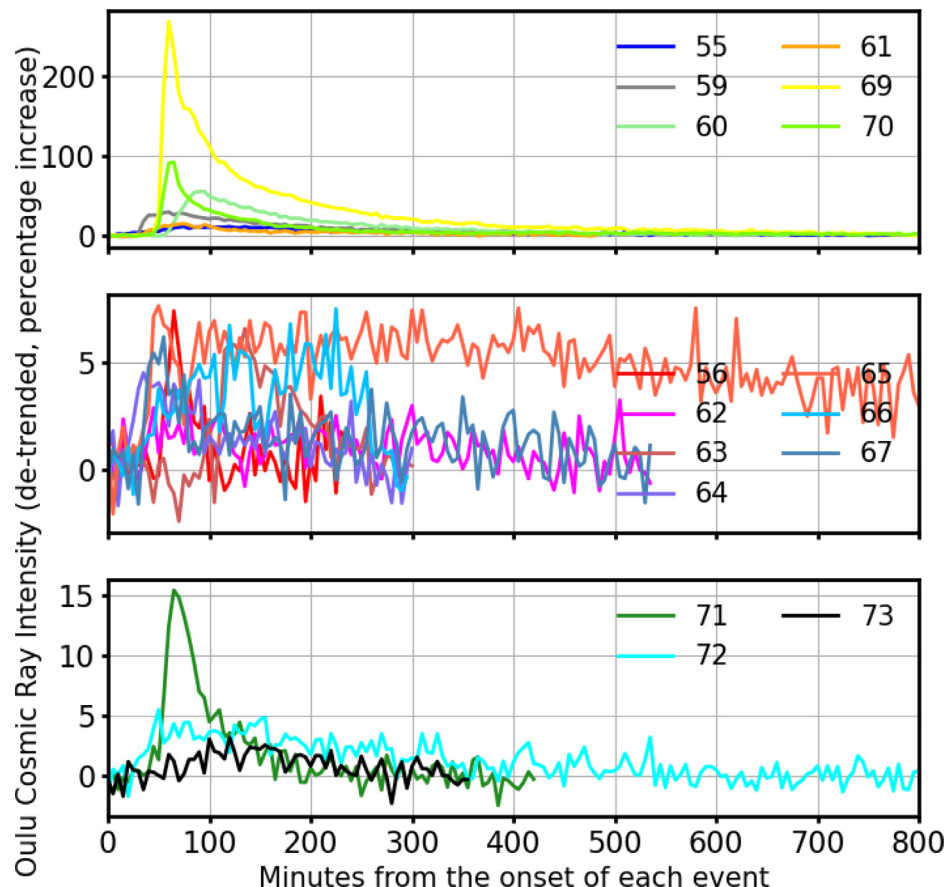


Fig. 8. Time profiles of GLE events 55–73 (except for events 57, 58 and 68, which have caused only marginal enhancements) as recorded by the Oulu NM station with cutoff rigidity of 0.8 GV. GLE numbers are shown in the legends. The top panel shows events during solar cycle 23 with a peak increase above 10%, the middle panel shows the smaller events from solar cycle 23, and the bottom panel shows the only two GLE events (GLE71 and GLE72) during solar cycle 24 and the one event so far (GLE73) during solar cycle 25. Data were downloaded from the International GLE Database <https://gle.oulu.fi> (detrended GLE data) with 5-min cadence.

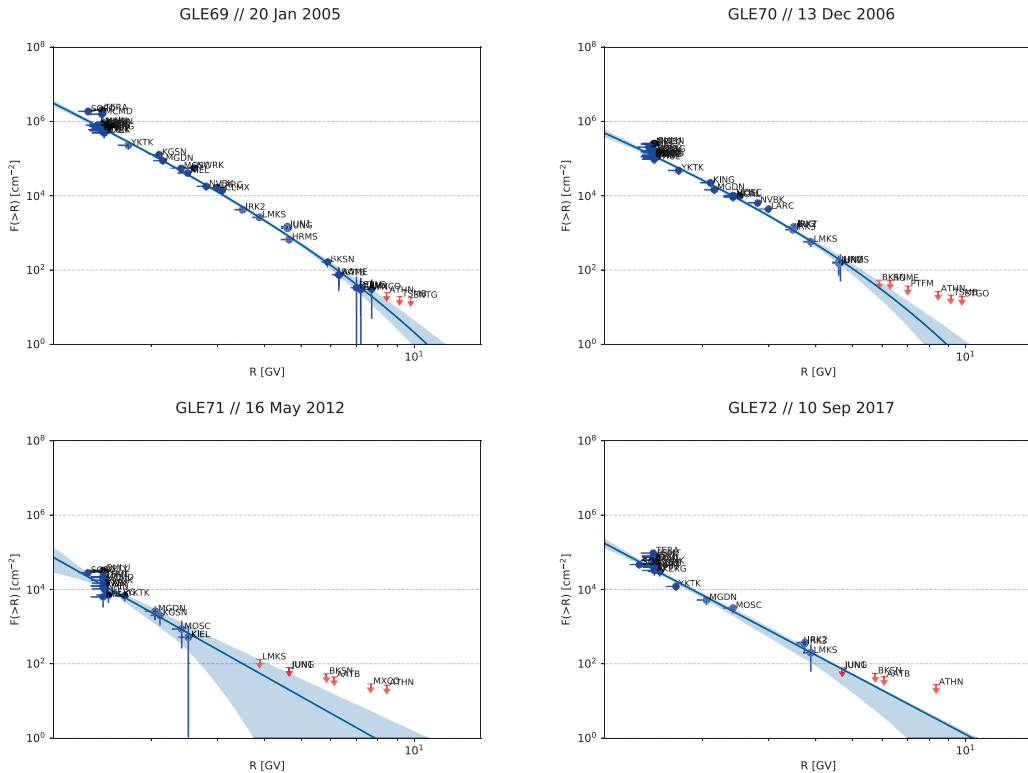


Fig. 9. Integral fluence spectra reconstructed for GLE events 69–72 (from Usoskin et al. (2020), reproduced with permission from the European Southern Observatory). Blue points with error bars depict reconstructions of the integral fluence from individual NMs, while red arrows denote the upper limits. Error bars represent the full-range uncertainties. The thick blue curve represents the best-fit spectral approximation with 1σ uncertainties. (For interpretation of the references to colour in this figure legend, the reader is referred to the web version of this article.)

In this section, we give a brief overview of the recent progress on GLE observations (and models developed in synergy with observations) and address a few issues that need to be better studied in the next few years.

3.2. Recent progress and current understanding

Joint SEP and GLE studies based on data from both space-borne and ground-based instruments have made major progress in the past few years. During the recent space age, GLE observations by NMs are often complemented by various sets of space-based particle data registered during the associated SEP events (see, e.g., Plainaki et al., 2014). High-energy SEP data with some associated with GLE events have been recorded over the past few years by the Electron Proton Helium Instrument (EPHIN) onboard SOHO (Kühl et al., 2017) and by the High Energy Proton and Alpha Detector (HEPAD) onboard GOES spacecraft (Onsager et al., 1996). Although recent space-borne measurements of particle fluxes above some hundreds of megaelectronvolts, e.g., the Payload for Antimatter Matter Exploration and Light-nuclei Astrophysics (PAMELA; Adriani et al., 2015), operating from 2006 to 2016, and AMS-02 (Aguilar et al., 2018), in operation since 2011, have significantly broadened our view on relativistic SEP events (e.g., Bruno et al., 2018), ground-based NM observations remain essential. At LEO altitude, Earth's

magnetosphere can shield and modulate SEPs arriving at these detectors, causing the SEP flux to vary intermittently as affected by the hosting satellites' orbit. Moreover, during such major SEP events, saturation effects caused by intense particle fluxes hitting the detectors are likely to result in greater uncertainties in the estimation of the event magnitudes, as already observed for payload onboard GEOS spacecraft (e.g., Reeves et al., 1992; Tylka et al., 1997). However, the high-energy space-borne data have recently been essentially revisited and corrected for known errors (see, e.g., Raukunen et al., 2020, for GOES data).

To reveal the properties of relativistic SEPs associated with GLE events, the identification of the primary SEP spectrum is necessary and has been realized by various studies. The primary SEP spectrum reconstruction has typically been done by best-fitting NM data (e.g., Belov et al., 2005; Plainaki et al., 2007; Plainaki et al., 2009a; Mishev and Usoskin, 2016; Mishev et al., 2018; Usoskin et al., 2020) and/or energy-dependent space-borne data (Raukunen et al., 2018; Bruno et al., 2019) to a predefined spectral shape and spatial distribution function associated with the primary SEP fluxes, containing free parameters that characterize the ongoing physical mechanisms. The identification of these best-fit parameters and of their uncertainties often allows some scenarios to be eliminated regarding the primary acceleration mechanism (e.g., Plainaki et al., 2014). A crucial input in these retrieval

models is the NM yield function, a topic for which important investigations have been performed in recent years (e.g., Clem and Dorman, 2000; Mishev et al., 2020). Recently, a new effective-energy analysis method was developed to reconstruct the high-rigidity part (1 GV or greater) of the spectral fluence of SEPs for GLE events, based on the use of NM data (Koldobskiy et al., 2018). Moreover, by combining data from low-energy (less than 300 MeV per nucleon) space-borne detectors located beyond the magnetosphere (e.g., at L1) with NM data, one can reconstruct the primary SEP spectrum and identify the spatial characteristics of the flux (e.g., anisotropy and spatial distribution at a specific altitude within Earth's atmosphere), taking also into consideration the NM asymptotic directions of viewing (e.g., Plainaki et al., 2009b). In this context, the use of ground-based data is particularly important since the registration (or lack of registration) of an event at different locations on Earth's surface provides direct information on the minimum cutoff energy of the primary particles responsible and the dominant direction of their propagation.

Before the era of ground-based detectors, some very large GLE events also left their footprint on Earth. SEPs with extremely high energies and fluxes can affect atmospheric chemistry, leading to the formation of nitrates or the production of cosmogenic radionuclides, such as radiocarbon ^{14}C . These signatures can be registered in the polar ice core or in tree rings. Recent years have seen much progress in reconstructing extreme historical SEP events with use of such information (see Section 7 in Cliver et al., 2022) to understand the features and occurrence probability of these events. However, it is still unclear if different physics is involved to make such extreme events distinguished from other GLE and SEP events or if they are merely large (McCracken et al., 2023). The accurate forecast of such extreme events continues to pose one of the biggest challenges for the space weather community.

In parallel to such extreme types of GLE events, there is also growing interest to study weak and short-term events, such as sub-GLE (Poluianov et al., 2017) and anisotropic cosmic-ray enhancement (ACRE) events (Gil et al., 2018). However, they generally have less contribution to the enhanced radiation environment. Sub-GLE events are those with a relatively weak SEP input that are not detected by sea-level NM stations but that are registered at high-elevation polar regions with negligible geomagnetic and reduced atmospheric rigidity cutoffs. In comparison, a GLE event has to be registered by at least two differently located NMs, including at least one NM near sea level and a corresponding enhancement in the proton flux measured by a space-borne instrument(s). Alternatively, ACRE events are associated with highly anisotropic GCR flux detected only by NMs with certain directions of acceptance of charged particles through Earth's magnetosphere. It may be not related to SEPs, but may be caused by the local

anisotropy of Forbush decreases or other disturbed heliospheric conditions (more details are provided in Section 4).

With the recent progress in planetary exploration, some particle detectors have been sent to the surface of other planetary bodies, such as the Radiation Assessment Detector (Hassler et al., 2012) on Mars and the Lunar Lander Neutron and Dosimetry instrument (Wimmer-Schweingruber et al., 2020) on the Moon. Thus, our detection and knowledge of GLE events has expanded to places other than Earth. Xu et al. (2020) reported the first SEP event detected on the lunar surface, on 2019 May 6, which had a rather low intensity. Because of the lack of an atmosphere or intrinsic magnetic field, SEPs can directly reach the lunar surface and interact with the lunar regolith to generate secondaries. Thus, the lunar surface radiation environment could be hazardous during SEP events for future lunar explorers. Similarly, Mars lacks an internal magnetic dynamo and its atmosphere is rather thin as compared with Earth's, allowing a good portion of the SEPs to reach its surface or to cause enhanced secondary radiation on Mars. The recent two GLE events registered at Earth (GLE72 and GLE73) were also detected at Mars (Guo et al., 2018; Guo et al., 2023). However, their properties are significantly different at the two planets, for which two factors should be carefully considered: (1) the different heliospheric locations of the planets mean that they may see different SEP intensities and energy spectra because of transport from the acceleration site (Section 2); (2) the different planetary environments (magnetic field, atmospheric structure and depth, regolith composition, etc.) have different influences (shielding) on the arriving SEPs. The former requires a global understanding of the SEP properties and distributions in the heliosphere, while the latter needs specific particle transport modeling through the planet's environment. The space weather at other planetary bodies is the subject of the ISWAT H4 cluster "Space weather at planetary bodies in the Solar System," and the subject of planetary space weather will be discussed in a future article.

In summary, on the basis of advances in recent years, we now have sufficient observation and modeling capabilities to do the following:

- We can assess, during SEP and GLE events, with acceptable accuracy the spatial distribution of the radiation environment above Earth's atmosphere in the rigidity range approximately above 1 GV.
- We can identify during GLE events, for a predefined SEP spectrum shape, the most representative parameters characterizing the particle acceleration and transport processes (e.g., power-law spectrum index).
- We understand, even though not exhaustively, the way the atmosphere affects primary SEP fluxes during GLE events, based on back-tracing and forward modeling techniques.

- We can derive with acceptable accuracy the acceptance cones at each ground-based detector given the intensity of the magnetic field in the near-surface region.
- We are starting to investigate the nature of different types of GLE, including weak sub-GLE and ACRE events as well as extreme GLE/SEP events, using their cosmogenic imprints.
- We are starting to detect and understand SEP and GLE events at other planetary bodies combined with synergistic observations near Earth and modeling approaches.

3.3. Limitations and open questions

The study of GLE events in the near future will remain important to answer a few open questions, from the pure space weather science point of view, summarized as follows:

- What is the essential and necessary condition that solar eruptions need to satisfy to produce a GLE event?
- What is the contribution of the interplanetary space structures in the SEP transport processes?
- What are the properties of the seed population necessary for producing a GLE event?
- How can we predict the onset times and properties of relativistic SEPs resulting in radiation storms and GLE events?
- What is the distribution of the primary SEP spectrum (in near-Earth space) responsible for GLE events?
- If and what different mechanisms are involved in making extreme types of SEP events?

From an operational point of view considering the monitoring and predictability of SEP and GLE events, we can still make improvements in the following directions, most of which are beneficial not only for GLE studies but also for a wider range of space weather topics:

- We need a denser and wider coverage of NM detectors (see [Mishev and Usoskin, 2020](#), for more detailed discussions). This will increase the certainty in the estimation of the modeled SEP parameters, reducing possible code bias effects, especially in cases of low-intensity GLE events.
- We should work toward implementing a reliable space-based and ground-based network of space weather assets, continuously operating and maintained. In particular, it is necessary to intercalibrate ground-based and space-based measurements since the derived results do not always agree with each other ([Miroshnichenko, 2018](#)) and there is a need for good coverage of space particle detectors in the energy range up to a few gigaelectronvolts.
- We need a fleet of spacecraft that can provide the necessary basis for testing and validating radiation models of different particle types over a wide range of energies and at different locations in the inner solar system.

- We will benefit from a dense coverage of ground-based magnetic observatories that could provide information in real time on the actual magnetic field conditions for better interpreting and possibly predicting the direction of the major radiation hazards in space due to GLE events.
- We need to use more information of historical events, even before the NM era, to better understand their nature and make predictions of such disastrous scenarios.

4. Galactic cosmic rays

4.1. Introduction

GCRs originate from outside the heliosphere and can have energies far greater than SEPs. Radiation induced by GCR nuclei, especially those with high energy (e.g., protons with energy above 100 MeV) and high-charge ions, remains one of the major concerns for long-term deep-space human and robotic missions ([Townsend et al., 1994](#); [Cucinotta et al., 2013](#); [Miyake et al., 2017](#); [Dachev et al., 2020](#); [Guo et al., 2021](#)).

Compared with SEPs (Section 2), the intensity and composition of GCRs are rather stable, but not constant as the charged GCR particles are affected by the varying heliospheric environment following solar activities (see reviews by [Cane et al., 1999](#); [Potgieter, 2013](#); [Rankin et al., 2022](#)). In the long term, the GCR flux was first observed to vary inversely with sunspot number ([Forbush, 1954](#); [Forbush, 1958](#)) and is known as the 11-year solar modulation of GCRs. Recent studies using historical cosmogenic isotope imprints have also revealed longer cycles of the modulation, such as the 2400-year Hallstatt cycle, the millennial Eddy cycle, and 210-year Suess/de Vries cycle (see the review by [Usoskin, 2023](#)). In recent decades, the decrease (or increase) in GCR intensity near the solar maximum (or minimum) has been studied and quantified with use of data from both ground-based NMs (see, e.g., [Usoskin et al., 2017](#), and Fig. 12) and high-energy particle detectors for space missions. As described in Section 3, NMs measure the secondary neutrons generated in Earth's atmosphere by primary cosmic rays, being GCRs or occasionally SEPs with particles reaching GLE energies. An example of continuous measurement of energy-resolved particles in space is shown in the bottom panel in Fig. 4, where the SEP-subtracted background flux measured by GOES spacecraft is anticorrelated with the solar-cycle sunspot number (top panel).

On short timescales of several days, GCR modulation is dominated by interplanetary transients such as ICMEs and SIRs. ICMEs are interplanetary counterparts of solar eruptive magnetic structures that evolve as they propagate in the interplanetary space and may pile up plasma and heliospheric magnetic field in the so-called sheath region as well as drive a shock ahead of the sheath (see, e.g., the overview by [Kilpua et al., 2017](#)). During their passage, a depression

can be observed in the GCR count, called a *Forbush decrease*, first discovered by [Forbush \(1937\)](#) and [Hess and Demmelmaier \(1937\)](#). SIRs are interplanetary transients formed by the interaction of the high-speed streams originating from coronal holes and the slow solar wind (see, e.g., the overview by [Richardson, 2018](#)). As ICMEs, they can cause short-term depressions in the GCR flux. They may recur in several solar rotations, in which case they are called *corotating interaction regions* (CIRs) and thus their corresponding short-term Forbush decreases in the GCR flux are recurrent following the 27-day solar rotation rate ([Richardson, 2004](#)). Sketches of an ICME and a SIR and the corresponding (recurrent) Forbush decreases are given in [Fig. 10](#). The ICME-related generic Forbush decrease (bottom-left panel) was obtained from modeling (for details, see [Dumbović et al., 2020](#)), whereas the SIR-related Forbush decrease generic profile (bottom-right panel) was obtained by superposed epoch analysis (for details, see [Dumbović et al., 2022](#)). For a comprehensive overview of ICMEs, SIRs, and other solar wind disturbance in the heliosphere, see [Temmer et al. \(2023\)](#).

In this section, we give a brief overview of the recent progress on GCR modulation and the physics of GCR

transport and address the limitations and open questions related to this topic.

4.2. Recent progress and current understanding

In the heliosphere, GCRs propagate against the expanding solar wind and interact with embedded magnetic irregularities. Thus, their intensities in the inner heliosphere differ from their local interstellar spectra (LIS) beyond the heliopause at about 120 AU ([Krimigis et al., 2013](#)). Although LIS are the essential ingredient of the solar modulation model, our knowledge of LIS is very limited because of the difficulty of direct measurement. Voyager 1 crossed the heliopause on 2012 August 25 at a radial distance 121.6 AU from the Sun, and observed the low-energy GCRs from the LIS ([Krimigis et al., 2013; Stone et al., 2013; Gloeckler and Fisk, 2014](#)). Six years later, on 2018 November 5, Voyager 2 also entered the interstellar space and measured the LIS ([Stone et al., 2019](#)). The LIS measured by Voyager 1 shows that nucleon spectra flatten and roll over below a few hundred megaelectronvolts per nucleon with respect to the approximate power-law dependence at higher energies, and the intensity of electrons (in-

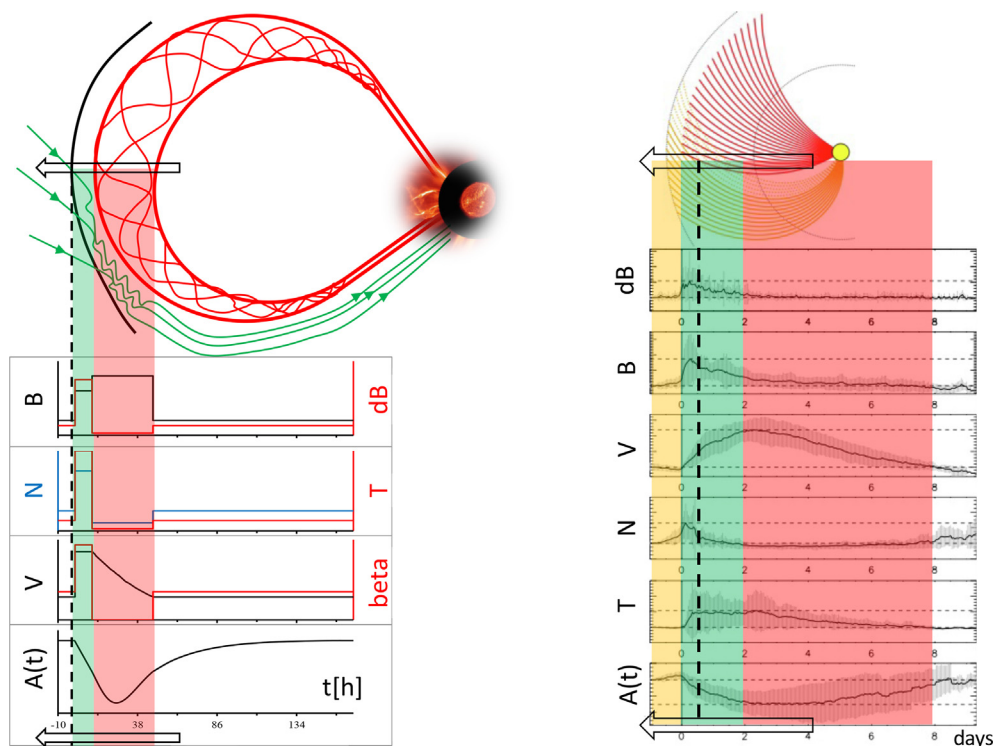


Fig. 10. Left: Sketch of an ICME consisting of the magnetic ejecta/flux rope (red) as well as the shock and sheath region (black line followed by a green region) with corresponding in situ measurements observed as the spacecraft crosses through the trajectory marked by an arrow. The in situ measurements show a generic ICME profile in (from top to bottom) magnetic field and fluctuations, density and temperature, speed and plasma beta, and cosmic ray count rate (adapted from [Dumbović et al., 2020](#)). Right: Sketch of a SIR with highlighted regions of slow solar wind (yellow), compression region (green; with stream interface marked by the dashed black line), and high-speed stream (red). Corresponding in situ measurements are given below observed as the spacecraft crosses through the trajectory marked by an arrow. The in situ measurements show a generic SIR profile in (from top to bottom) magnetic field fluctuations, magnetic field strength, solar wind speed, density, temperature, and cosmic ray count rate (adapted from [Dumbović et al., 2022](#)). (For interpretation of the references to colour in this figure legend, the reader is referred to the web version of this article.)

cluding positrons) exceeds that of protons below approximately 50 MeV (Cummings et al., 2016). The two Voyager probes provided invaluable information on the unmodulated GCR energy spectrum, as shown in Fig. 11. However, their energy range is very limited, from a few megaelectronvolts per nucleon to a few hundred megaelectronvolts per nucleon, so the complete LIS are still primarily based on model predictions.

During the propagation in the heliosphere, GCRs are subjected to four major modulation processes: convection and adiabatic energy losses caused by the expanding solar wind, diffusion due to the random motion on the irregularities of the heliospheric magnetic field, and drift motions resulting from gradients and curvatures in the heliospheric magnetic field as well as the abrupt change of the magnetic field direction above and below the HCS (Potgieter, 2013; Moraal, 2013). The modulation effect is significant for particles with energy below approximately 10 GeV with an energy dependence (Gieseler et al., 2017) and varies with time and position. The solar-cycle variation of GCRs has long been observed at Earth by ground-based NMs as well as high-energy particle detectors onboard space missions (e.g., Heber et al., 2006; Picozza et al., 2007; Kounine, 2012; Usoskin et al., 2017; Fu et al., 2021). Recently, this modulation effect was also observed and studied at other planets/locations in the heliosphere, such as at Mars (Guo et al., 2021), Saturn (Roussos et al., 2020), ROSETTA en route to comet 67P/Churyumov–Gerasimenko (Honig et al., 2019), and New Horizons en route to Pluto (Wang et al., 2022).

Since GCRs drift along opposite trajectories during opposite heliospheric magnetic field polarity cycles, their

intensities reflect not only the 11-year solar activity cycle but also the 22-year solar (heliospheric) magnetic polarity cycle. Numerous studies have explored the anticorrelation of the GCR count rate and various solar and heliospheric parameters, such as the sunspot number, the solar radio flux, the strength and turbulence level of the heliospheric magnetic field, the HCS tilt angle, and the open solar magnetic flux (e.g., Heber et al., 2006; Usoskin et al., 1998; Cliver and Ling, 2001; Alanko-Huotari et al., 2007; Potgieter, 2013; Wang et al., 2022), and empirical functions describing the GCR dependence on different solar-cycle parameters have been proposed (e.g., Dorman, 2001; Usoskin et al., 2011; Wang et al., 2022). Fig. 12 (top panel) shows a comparison of normalized GCR counts recorded at eight different NM stations with different cutoff rigidity. It seems that in the case of high cutoff rigidity (which requires the primary GCRs to have higher energies overcoming Earth's magnetic shielding), the variation of the GCR count rate over different phases of the solar activity cycle is smaller. This may be because high-energy GCR particles have a weaker solar modulation effect than GCRs with lower energies. Recently, the GCR anisotropy and its dependence on the 22-year magnetic cycle have also been observed and are attributed to the magnetic field turbulence, solar wind convection, particle diffusion and drift processes, and the combined effects with the existing GCR gradients (see, e.g., Wozniak et al., 2023).

The transport of GCRs in the heliosphere is described by the transport equation (TPE; also referred to as the *Parker TPE*; Parker, 1965) including all major modulation processes. In the most general case, the TPE is a 3D rigidity-dependent, time-dependent, and space-dependent

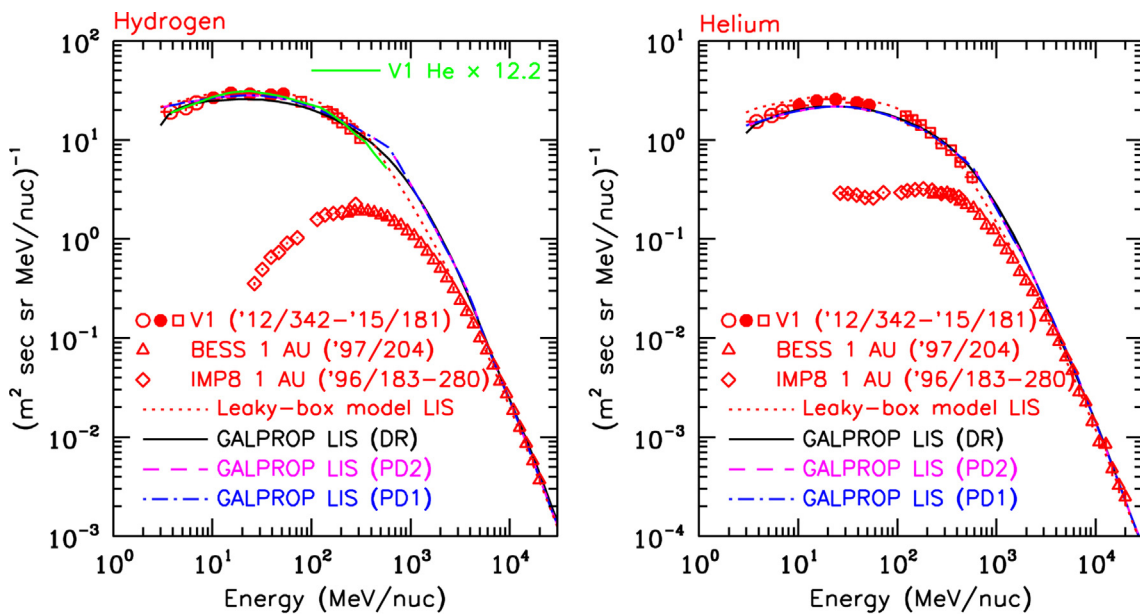


Fig. 11. Differential energy spectra of LIS H (left) and He (right) from Voyager 1 for the period from 2012/342 to 2015/181, and solar-modulated spectra at 1 AU from a Balloon-borne Experiment with a Superconducting Spectrometer (BESS) balloon flight in 1997 and from IMP-8 in the latter part of 1996. Several modeled GCR spectra are also plotted as a comparison. (From Cummings et al. (2016), reproduced with permission from the American Astronomical Society).

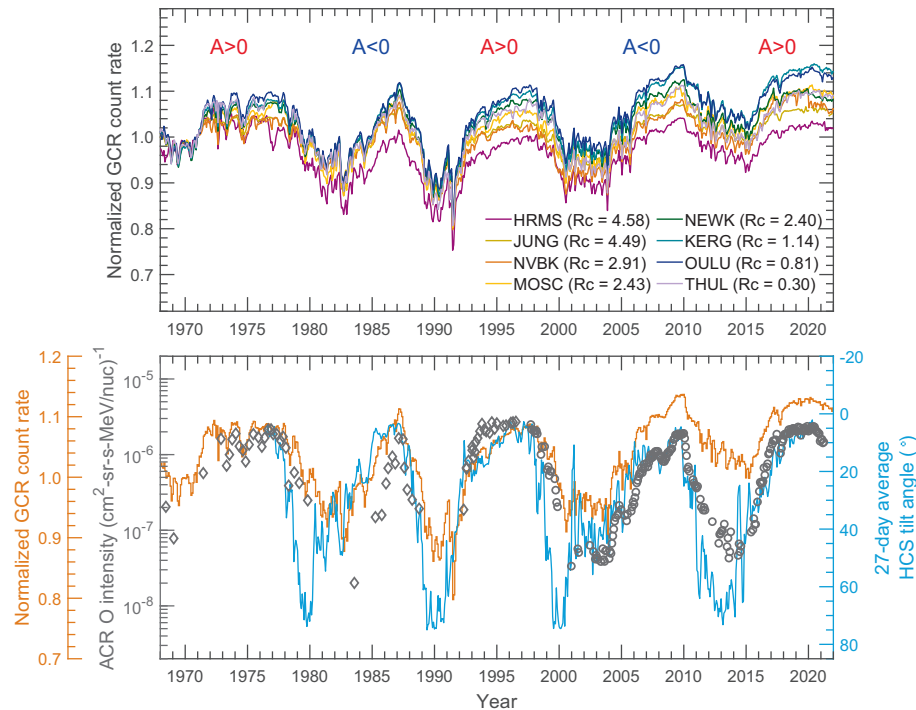


Fig. 12. Top: Time profiles of the count rate of secondary particles generated by GCRs as measured by eight different NMs with different rigidity cutoffs (Rc) from 1968 to 2022, each normalized to its long-term average level. Bottom: GCR count rate calculated as the average from the aforementioned eight stations (orange curve scaled by the first left axis), ACR oxygen intensity (black points scaled by the second left axis), and the HCS tilt angle (cyan curve scaled by the right axis, where an inverted scale is applied for a more intuitive comparison). (Image obtained via private communication with Fu Shuai from Macau University of Science and Technology.). (For interpretation of the references to colour in this figure legend, the reader is referred to the web version of this article.)

partial differential equation with a second-order diffusion tensor, which can be solved numerically (see, e.g., the review by Strauss and Effenberger, 2017). However, solving the full TPE is very complex, is computationally expensive, and might suffer from the numerical stability problem. Therefore, a much simpler, 1D approximate solution, called the *force-field approximation method*, is widely used. It can be derived from the TPE assuming a 1D steady state and spherical symmetry and ignoring adiabatic cooling and drifts (for more description and discussion, see, e.g., Gleeson and Axford, 1968; Caballero-Lopez and Moraal, 2004; Moraal, 2013). The force-field approximation is popular because it is easy to use with an analytical method describing the modulation level with a single parameter. In recent years, the stochastic differential equation method has often been applied in solving the 2D or 3D Parker equations because of the unconditional numerical stability and advances in computational resources (Kappl, 2016; Potgieter, 2017; Boschini et al., 2018). The Parker TPE is transformed into a set of stochastic differential equations and then the solution is sampled via Monte Carlo simulations. Regardless of whether one seeks a solution of a full TPE or a simpler but approximate solution, one needs to apply boundary conditions, i.e., information on the LIS of GCRs is necessary.

Recently, precise measurements of the energy and time dependence of GCR intensities throughout an entire solar

cycle by PAMELA (onboard the Resurs DK1 satellite since 2006; Bonvicini et al., 2001) and AMS-02 (installed on the International Space Station in 2011 May; Bindi et al., 2017) shed light on the LIS and improved understanding of the details of solar modulations. These measurements cover the long solar minimum between cycle 23 and cycle 24, the solar maximum and solar polar reversal, and the recent solar minimum in cycle 24/25. A number of complex numerical models have been built to investigate the monthly measurements of GCR spectra by these experiments (see, e.g., a comprehensive model-data comparison by Liu et al. (2024)). The classic force-field approximation method is not sufficient to interpret these precise data; thus, modification of the force-field approximation or more advanced models are needed (Corti et al., 2016; Cholis et al., 2016; Shen et al., 2021). With the developed solar modulation models and measurements from the Voyager probes, PAMELA, and AMS-02, several new LIS models have also been constructed (Potgieter, 2014; Corti et al., 2016; Herbst et al., 2017; Gieseler et al., 2017; Zhu et al., 2018; Boschini et al., 2018; Bisschoff et al., 2019; Wang et al., 2019; Boschini et al., 2020; Wang et al., 2022).

Studies of GCR modulation help us to conclude the following (e.g., Tomassetti et al., 2017; Di Felice et al., 2017; Corti et al., 2019; Wang et al., 2019; Ngobeni et al., 2020; Aslam et al., 2021; Song et al., 2021; Fiandrini et al., 2021; Roussos et al., 2020; Wang et al., 2022; Wang et al., 2022):

- The GCR modulation effect is rigidity dependent (stronger for particles with lower rigidity), location dependent (generally stronger modulation at distances closer to the Sun), and time dependent (ranging from a few hours as modulated by ICMEs to more than a solar cycle and even over millennia).
- There is a time lag in the variation of GCR intensity relative to the solar activity, although this lag is not constant, but rather rigidity dependent, polarity dependent, location dependent, and time dependent.
- The radial gradient of the GCR flux within about 10 AU is mostly between 2% and 4% per astronomical unit, which is, however, rigidity dependent, location dependent, and time dependent.
- The rigidity dependence of the diffusion coefficient varies with time and location.
- During the high solar activity epochs, the drift effects are suppressed.

As noted earlier, on timescales of several days/weeks, GCR flux is modulated by interplanetary disturbances and observed as so-called Forbush decreases (Fig. 10). The variety of Forbush decreases detected, from spacecraft to ground-based observations both at Earth and at other planets, such as Mars, has provided further insights into the characterization of Forbush decrease events at different locations in the heliosphere, as well as during different times in the solar cycle. Their properties are as follows:

- The time evolution of the Forbush decrease is characterized by a decrease followed by a recovery period. However, the intensity of the decrease (as in the maximum reduction of the GCR count rate), the speed of the decrease, and the speed of the recovery all vary depending on its interplanetary causes (see, e.g., the review by Cane, 2000; Belov, 2008).
- The relative trajectory of the detector through the interplanetary transient can also affect the shape of the detected Forbush decrease.
- The Forbush decrease magnitude depends on the interplanetary transient, the location in the heliosphere where it was observed, and the instrument energy coverage of the GCR spectra (e.g., Witasse et al., 2017; Winslow et al., 2018; Guo et al., 2018; Freiherr von Forstner et al., 2018; Dumbović et al., 2020; Freiherr von Forstner et al., 2020).
- The energy spectrum of GCRs can change during Forbush decreases as directly observed (by, e.g., PAMELA; Usoskin et al., 2015) and the changes may depend on the state of the turbulence of the interplanetary magnetic field (Alania and Wawrzynszak, 2012).
- With long-term spacecraft detection of transient structures such as SIRs and CMEs by Wind, ACE, etc., as well as GCRs on the ground by, for example, NMIs or in space by, for example, AMS-02, it is now possible to analyze statistically large samples of Forbush decrease events in relation to interplanetary transients.

- Observations reveal how the compression region ahead of these structures (the sheath), the magnetic structure inside them (the magnetic ejecta/cloud), and also the speed at which these events travel can all play a role in driving Forbush decrease of different intensities (e.g., Badruddin, 2016; Masías-Meza et al., 2016; Janvier et al., 2021). For example, the effect of the shock (or the sheath) is normally reported as a sudden jump downward for the Forbush decrease when crossing the discontinuity, unlike the typical smooth continuous decrease (with varying slopes).
- In general, the effect can be described with use of the TPE approach (e.g., Dumbović et al., 2018; Petukhova et al., 2019; Benella et al., 2020; Vršnak et al., 2022), although different models might use slightly different assumptions and simplifications; for example, the simplified force-field approximation can also be used to describe some Forbush decreases (Usoskin et al., 2015).

4.3. Limitations and open questions

Although it has been well observed for about six solar cycles that the GCR flux can be correlated with various solar and heliospheric parameters, some observations still cannot be fully explained (e.g., Ross and Chaplin, 2019). For instance, it has been found that the GCR intensity lags behind the variation of the sunspot number and this lag time during odd cycles is often longer than that during sequential even cycles. Many early studies explained this time lag as driven by the outward solar wind convection and the inward GCR transport whereby the drift direction of particles reverses during positive and negative solar (heliospheric) magnetic field polarity cycles (Van Allen, 2000; Dorman, 2001; Usoskin et al., 2011; Cliver and Ling, 2001; Thomas et al., 2014). Some others suggest that this lag is primarily due to the late opening of the solar magnetic field with respect to the sunspot number, which already shows an odd–even cyclic pattern (Wang et al., 2022). Besides, the energy dependence of the time lag is also poorly quantified because of the lack of continuous and accurate energy-dependent GCR data. Some recent work suggests a shorter delay for higher-energy GCRs (Shen et al., 2020), an effect that may be attributed to the energy-dependent transport of GCRs in the heliosphere (Moloto and Engelbrecht, 2020). But detailed quantification based on more observations is still needed for a precise physical description of the energy-dependent transport process. Another important index that can be contrasted against different transport model predictions is the radial intensity gradient of GCRs. However, it is rather difficult to quantify because of the rareness of continuous and simultaneous measurements at different heliospheric locations and also the diverse datasets obtained by instruments with different energy responses. Many studies are subject to various uncertainties, and further assessment at different time periods and locations is essential (Roussos et al., 2020).

The limitations regarding GCR transport and modulation modeling are well summarized in reviews by Vainio et al. (2009), Potgieter (2013), and Engelbrecht et al. (2022). For comprehensive modeling, reliable numerical schemes are needed with appropriate LIS as boundary conditions and properly estimated transport parameters. The latter still pose a huge challenge, as the diffusion tensor cannot be directly measured or easily estimated, especially given our limited understanding of the turbulence in the solar wind, which is the main “ingredient” of diffusion (e.g., Zank et al., 1998; Matthaeus and Velli, 2011). Several theories have been developed to describe the diffusion coefficient (e.g., Bieber et al., 1994; Teufel and Schlickeiser, 2003; Qin, 2007; Wiengarten et al., 2016; Zhao et al., 2017; Zhao et al., 2018; Shalchi, 2020). However, because of its complexity, most models still use simpler empirical formulas, e.g., a rigidity-dependent linear or smoothly broken power law for the mean free path, and a simple spatial dependence related to the heliospheric magnetic field distribution. The empirical formulas often have some free parameters and cause large diversities in the underlying process for assessing the solar modulation effect. For instance, in the previously mentioned models, the monthly PAMELA and AMS-02 measurements could be reproduced with different sets of free parameters and LIS. Furthermore, the degeneracy among normalization of the diffusion coefficient, the rigidity index of the diffusion coefficient, and the level of drift effect makes it hard to find the best-fit parameters. The Markov chain Monte Carlo method could be somewhat helpful but does not provide a distinct improvement or clear up the confusion (Song et al., 2021). The monthly flux of protons, antiprotons, electrons, and positrons could improve the clarification on the degeneracy. More effort to compute the transport of turbulence and use of the latest diffusion theory are needed to build a reliable diffusion coefficient, to result in more realistic LIS and to make improvements for studying solar modulation processes (e.g., Zank et al., 2012; Engelbrecht and Burger, 2013; Zank et al., 2017; Zhao et al., 2017; Zhao et al., 2018; Moloto et al., 2018; Oughton and Engelbrecht, 2021; Engelbrecht and Moloto, 2021; Wang et al., 2022; Adhikari et al., 2023; Kleimann et al., 2023).

Moreover, the transport of GCRs in the heliosphere is governed by the properties of the heliosphere, such as the magnetic field structure, the solar wind speed, the HCS structure, and the heliospheric boundary. A realistic description of the dynamic heliospheric environment is essential but poses big challenges, as listed below:

- During the solar minimum, the solar magnetic field can be approximated as a tilted dipole field. But during the solar maximum and the polarity reversal periods, the solar and heliospheric magnetic fields may not follow a regular form but may have chaotic and dynamic structures (e.g., Bindi et al., 2017). Thus, the classic (or mod-

ified) Parker magnetic field structures (Jokipii and Kóta, 1989; Fisk, 1996) are not appropriate to compute the drift velocity.

- The solar wind speed as a main input parameter in the modulation model exhibits a distinctively latitudinal dependence in the solar minimum and is relatively uniform in the solar maximum, but such a pattern is not clear during other solar activity levels (McComas et al., 2002; Zurbuchen, 2007). Most continuous solar wind measurements so far have been constrained at the equatorial plane near 1 AU so could not provide a full view of the solar wind speed. Only the indirect method based on observations via interplanetary scintillations and backscattered Ly α mapping of the interplanetary H can provide the latitudinal variation of the solar wind flow (Bzowski et al., 2003; Sokół et al., 2013).
- The large-scale heliospheric magnetic structure determines the open solar flux, heliospheric magnetic field properties, and HCS structures and tilt angles. However, information on these parameters is highly model dependent (such as based on force-free field extrapolation) and this results in large uncertainties during extreme solar activities (Potgieter, 2013).
- It is generally accepted that the terminal shock and heliosphere structure are significantly asymmetric in terms of a nose-tail direction with a blunt shape (Zank, 1999; Jokipii et al., 2004; Opher et al., 2009; Pogorelov et al., 2009). However, in the solar modulation model, for simplicity, the terminal shock and heliopause are often modeled as a spherical structure.

The further combination of the magnetohydrodynamics simulation and the transport of GCRs may give a more accurate description of the heliosphere condition and will refine solar modulation models (Florinski et al., 2003; Ball et al., 2005; Luo et al., 2013). It is also important to accumulate data on cosmic ray variations at multiple locations in the heliosphere (differing in heliospheric distance and latitude), which will improve our understanding of solar modulation (De Simone et al., 2011; Vos and Potgieter, 2016; Honig et al., 2019; Modzelewska et al., 2019; Knutson et al., 2021; Roussos et al., 2020; Wang et al., 2022).

Regarding the short-term effect caused by corotating interaction regions and ICMEs, there are still many limitations in our current understanding and there is still need to improve our observational and theoretical capabilities in the following aspects.

First, there is a lack of extensive comparison between models and observations taking into account the measured particle energy range. In particular, we have limited opportunities for comparing data obtained at different heliospheric positions, limited by different energy responses of different detectors. For future studies, considering the energy response of the detector will be of great importance and might help to resolve some long-standing issues.

Second, the dual nature of ICME-related Forbush decrease has been known for decades: the existence of so-called two-step Forbush decreases was confirmed by many studies, and it is generally accepted that their two-step nature is related to the substructures (shock, sheath, and magnetic ejecta regions) of ICMEs (for an overview, see, e.g., Cane, 2000). However, not all ICMEs that have both regions will produce observable two-step depressions, which in turn made some authors question their causes (Jordan et al., 2011). Furthermore, it has not been fully resolved whether these two steps are a cumulative effect or separate effects or what determines their relative contribution to the total depression. Richardson and Cane (2011) and more recently Janvier et al. (2021) found that near Earth, on average, both ejecta and sheath effects contribute approximately the same to the total depression. Cane et al. (1994) and later Blanco et al. (2013) found indications that the ejecta effect weakens with time, whereas Freiherr von Forstner et al. (2020) found that the sheath effect becomes more prominent with time. However, the contribution of each substructure in driving a Forbush decrease, to what intensity, and to what effect when combined, still needs to be fully understood. Thus, a conclusive answer on the nature of the two-step Forbush decreases remains elusive.

Besides, our limited ability to compare the Forbush decrease effect as detected by different instruments is the main reason for yet another long-standing issue: what do early/late Forbush decreases look like, i.e. what do different “evolutionary stages” of a Forbush decrease look like? It is suspected that a Forbush decrease should reflect the evolutionary stage of its complementary interplanetary disturbance; however, this is yet to be shown conclusively and can be achieved only through systematic multispacecraft studies.

Finally, with better knowledge and understanding of Forbush decreases and especially their evolutionary stage, which presumably reflects that of their interplanetary cause, Forbush decreases can be used as a means for ICME/SIR analysis in conditions where measurements other than cosmic ray counts are not available. For instance, Lefèvre et al. (2016) and Vernerstrom et al. (2016) used Forbush decreases as an indication of ICMEs in the presatellite era at Earth, Möstl et al. (2015) and Freiherr von Forstner et al. (2018) used Forbush decreases as an indication of ICME arrival at Mars, and Winslow et al. (2018) and Witasse et al. (2017) tracked ICMEs across different locations in the heliosphere using Forbush decreases. With better understanding, Forbush decreases might provide more information on the ICME and SIR properties than simply the arrival time. Moreover, since they can be detected by relatively cheap, small, and simple detectors that can be put aboard practically any spacecraft, Forbush decreases can be easily used for space weather monitoring and diagnostic

purposes, i.e., to probe and track interplanetary transients across the heliosphere.

5. Anomalous cosmic rays

5.1. Introduction

As a result of the solar modulation, the low-energy GCR intensities should decrease with decreasing particle energy. However, the analysis of cosmic ray spectra in the early 1970s revealed an anomalous enhancement at low energies (Garcia-Munoz et al., 1973). This enhanced component is called *anomalous cosmic rays* (ACRs).

Low-energy ACRs are primarily singly ionized, which distinguishes them from SEPs (Section 2) and GCRs (Section 4). However, ACRs with higher charge states are present and become dominant, with total energies above approximately 350 MeV (Klecker et al., 1995; Cummings and Stone, 2007). High-energy ACRs take more time to accelerate, and thus there is more ionization via charge stripping. The abundance of multiply charged elements constrains the acceleration timescale, which must be on the order of 1 year (Mewaldt et al., 1996).

The most abundant ACR elements are H, He, N, O, Ne, and Ar, which have significant neutral abundance in the local interstellar medium. Fisk et al. (1974) first suggested the source of ACRs is pickup ions. Pickup ions originate from the interstellar neutral atoms, which penetrate into the heliosphere and become ionized mainly by solar radiation via photoionization and/or by solar wind ions via charge exchange. Then these particles are picked up by the solar wind magnetic field and are convected into the outer heliosphere. Since the energy of pickup ions is approximately 1 keV per nucleon, they must be accelerated by about four orders of magnitude to become ACRs, for which a very efficient particle acceleration mechanism is needed.

5.2. Recent progress and current understanding

Before the Voyager probes crossed the termination shock (Section 4), it was believed that ACRs are accelerated through a diffusive shock acceleration mechanism at the termination shock (Pesses et al., 1981). But the Voyager probes observed that the intensity of ACR helium did not peak at the shock, suggesting that the acceleration source is elsewhere on the shock or in the heliosheath (Stone et al., 2005; Stone et al., 2008). For particles at energies below approximately 1 MeV, called *termination shock particles* (TSPs), however, the Voyager probes observed a significant flux enhancement at the time of the shock crossing (Decker et al., 2005; Decker et al., 2008). As the Voyager probes moved further into the heliosheath, the intensity of particles with energy above a few megaelectronvolts continued to rise and eventually exhibited an approximate power-law spectrum, while TSPs were observed to be nearly uniform in the heliosheath (Cummings et al., 2008).

McComas and Schwadron (2006) first noted that the blunt-shaped structure of the termination shock has a significant effect on the acceleration of particles and proposed a simple geometric interpretation of the observations of the Voyager probes (see Fig. 13). The intersection points between the field line and the termination shock move along the shock from the nose toward the flanks as the field line is pulled out by the solar wind into the heliosheath. As the intersection points move toward the flanks, pickup ions have longer time to be accelerated and become ACRs (Schwadron et al., 2008). The peak fluxes of ACRs are in the flanks, remote from the Voyager probes, and these particles are transported within the heliosheath. Thus, the Voyager probes observed the peak of ACRs in the heliosheath rather than at the shock nose. Alternatively, TSPs are accelerated over a short time with a power-law distribution and remain near the point of injection. These low-energy particles thus have their peak flux at the nose of termination shock, where the Voyager probes explored.

This blunt-shock concept was confirmed later by numerical computations performed by Kóta and Jokipii (2008) and Schwadron et al. (2008). A 2D hybrid simulation suggested that accelerated TSPs at the termination shock are uniformly distributed along the termination shock, and are likely quite uniform throughout the entire heliosheath (Giacalone et al., 2021). Cummings et al. (2019) analyzed the ACR anisotropies and found that a diffusive streaming of ACRs comes from the flanks of the heliosphere, further supporting the geometric explanation shown in Fig. 13. However, it has also been suggested that the shock interacting with large-scale plasma turbulence may result in a similar effect as the blunt shock if the shock surface becomes rippled and the scale of the ripples is larger than the char-

acteristic scale associated with the particle diffusion (Li and Zank, 2006; Kóta, 2010; Guo et al., 2010). The meandering magnetic field lines caused by the turbulent plasma upstream of the shock could also produce similar effects (Kóta and Jokipii, 2008).

In the heliosphere, ACRs travel in the same plasma as GCRs, and they therefore also experience the solar modulation effect and exhibit the 11-year cycle and the 22-year cycle. Fig. 12 (bottom panel), similarly to Fig. 5 in Fu et al. (2021), shows the time profiles of the ACR and GCR intensity (represented by the neutron count rate averaged over the long-term normalized values from eight different stations) and the HCS tilt angle (shown on an inverted y scale). As suggested by Fu et al. (2021) on the basis of particle data from both NMs and the ACE spacecraft, the ACR evolution is better correlated with the HCS tilt angle, which is a popular proxy for solar activity and is more closely related to the solar modulation than the sunspot number. Meanwhile, the GCR evolution recorded by different NMs may also differ, and this may depend on the cutoff rigidity of the station, as shown in the top panel in Fig. 12. Comparing the two panels in Fig. 12, one may speculate that the GCR count rate from a station with high cutoff rigidity could better match the ACR count rate, especially in the two recent cycles (23 and 24). However, the exact cause of this phenomenon still needs careful investigation.

5.3. Limitations and open questions

We still have many open questions in our current understanding of ACRs, constrained both by limited observations and by lack of theories that can fully explain the observations.

The acceleration mechanism of ACRs is still debated. Fisk and Gloeckler (2009) proposed that ACRs are accelerated through diffusive compression acceleration near the heliopause and subsequently diffuse back into the heliosheath. It was also suggested that magnetic reconnection is a source of ACR acceleration (Lazarian and Opher, 2009; Drake et al., 2010; Zhao et al., 2019). We refer to reviews by Giacalone et al. (2012, 2022) for detailed discussion and open questions on the acceleration mechanism of ACRs.

Concerning the transport process, although both ACR and GCR particles are modulated by the heliospheric magnetic field, the difference in the ACR and GCR variation with the solar cycle is not yet well understood. During the last two solar minimum periods (2008–2009 with $A < 0$ and 2019–2020 with $A > 0$), cosmic ray intensities were much higher than in earlier cycles because of weaker solar modulation (Mewaldt et al., 2010). However, the ACR intensities do not show the same tendency and are comparable to or below their level in previous solar minimum periods as shown in Fig. 12 (also see Fu et al., 2021). This indicates a different modulation mechanism between ACRs and GCRs.

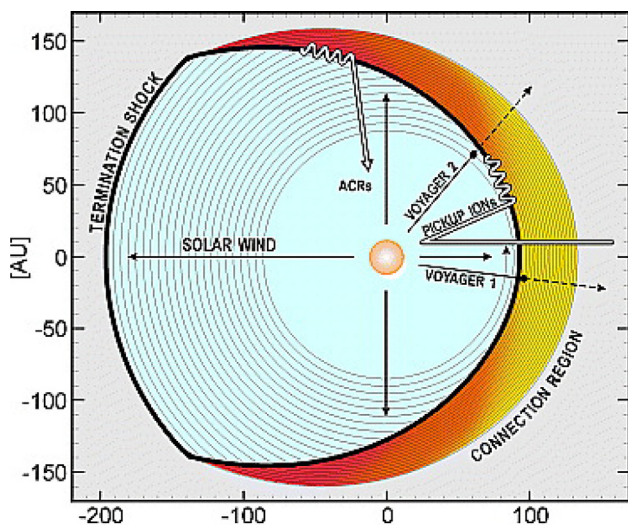


Fig. 13. Blunt-shaped heliosphere termination shock (thick black line), heliospherical magnetic field (gray line), trajectory of pickup ions and ACRs (long arrows), and ecliptic projection of the orbits of the Voyager probes. (From McComas and Schwadron, 2006, reproduced with permission from the American Geophysical Union).

Progress on the cosmic ray LIS and transport in the heliosphere could help us to investigate the origin and transport of ACRs. All the improvements mentioned for GCRs (Section 4) are suitable for application to ACR studies, and vice versa. Some additional effort is needed in the following aspects:

- We should use time-dependent models including the acceleration at the acceleration site and transport in the heliosphere to compute the ACR flux and compare this with observations from different spacecraft at different locations and different times.
- We should use the same set of heliospheric parameters to reproduce the observations for ACR and GCR energy spectra and to infer the unmodulated ACR spectra and transport parameters.
- We should use observations to investigate ACR gradients, which may improve our understanding of the transport processes.

6. Future focuses and recommendations

In previous sections we reviewed the current status of our understanding of energetic particles (SEPs, GCRs, and ACRs) in the heliosphere. We also pointed out our knowledge gaps in observing, modeling, physical understanding of, and forecasting capabilities for the helio-

spheric radiation environment. In this section, we offer suggestions for narrowing these gaps and moving the field forward in the next 5–10 years, as illustrated in Fig. 14.

6.1. Requirements of observations

As a first step, it is most pragmatic to further exploit existing radiation datasets from different regions in the circumterrestrial space and in the heliosphere, e.g., the near geospace (LEO and geosynchronous equatorial orbit satellites), the terrestrial NMIs, the vicinity of other planets (e.g., BepiColombo, MAVEN, TianWen-I, MSL, Juno, etc.), and near-Sun regions (PSP and Solar Orbiter). We stress the following aspects:

- Well-organized community effort is important. For instance, the EU-supported Solar Energetic Particle Analysis Platform for the Inner Heliosphere (SERPENTINE; <https://serpentine-h2020.eu>) project is currently developing various open catalogs of transient phenomena related to SEP events and a series of new data products for the ongoing particle measurements from the Solar Orbiter, PSP, and BepiColombo missions.
- An interdisciplinary effort to combine data of different types (such as space-borne and ground-based, radiation dose and particle flux) should be also encouraged.

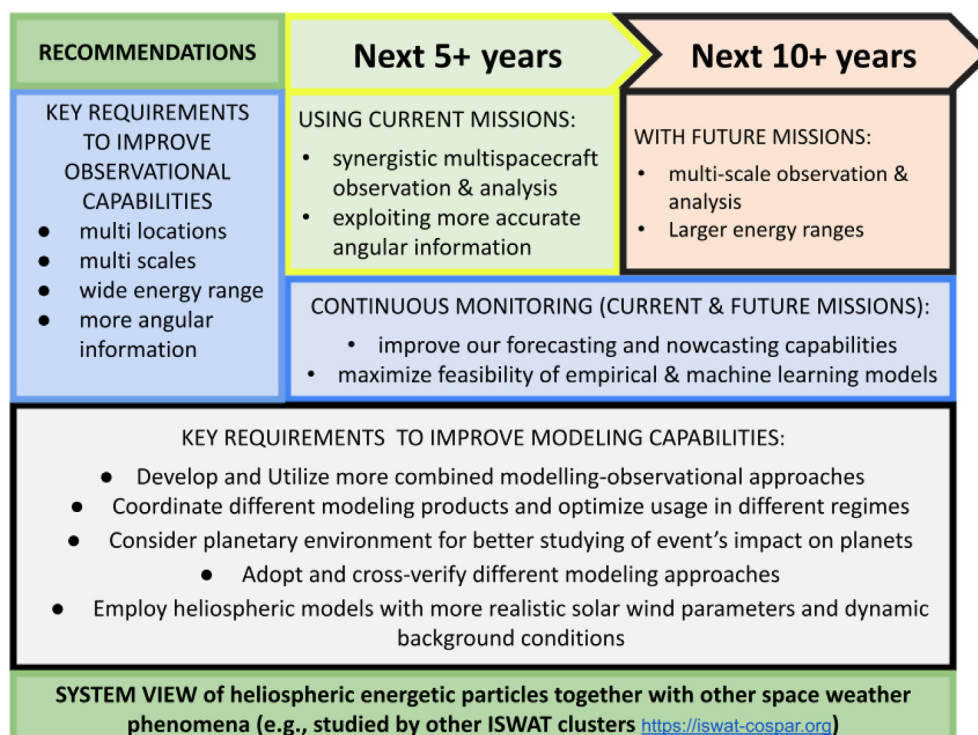


Fig. 14. Recommendation for improving observational and modeling capabilities in the next 5–10 years.

- Adopting a planetary space weather approach based on joint-science investigations for more than one planetary body in the heliosphere could be of significant help for better understanding the radiation environment properties at different locations in the solar system (see, e.g., Plainaki et al., 2020).

Planning for future missions, more observations are still needed in the following aspects.

First, at multiple well-separated locations (in longitude, latitude, and radial distance) we need to maintain or increase the following observations:

- Most multipoint observations of SEP flux so far are based on two or three observers at a solar distance of approximately 1 AU. Recent joint observations retrieved near Earth and at a few other locations with available spacecraft (STEREO-A, Solar Orbiter, PSP, etc.) such as by Kollhoff et al. (2021) make it clear that we still have many questions in interpreting widespread SEP events and that multipoint observations can greatly advance our understanding of the acceleration and transport processes.
- Similarly, multispacecraft observations of ACRs and GCRs over large heliospheric scales for a continuous period are too scarce for us to understand their sources and transport processes or to explain their features, such as the modulation phase lagging behind the sunspot number or the energy-dependent radial gradient. Much of our knowledge of ACR and GCR source populations and transport is based only on theories and transport models as described in Sections 4 and 5.
- Short-term GCR depressions directly depend on the local interplanetary conditions, which are greatly influenced by transients such as SIRs and ICMEs. It is therefore recommended that multispacecraft measurements of both recurrent and nonrecurrent Forbush decreases are used on a regular basis to track and analyze interplanetary transients throughout the heliosphere.

Second, we also need to have more observations at various different scales (both global and local) as explained as below:

- SEP sources span a huge range of spatial scales. For the most energetic events, the maximum acceleration may happen within a few solar radii of the Sun; however, accelerating shocks can extend over more than 180° in heliolongitude and can persist to the outer regions of the heliosphere. Variations of the shock parameters over mesoscales (and how they affect particle acceleration) are nearly completely unknown.
- We also need observations more densely populated at smaller scales so we can understand important dynamics of SEP acceleration (e.g., between L1 and Earth's bow shock and at scales resolving the perpendicular shock front, where acceleration occurs).

- Following the injection/release of SEPs, GCRs, or ACRs from their source regions, the mean free paths of particles can be on the order of 1 AU or much smaller. The details of their transport—in particular, whether it is relatively “scatter-free” or it is dominated by diffusion and/or drifts—should clearly depend on the circumstances, including the background conditions into which the particles propagate. Multipoint measurements of pitch-angle distributions together with contextual information on the local background and the larger-scale settings of the local measurements (e.g., from in situ plasma and field, and solar imaging observations) can lead to improved concepts and models for the global (re) distributions of heliospheric particles from both internal and external sources.

Third, heliospheric particles should be monitored over a larger and continuous energy range (from superthermal to nonthermal and relativistic energies):

- While superthermal particles are considered to play a key role in providing the seed population for SEP acceleration, particles in this energy range (tens of kiloelectronvolts to a few megaelectronvolts) are not routinely measured, and their composition, spectra, and spatial distributions are still poorly understood. There have been a few potentially useful instruments flown (e.g., the Ultra Low Energy Isotope Spectrometer on ACE and SIT on STEREO), but this remains a population where a gap needs to be filled more routinely by including it in heliospheric particle detector suites.
- At energies of tens of megaelectronvolts where SEP proton flux and radiation effects can be significantly enhanced, we are currently largely depending on the EPHIN and ERNE (Energetic and Relativistic Nuclei and Electron experiment) detectors on board SOHO to record the radiation environment near Earth. However, SOHO will soon retire and particle measurement in this critical energy range at Earth's L1 point will be missing if not covered by future missions.
- At energies above hundreds of megaelectronvolts, direct observations are rare and yet they are critical in terms of radiation impacts on aviation, space hardware, and humans in space. Although there are a couple of instruments (AMS-02 and PAMELA) near Earth, the periodic influences of Earth's magnetosphere often prevent their use for onset-time analysis. For higher energies, low-cost ground-based NM measurements have been very useful for deriving particle spectra above the local atmospheric and magnetic cutoff energy (Section 3). However, SEP spectra derived from NMs depend on calculated atmospheric response models, which may carry unknown uncertainties. Moreover, the direct validation of these spectra is often difficult because of the lack of space observations in this high-energy range (at least above approximately 400 MeV, which is the atmospheric cutoff

energy). Future lunar outposts and Earth-orbiting space stations will provide potential platforms for more regular monitoring in this energy range.

- For studying ACRs and GCRs, which can have larger and higher energy ranges than SEPs, the availability of energy-resolved observations is even less. Fluxes integrated over a wide energy range are often used and compared across different instruments. This can be misleading, for example, when one is studying solar modulation of GCRs as a transient disturbance while a solar eruption passes different observers. For existing measurements, it is necessary that the energy responses of different detectors are taken into account, so that the evolutionary effects can be disentangled from the detector response. More energy-resolved measurements in the future (starting at hundreds of megaelectronvolts per nucleon) will better reveal the physics of the high-energy particle transport or modulation process.

Besides, more accurate angular distribution information is important for understanding the source and transport of high-energy particles in space:

- Most SEP observations contain little information on anisotropies, which can provide considerable insight into the physics. For example, counterstreaming SEP fluxes can indicate “reservoirs” produced by local magnetic trapping, while the pitch-angle distribution indicates the role of scattering during transport to the detection site. Modern detection techniques allowing accurate measurements of this property can help better constrain SEP event sources and inform modeling efforts.
- Similarly, suprathermal particle, ACR, and GCR anisotropies contain insights into their sources and transport. For example, newly created heliospheric pickup ions will retain vestiges of their initial ring-beam distribution function before they are scattered by ambient magnetic fluctuations or self-excited waves become unstable to ion cyclotron wave generation. The subsequent acceleration of these pickup ion seed populations toward their becoming ACRs can be diagnosed if the angular distribution is known. In the case of ACRs and GCRs, information about the larger heliosphere shape and state, e.g., over the solar cycle, is contained in the decadal timescale, global directional modulation of these populations. The Interstellar Mapping and Acceleration Probe (IMAP, [McComas et al., 2018](#)) is dedicated to increasing knowledge in these areas, but sustained measurements will hopefully be inspired given the importance/necessity of long-term information.

Finally, for better forecasting the space weather impact of energetic particles in the heliosphere, more observations are undoubtedly needed in the above aspects (more locations, multiple scales, more energy coverage, and angular information) as better understanding of the physics is essential for improving the application capabilities. More-

over, continuous monitoring with real-time data available from multiple locations within the inner heliosphere and at 1 AU would improve SEP forecasting and nowcasting capabilities, including for locations away from Earth, such as at Mars, which are increasingly important for robotic and human space exploration activities. Continuous measurements in regions where radiation information is critical for aviation and satellite operations but not yet sufficient (such as between LEO and geosynchronous orbit) and by a range of space weather monitoring instruments (when feasibility is not an issue) so that we can better nowcast the radiation effects of SEP events (because of their unpredictability) for space industries.

In summary, we still require more observations at more locations (such as at well-separated longitudes, at distances both close to the Sun and beyond 1 AU, and at other latitudes away from the equatorial plane), at both small and global scales, measuring energies extending from superthermal to relativistic energy ranges, and with improved angular resolution and coverage. Since particle detectors generally have the advantage of relatively low mass, low power, and low cost, we recommend carrying one on each of the future interplanetary missions, including Earth-monitoring spacecraft, solar observatories, and even planetary missions if possible. For instance, the BepiColombo mission to explore Mercury carries the Solar Intensity X-ray and Particle Spectrometer (SIXS), which is capable of broadband measurements of X-ray, proton, and electron spectra on its way to Mercury and in orbit ([Huovelin et al., 2020](#)).

6.2. Requirements of modeling efforts

In parallel to the need for improved observations as discussed above, a more aggressive effort is still needed to bring together the modeling efforts and the existing observations with the following emphases:

- Tie to observations at both ends. Observations should be used both as inputs, for constraining model parameters, and finally for testing outputs. This also echoes our previous recommendation that more observations are needed, both from a particle energy and directional distribution perspective and from a spatial sampling perspective.
- Coordinate different modeling products and optimize use in different regimes. Modeling efforts consist of several types that produce different results and have different applications. For example, some empirical SEP models produce a peak flux or event-integrated flux, while others aim to produce a complete event flux versus time profile. Similarly, some provide a single-point observer view of the event, while others provide a heliosphere-wide view. Identifying the particular value (s) and challenges of each of these is important for the purposes of coordinating and prioritizing ongoing and new efforts.

- Consider accurate and timely modeling for magnetospheric shielding of particles. Modeling efforts on how magnetic shielding affects SEP intensity and transport inside Earth's magnetosphere (and in the near-Earth region) are needed to both effectively interpret measurements such as those from the GOES geosynchronous orbit missions and to predict SEP hazards for Earth-orbiting space stations under different geomagnetic activity conditions. The computational tools now exist for making realistic simulations of SEPs in Earth's environment, but it is still difficult to put them into practice on a regular basis. In particular, the realistic modeling of this shielding requires realistic modeling of the magnetospheric response to heliospheric transients (see efforts in the ISWAT G1 cluster "Geomagnetic environment"; <https://www.iswat-cospar.org/g1>), which is still being developed and tested for real-time applications. Similarly, we may also need to consider modeling of particles reaching other planets with different magnetospheric conditions, such as Mercury or Mars.
- Modeling of both SEP and GCR/ACR transport should adopt more realistic heliospheric models (see efforts in the ISWAT H1 cluster "Heliospheric magnetic field and solar wind"), where both large-scale solar wind and interplanetary magnetic field and small-scale turbulence should be considered. Current models often rely on various ad hoc and adjustable parameters, whose values cannot be directly verified but are chosen to fit the modeling results with observations. Instead, a modeling-observational approach is needed to constrain the nonobservable parameters such as the diffusion tensor. For GCR/ACR models, it is also important to appropriately constrain the boundary conditions; therefore, it would be prudent to further improve our knowledge of LIS through ongoing and future observations.
- Consider the varying background fluxes affected by interplanetary transients. ICME/SIR-induced Forbush decreases of the background radiation should be incorporated within the SEP/GLE modeling to more accurately describe the temporal evolution of the radiation before, during, and after the SEP events. Forbush decrease modeling can benefit from space-based data in the circumterrestrial environment together with different ground-based NM observations as well as solar wind and interplanetary magnetic field observations.
- Adopt and combine different modeling approaches. Physics-based models, which are very useful for post-event studies, are often computationally expensive, with limited ability to produce a prediction in real time. Forecasting for operations also needs empirical models and machine learning techniques. These models are based on existing data to identify the dependence of SEP properties on other parameters and can give rapid forecasts and are easily incorporated into forecasting and operations. To improve the forecasting capability of such models, very large datasets are needed and will directly

benefit from more observations as discussed earlier; such models should also be studied and tested together with physics-based models.

In summary, it is critical to improve the scientific understanding of SEP events and GCR/ACR transport and use this understanding to develop and improve radiation modeling capabilities to support operations. In particular, [Whitman et al. \(2023\)](#) summarized all SEP models currently developed in the scientific community, including a description of model approach, inputs and outputs, free parameters, and any published validations or comparisons with data. They concluded that "the SEP modeling community has developed a rich and diverse set of SEP models that exhibit a wide array of capabilities but currently have significant limitations, in particular arising from the gaps in real-time observations. If supported with the necessary observations, and with further developments, for example in computational capabilities and the application of artificial intelligence and machine learning, the field is poised for continued growth with a great potential to contribute significantly both to space weather operations and advances in the understanding of the physics of SEP events."

6.3. System view of the problem in synergy with other heliospheric studies

We need a coordinated effort to combine the results of individual space weather efforts in the field of radiation enabling research activities at large. Along this path, much has already been discussed throughout this section, and we provide a brief summary below.

SEPs should be studied as part of a system where the magnetic features on the Sun can evolve to drive solar eruptions such as flares, CMEs, and shocks that may accelerate energetic particles that can escape into interplanetary space while being conditioned by the solar wind during their transport and can also interact with the planetary environment when they arrive at a planetary body (i.e., topics studied by "S: Space weather origins at the Sun," "H: Heliosphere variability," and "G: Coupled geospace system" within the ISWAT framework, <https://iswat-cospar.org>; see also related articles in this special issue).

Similarly, ACRs and GCRs should also be studied as part of a system where the global magnetic field of the heliosphere (from the inner heliosphere to the outer heliosphere and to the heliospheric boundary) is treated in a realistic and dynamic manner whereby the small-scale turbulence in the solar wind is appropriately addressed. Meanwhile, the mesoscale solar transient disturbances and short-term variations are considered as modulation factors that may have an accumulative effect on the global transport. Finally, their interaction with the planetary environment and the impact of radiation on long-term interplanetary missions are to be explored by an interdisciplinary approach.

7. Conclusion

Space radiation is a significant concern for the safety of robotic and human exploration both in the near-Earth environment and toward deep space and other planets, such as Mars. Studying energetic particle radiation in the heliosphere is essential for improving space weather forecasting capability and also for better understanding the physics of particle energization and transport processes.

We have reviewed the scientific aspects of the major sources of energetic particle radiation in the heliosphere: SEP, GLE events, GCRs, and ACRs (in Sections 2–5). We have also reviewed the advances in recent decades concerning current scientific understanding and predictive capabilities. We also pointed out our knowledge gaps in observing, modeling, physical understanding of, and forecasting capabilities for the heliospheric radiation environment. Finally, we offered considerations related to the planning of future space observations in Section 6. COSPAR's ISWAT H3 cluster "Radiation environment in heliosphere" (<https://www.iswat-cospar.org/h3>) will continue providing a scientific platform for researchers around the world to work together with the common goal to understand, characterize, and predict the energetic particle radiation in the heliosphere and to mitigate radiation risks associated with aerospace activities, the satellite industry, and human space explorations.

Declaration of Competing Interest

The authors declare that they have no known competing financial interests or personal relationships that could have appeared to influence the work reported in this paper.

Acknowledgments

We thank the four anonymous referees for their time and effort in reviewing this article. We acknowledge the COSPAR ISWAT community and their effort in organizing this special activity, in particular the dedicated endeavor of Masha Kuznetsova and Mario Bisi. J.G. is supported by the National Natural Science Foundation of China (grants 42188101, 42074222, 42130204) and the Strategic Priority Program of the Chinese Academy of Sciences (grant XDB41000000). B.W. was supported in part by a US National Science Foundation EPSCoR RII-Track-1 Cooperative Agreement (OIA-2148653). C.C. is supported by NASA grants NNN06AA01C, 80NSSC18K1446, 80NSSC18K0223, and JHU. APL173063. S.D. acknowledges support from the UK Natural Environment Research Council (grant NE/V002864/1) and the UK Science and Technology Facilities Council (grant ST/V000934/1). M.D. acknowledges support from the Croatian Science Foundation under the project IP-2020-02-9893 (ICOHOSS). L.W. is supported in part by the National Natural Science Foundation of China under contracts 42225404, 42127803, and 42150105. H.M.B. con-

ducted this work while supported by Cooperative Agreement award NA17OAR4320101. The Integrated Solar Energetic Proton Alert/Warning System project transitioning SEP models to real-time operations and the development of the SEP Scoreboard is supported by the Advanced Exploration Systems Division under the Human Exploration and Operations Mission Directorate of NASA and is performed in support of the Human Health and Performance Contract for NASA (NNJ15HK11B). Part of the research described in this article was performed at the Jet Propulsion Laboratory, California Institute of Technology, under a contract with NASA (80NM0018D0004).

References

Adhikari, L., Zank, G.P., Wang, B., Zhao, L., Telloni, D., Pitna, A., Opher, M., Shrestha, B., McComas, D.J., Nykyri, K., 2023. Theory and transport of nearly incompressible magnetohydrodynamic turbulence: high plasma beta regime. *Astrophys. J.* 953, 44–58. <https://doi.org/10.3847/1538-4357/acde57>.

Adriani, O., Barbarino, G., Bazilevskaya, G., Bellotti, R., Boezio, M., Bogomolov, E., Bongi, M., Bonvicini, V., Bottai, S., Bravar, U., et al., 2015. PAMELA's measurements of magnetospheric effects on high-energy solar particles. *Astrophys. J. Lett.* 801, L3. <https://doi.org/10.1088/2041-8205/801/1/L3>.

Aguilar, M., Cavasonza, L.A., Alpat, B., Ambrosi, G., Arruda, L., Attig, N., Aupetit, S., Azzarello, P., Bachlechner, A., Barao, F., et al., 2018. Observation of fine time structures in the cosmic proton and helium fluxes with the Alpha Magnetic Spectrometer on the International Space Station. *Phys. Rev. Lett.* 121, 051101. <https://doi.org/10.1103/PhysRevLett.121.051101>.

Alania, M.V., Wawrzynczak, A., 2012. Energy dependence of the rigidity spectrum of Forbush decrease of galactic cosmic ray intensity. *Adv. Space Res.* 50, 725–730. <https://doi.org/10.1016/j.asr.2011.09.027>.

Alanko-Huotari, K., Usoskin, I., Mursula, K., Kovaltsov, G., 2007. Cyclic variations of the heliospheric tilt angle and cosmic ray modulation. *Adv. Space Res.* 7, 1064–1069. <https://doi.org/10.1016/j.asr.2007.02.007>.

Anastasiadis, A., Lario, D., Papaioannou, A., Kouloumvakos, A., Vourlidas, A., 2019. Solar energetic particles in the inner heliosphere: status and open questions. *Philos. Trans. R. Soc. A Math. Phys. Eng. Sci.* 377, 20180100. <https://doi.org/10.1098/rsta.2018.0100>.

Aran, A., Sanahuja, B., Lario, D., 2006. SOLPENCO: a solar particle engineering code. *Adv. Space Res.* 37, 1240–1246. <https://doi.org/10.1016/j.asr.2005.09.019>.

Arnoldy, R., Kane, S., Winckler, J., 1968. Energetic solar flare X-rays observed by satellite and their correlation with solar radio and energetic particle emission. *Astrophys. J.* 151, 711–736. <https://doi.org/10.1086/149470>.

Aschwanden, M.J., 2012. GeV particle acceleration in solar flares and ground level enhancement (GLE) events. *Space Sci. Rev.* 171, 3–21. <https://doi.org/10.1007/s11214-011-9865-x>.

Aslam, O.P.M., Bisschoff, D., Ngobeni, M.D., Potgieter, M.S., Munini, R., Boezio, M., Mikhailov, V.V., 2021. Time and charge-sign dependence of the heliospheric modulation of cosmic rays. *Astrophys. J.* 909, 215–228. <https://doi.org/10.3847/1538-4357/abdd35>.

Badruruddin, Kumar, A., 2016. Study of the cosmic-ray modulation during the passage of ICMEs and CIRs. *Sol. Phys.* 291, 559–580. doi:10.1007/s11207-015-0843-4.

Bain, H.M., Copeland, K., Onsager, T.G., Steenburgh, R.A., 2023a. NOAA Space Weather Prediction Center radiation advisories for the International Civil Aviation Organization. *Space Weather* 21, e2022SW003346. doi:10.1029/2022SW003346. e2022SW003346 2022SW003346.

Bain, H.M., Mays, M.L., Luhmann, J.G., Li, Y., Jian, L.K., Odstrcil, D., 2016. Shock connectivity in the August 2010 and July 2012 solar energetic particle events inferred from observations and ENLIL modeling. *Astrophys. J.* 825, 1. <https://doi.org/10.3847/0004-637X/825/1/1>.

Bain, H.M., Onsager, T.G., Mertens, C.J., Copeland, K., Benton, E.R., Clem, J., Mangeard, P.S., Green, J.C., Guild, T.B., Tobiska, W.K., Shelton-Mur, K., Zheng, Y., Halford, A.J., Carlson, S., Pulkkinen, A., 2023. Improved space weather observations and modeling for aviation radiation. *Front. Astron. Space Sci.* 10. <https://doi.org/10.3389/fspas.2023.1149014>.

Bain, H.M., Steenburgh, R.A., Onsager, T.G., Stitely, E.M., 2021. A summary of National Oceanic and Atmospheric Administration Space Weather Prediction Center proton event forecast performance and skill. *Space Weather* 19. <https://doi.org/10.1029/2020SW002670>, e2020SW002670.

Balch, C.C., 1999. SEC proton prediction model: verification and analysis. *Radiat. Meas.* 30, 231–250. [https://doi.org/10.1016/S1350-4487\(99\)00052-9](https://doi.org/10.1016/S1350-4487(99)00052-9).

Balch, C.C., 2008. Updated verification of the space weather prediction center's solar energetic particle prediction model. *Space Weather* 6, S01001. <https://doi.org/10.1029/2007SW000337>.

Ball, B., Zhang, M., Rassoul, H., Linde, T., 2005. Galactic cosmic-ray modulation using a solar minimum MHD heliosphere: a stochastic particle approach. *Astrophys. J.* 634, 1116–1125. <https://doi.org/10.1086/496965>.

Belov, A., 2008. Forbush effects and their connection with solar, interplanetary and geomagnetic phenomena. *Proc. Int. Astron. Union* 4, 439–450. <https://doi.org/10.1017/S1743921309029676>.

Belov, A., Eroshenko, E., Mavromichalaki, H., Plainaki, C., Yanke, V., 2005. Solar cosmic rays during the extremely high ground level enhancement on 23 February 1956. *Ann. Geophys.* 23, 2281–2291. <https://doi.org/10.5194/angeo-23-2281-2005>.

Benella, S., Laurenza, M., Vainio, R., Grimani, C., Consolini, G., Hu, Q., Afanasiev, A., 2020. A new method to model magnetic cloud-driven Forbush decreases: the 2016 August 2 event. *Astrophys. J.* 901, 21–30. <https://doi.org/10.3847/1538-4357/abac59>.

Bieber, J.W., Matthaeus, W.H., Smith, C.W., Wanner, W., Kallenrode, M.B., Wibberenz, G., 1994. Proton and electron mean free paths: the Palmer consensus revisited. *Astrophys. J.* 420, 294–306. <https://doi.org/10.1086/173559>.

Bindi, V., Corti, C., Consolandi, C., Hoffman, J., Whitman, K., 2017. Overview of galactic cosmic ray solar modulation in the AMS-02 era. *Adv. Space Res.* 60, 865–878. <https://doi.org/10.1016/j.asr.2017.05.025>.

Bisschoff, D., Potgieter, M.S., Aslam, O.P.M., 2019. New very local interstellar spectra for electrons, positrons, protons, and light cosmic ray nuclei. *Astrophys. J.* 878, 59. <https://doi.org/10.3847/1538-4357/ab1e4a>.

Blanco, J.J., Hidalgo, M.A., Gómez-Herrero, R., Rodríguez-Pacheco, J., Heber, B., Wimmer-Schweingruber, R.F., Martín, C., 2013. Energetic-particle-flux decreases related to magnetic cloud passages as observed by the Helios 1 and 2 spacecraft. *Astron. Astrophys.* 556, A146. <https://doi.org/10.1051/0004-6361/201321739>.

Blasi, P., 2013. The origin of galactic cosmic rays. *Astron. Astrophys. Rev.* 21, 70. <https://doi.org/10.1007/s00159-013-0070-7>.

Bombardieri, D., Duldig, M., Humble, J., Michael, K., 2008. An improved model for relativistic solar proton acceleration applied to the 2005 January 20 and earlier events. *Astrophys. J.* 682, 1315–1327. <https://doi.org/10.1086/589494>.

Bonvicini, V., Barbiellini, G., Boezio, M., Mocchiutti, E., Schiavon, P., Scian, G., Vacchi, A., Zampa, G., Zampa, N., Bergström, D., et al., 2001. The PAMELA experiment in space. *Nucl. Instrum. Methods Phys. Res. Sect. A Accel. Spectrom. Detect. Associated Equip.* 461, 262–268. [https://doi.org/10.1016/S0168-9002\(00\)01221-3](https://doi.org/10.1016/S0168-9002(00)01221-3).

Boschini, M.J., Della Torre, S., Gervasi, M., Grandi, D., Jóhannesson, G., La Vacca, G., Masi, N., Moskalenko, I.V., Pensotti, S., Porter, T.A., Quadrani, L., Rancoita, P.G., Rozza, D., Tacconi, M., 2018. Deciphering the local interstellar spectra of primary cosmic-ray species with HELMOD. *Astrophys. J.* 858, 61–71. <https://doi.org/10.3847/1538-4357/aabc54>.

Boschini, M.J., Della Torre, S., Gervasi, M., Grandi, D., Jóhannesson, G., La Vacca, G., Masi, N., Moskalenko, I.V., Pensotti, S., Porter, T.A., Quadrani, L., Rancoita, P.G., Rozza, D., Tacconi, M., 2020. Inference of the local interstellar spectra of cosmic-ray nuclei Z 28 with the GALPROP-HELMOD framework. *Astrophys. J. Suppl. Ser.* 250, 27–56. <https://doi.org/10.3847/1538-4365/aba901>.

Boschini, M.J., Della Torre, S., Gervasi, M., La Vacca, G., Rancoita, P.G., 2018. Propagation of cosmic rays in heliosphere: the HELMOD model. *Adv. Space Res.* 62, 2859–2879. <https://doi.org/10.1016/j.asr.2017.04.017>.

Bruno, A., Bazilevskaya, G., Boezio, M., Christian, E.R., de Nolfo, G., Martucci, M., Merge, M., Mikhailov, V., Munini, R., Richardson, I., et al., 2018. Solar energetic particle events observed by the PAMELA mission. *Astrophys. J.* 862, 97–113. <https://doi.org/10.3847/1538-4357/aacc26>.

Bruno, A., Christian, E., De Nolfo, G., Richardson, I.G., Ryan, J., 2019. Spectral analysis of the September 2017 solar energetic particle events. *Space Weather* 17, 419–437. <https://doi.org/10.1029/2018SW002085>.

Bzowski, M., Mäkinen, T., Kyrölä, E., Summanen, T., Quémérais, E., 2003. Latitudinal structure and north-south asymmetry of the solar wind from Lyman-alpha remote sensing by SWAN. *Astron. Astrophys.* 408, 1165–1177. <https://doi.org/10.1051/0004-6361:20031022>.

Caballero-Lopez, R.A., Moraal, H., 2004. Limitations of the force field equation to describe cosmic ray modulation. *J. Geophys. Res. Space Phys.* 109, A01101. <https://doi.org/10.1029/2003JA010098>.

Cane, H., Mewaldt, R., Cohen, C., Von Rosenvinge, T., 2006. Role of flares and shocks in determining solar energetic particle abundances. *J. Geophys. Res. Space Phys.* 111, A06S90. <https://doi.org/10.1029/2005JA011071>.

Cane, H., Wibberenz, G., Richardson, I., Von Rosenvinge, T., 1999. Cosmic ray modulation and the solar magnetic field. *Geophys. Res. Lett.* 26, 565–568. <https://doi.org/10.1029/1999GL900032>.

Cane, H.V., 2000. Coronal mass ejections and Forbush decreases. *Space Sci. Rev.* 93, 55–77. <https://doi.org/10.1023/A:1026532125747>.

Cane, H.V., Richardson, I.G., von Rosenvinge, T.T., Wibberenz, G., 1994. Cosmic ray decreases and shock structure: a multispacecraft study. *J. Geophys. Res. Space Phys.* 99, 21429–21442. <https://doi.org/10.1029/94JA01529>.

Cane, H.V., von Rosenvinge, T.T., Cohen, C.M.S., Mewaldt, R.A., 2003. Two components in major solar particle events. *Geophys. Res. Lett.* 30, 8017–8020. <https://doi.org/10.1029/2002GL016580>.

Cholis, I., Hooper, D., Linden, T., 2016. A predictive analytic model for the solar modulation of cosmic rays. *Phys. Rev. D* 93, 043016. <https://doi.org/10.1103/PhysRevD.93.043016>.

Clem, J.M., Dorman, L.I., 2000. Neutron monitor response functions. *Space Sci. Rev.* 93, 335–359. <https://doi.org/10.1023/A:1026508915269>.

Cliver, E., 2016. Flare versus shock acceleration of high-energy protons in solar energetic particle events. *Astrophys. J.* 832, 128–135. <https://doi.org/10.3847/0004-637X/832/2/128>.

Cliver, E., Forrest, D., Cane, H., Reames, D., McGuire, R., Von Rosenvinge, T., Kane, S., MacDowall, R., 1989. Solar flare nuclear gamma-rays and interplanetary proton events. *Astrophys. J.* 343, 953–970. <https://doi.org/10.1086/167765>.

Cliver, E.W., Ling, A.G., 2001. 22 year patterns in the relationship of sunspot number and tilt angle to cosmic-ray intensity. *Astrophys. J. Lett.* 551, L189–L192. <https://doi.org/10.1086/320022>.

Cliver, E.W., Schrijver, C.J., Shibata, K., Usoskin, I.G., 2022. Extreme solar events. *Living Rev. Sol. Phys.* 19, 2. <https://doi.org/10.1007/s41116-022-00033-8>.

Cohen, C., Mewaldt, R., Leske, R., Cummings, A., Stone, E., Wiedenbeck, M., Christian, E., Von Rosenvinge, T., 1999. New observations of heavy-ion-rich solar particle events from ACE. *Geophys. Res. Lett.* 26, 2697–2700. <https://doi.org/10.1029/1999GL900560>.

Cohen, C.M.S., Li, G., Mason, G.M., Shih, A.Y., Wang, L., 2021. Solar energetic particles, in: Raouafi, N.E., Vourlidas, A. (Eds.), *Solar Physics and Solar Wind*, American Geophysical Union, Washington, DC. pp. 133–178. doi:10.1002/9781119815600.ch4.

Copeland, K., Sauer, H.H., Duke, F.E., Friedberg, W., 2008. Cosmic radiation exposure of aircraft occupants on simulated high-latitude flights during solar proton events from 1 January 1986 through 1 January 2008. *Adv. Space Res.* 42, 1008–1029. <https://doi.org/10.1016/j.asr.2008.03.001>.

Corti, C., Bindi, V., Consolandi, C., Whitman, K., 2016. Solar modulation of the local interstellar spectrum with Voyager 1, AMS-02, PAMELA, and BESS. *Astrophys. J.* 829, 8–16. <https://doi.org/10.3847/0004-637X/829/1/8>.

Corti, C., Potgieter, M.S., Bindi, V., Consolandi, C., Light, C., Palermo, M., Popkow, A., 2019. Numerical modeling of galactic cosmic-ray proton and helium observed by AMS-02 during the solar maximum of solar cycle 24. *Astrophys. J.* 871, 253–267. <https://doi.org/10.3847/1538-4357/aafac4>.

Corti, C., Whitman, K., Desai, R., Rankin, J., Strauss, D.T., Nitta, N., Turner, D., Chen, T.Y., 2023. Galactic cosmic rays and solar energetic particles in cis-lunar space: need for contextual energetic particle measurements at Earth and supporting distributed observations. doi:10.48550/arXiv.2209.03635. White paper submitted to Decadal Survey for Solar and Space Physics (Heliophysics) 2024–2033.

Crosby, N., Heynderickx, D., Jiggens, P., Aran, A., Sanahuja, B., Truscott, P., Lei, F., Jacobs, C., Poedts, S., Gabriel, S., et al., 2015. SEPEM: a tool for statistical modeling the solar energetic particle environment. *Space Weather* 13, 406–426. <https://doi.org/10.1002/2013SW001008>.

Cucinotta, F.A., Durante, M., 2006. Cancer risk from exposure to galactic cosmic rays: implications for space exploration by human beings. *Lancet Oncol.* 7, 431–435. [https://doi.org/10.1016/S1470-2045\(06\)70695-7](https://doi.org/10.1016/S1470-2045(06)70695-7).

Cucinotta, F.A., Kim, M.H.Y., Chappell, L.J., Huff, J.L., 2013. How safe is safe enough? Radiation risk for a human mission to Mars. *PLoS One* 8, e74988. <https://doi.org/10.1371/journal.pone.0074988>.

Cucinotta, F.A., To, K., Cacao, E., 2017. Predictions of space radiation fatality risk for exploration missions. *Life Sci. Space Res.* 13, 1–11. <https://doi.org/10.1016/j.lssr.2017.01.005>.

Cummings, A., Stone, E., Heikkila, B.C., Lal, N., Richardson, J., 2019. Voyager 2 observations of the anisotropy of anomalous cosmic rays in the heliosheath, in: 36th International Cosmic Ray Conference (ICRC2019), p. 1071.

Cummings, A.C., Stone, E.C., 2007. Composition of anomalous cosmic rays. *Space Sci. Rev.* 130, 389–399. <https://doi.org/10.1007/s11214-007-9161-y>.

Cummings, A.C., Stone, E.C., Heikkila, B.C., Lal, N., Webber, W.R., Jóhannesson, G., Moskalenko, I.V., Orlando, E., Porter, T.A., 2016. Galactic cosmic rays in the local interstellar medium: Voyager 1 observations and model results. *Astrophys. J.* 831, 18–38. <https://doi.org/10.3847/0004-637X/831/1/18>.

Cummings, A.C., Stone, E.C., McDonald, F.B., Heikkila, B.C., Lal, N., Webber, W.R., 2008. Anomalous cosmic rays in the heliosheath. In: Li, G., Hu, Q., Verkhoglyadova, O., Zank, G.P., Lin, R.P., Luhmann, J. (Eds.), *Particle Acceleration and Transport in the Heliosphere and Beyond: 7th Annual International AstroPhysics Conference*, pp. 343–348. <https://doi.org/10.1063/1.2982469>.

Dachev, T.P., Tomov, B.T., Matviichuk, Y.N., Dimitrov, P.G., Semkova, J.V., Koleva, R.T., Jordanova, M.M., Bankov, N.G., Shurshakov, V. A., Benghin, V.V., 2020. Solar modulation of the GCR flux and dose rate, observed in space between 1991 and 2019. *Life Sci. Space Res.* 26, 114–124. <https://doi.org/10.1016/j.lssr.2020.06.002>.

Dalla, S., Balogh, A., Krucker, S., Posner, A., Müller-Mellin, R., Anglin, J.D., Hofer, M.Y., Marsden, R.G., Sanderson, T.R., Tranquille, C., Heber, B., Zhang, M., McKibben, R.B., 2003. Properties of high heliolatitude solar energetic particle events and constraints on models of acceleration and propagation. *Geophys. Res. Lett.* 30, 8035. <https://doi.org/10.1029/2003GL017139>.

Dalla, S., de Nolfo, G.A., Bruno, A., Giacalone, J., Laitinen, T., Thomas, S., Battarbee, M., Marsh, M.S., 2020. 3D propagation of relativistic solar protons through interplanetary space. *Astron. Astrophys.* 639, A105. <https://doi.org/10.1051/0004-6361/201937338>.

Dalla, S., Marsh, M.S., Kelly, J., Laitinen, T., 2013. Solar energetic particle drifts in the Parker spiral. *J. Geophys. Res. Space Phys.* 118, 5979–5985. <https://doi.org/10.1002/jgra.50589>.

De Simone, N., Di Felice, V., Gieseler, J., Boezio, M., Casolino, M., Picozza, P., Heber, B. PAMELA Collaboration, 2011. Latitudinal and radial gradients of galactic cosmic ray protons in the inner heliosphere - PAMELA and Ulysses observations. *Astrophys. Space Sci. Trans.* 7, 425–434. <https://doi.org/10.5194/astra-7-425-2011>.

Decker, R.B., Krimigis, S.M., Roelof, E.C., Hill, M.E., Armstrong, T.P., Gloeckler, G., Hamilton, D.C., Lanzerotti, L.J., 2005. Voyager 1 in the foreshock, termination shock, and heliosheath. *Science* 309, 2020–2024. <https://doi.org/10.1126/science.1117569>.

Decker, R.B., Krimigis, S.M., Roelof, E.C., Hill, M.E., Armstrong, T.P., Gloeckler, G., Hamilton, D.C., Lanzerotti, L.J., 2008. Mediation of the solar wind termination shock by non-thermal ions. *Nature* 454, 67–70. <https://doi.org/10.1038/nature07030>.

Desai, M., Giacalone, J., 2016. Large gradual solar energetic particle events. *Living Rev. Sol. Phys.* 13, 3. <https://doi.org/10.1007/s41116-016-0002-5>.

Di Felice, V., Munini, R., Vos, E.E., Potgieter, M.S., 2017. New evidence for charge-sign-dependent modulation during the solar minimum of 2006 to 2009. *Astrophys. J.* 834, 89–97. <https://doi.org/10.3847/1538-4357/834/1/89>.

Dierckxens, M., Tziotziou, K., Dalla, S., Patsou, I., Marsh, M.S., Crosby, N.B., Malandraki, O., Tsiroupolou, G., 2015. Relationship between solar energetic particles and properties of flares and CMEs: statistical analysis of solar cycle 23 events. *Sol. Phys.* 290, 841–874. <https://doi.org/10.1007/s11207-014-0641-4>.

Dobyns, M., Harikumaran, J., Guo, J., Wheeler, P., Galea, M., Buticchi, G., 2024. Cosmic radiation reliability analysis for aircraft power electronics. *IEEE Trans. Transp. Electrif.* 10, 344–352. <https://doi.org/10.1109/TTE.2023.3278319>.

Dobyns, M., Shprits, Y., Drozdov, A., Hoffman, J., Li, J., 2021. Beating 1 Sievert: optimal radiation shielding of astronauts on a mission to mars. *Space Weather* 19. <https://doi.org/10.1029/2021SW002749>.

Domingo, V., Fleck, B., Poland, A., 1995. SOHO: the solar and heliospheric observatory. *Space Sci. Rev.* 72, 81–84. <https://doi.org/10.1007/BF00768758>.

Dorman, L.I., 2001. Cosmic ray long-term variation: even-odd cycle effect, role of drifts, and the onset of cycle 23. *Adv. Space Res.* 27, 601–606. [https://doi.org/10.1016/S0273-1177\(01\)00088-6](https://doi.org/10.1016/S0273-1177(01)00088-6).

Drake, J.F., Opher, M., Swisdak, M., Chamoun, J.N., 2010. A magnetic reconnection mechanism for the generation of anomalous cosmic rays. *Astrophys. J.* 709, 963–974. <https://doi.org/10.1088/0004-637X/709/2/963>.

Dresing, N., Gómez-Herrero, R., Heber, B., Klassen, A., Malandraki, O., Dröge, W., Kartavykh, Y., 2014. Statistical survey of widely spread out solar electron events observed with STEREO and ACE with special attention to anisotropies. *Astron. Astrophys.* 567, A27. <https://doi.org/10.1051/0004-6361/201423789>.

Dumbović, M., Heber, B., Vršnak, B., Temmer, M., Kirin, A., 2018. An analytical diffusion-expansion model for Forbush decreases caused by flux ropes. *Astrophys. J.* 860, 71–82. <https://doi.org/10.3847/1538-4357/aac2de>.

Dumbović, M., Vršnak, B., Guo, J., Heber, B., Dissauer, K., Carcaboso, F., Temmer, M., Veronig, A., Podladchikova, T., Möstl, C., Amerstorfer, T., Kirin, A., 2020. Evolution of coronal mass ejections and the corresponding Forbush decreases: modeling vs. multi-spacecraft observations. *Sol. Phys.* 295, 104. <https://doi.org/10.1007/s11207-020-01671-7>.

Dumbović, M., Vršnak, B., Temmer, M., Heber, B., Kühl, P., 2022. Generic profile of a long-lived corotating interaction region and

associated recurrent Forbush decrease. *Astron. Astrophys.* 658, A187. <https://doi.org/10.1051/0004-6361/202140861>.

Ellison, D.C., Ramaty, R., 1985. Shock acceleration of electrons and ions in solar flares. *Astrophys. J.* 298, 400–408. <https://doi.org/10.1086/163623>.

Engelbrecht, N.E., Burger, R.A., 2013. An ab initio model for cosmic-ray modulation. *Astrophys. J.* 772, 46–57. <https://doi.org/10.1088/0004-637X/772/1/46>.

Engelbrecht, N.E., Effenberger, F., Florinski, V., Potgieter, M.S., Ruffolo, D., Chhiber, R., Usmanov, A.V., Rankin, J.S., Els, P.L., 2022. Theory of cosmic ray transport in the heliosphere. *Space Sci. Rev.* 218, 33. <https://doi.org/10.1007/s11214-022-00896-1>.

Engelbrecht, N.E., Moloto, K.D., 2021. An ab initio approach to antiproton modulation in the inner heliosphere. *Astrophys. J.* 908, 167–177. <https://doi.org/10.3847/1538-4357/abd3a5>.

Fiandrini, E., Tomassetti, N., Bertucci, B., Donnini, F., Graziani, M., Khiali, B., Reina Conde, A., 2021. Numerical modeling of cosmic rays in the heliosphere: analysis of proton data from AMS-02 and PAMELA. *Phys. Rev. D* 104, 023012. <https://doi.org/10.1103/PhysRevD.104.023012>.

Fisk, L.A., 1996. Motion of the footpoints of heliospheric magnetic field lines at the Sun: implications for recurrent energetic particle events at high heliographic latitudes. *J. Geophys. Res. Space Phys.* 101, 15547–15554. <https://doi.org/10.1029/96JA01005>.

Fisk, L.A., Gloeckler, G., 2009. The acceleration of anomalous cosmic rays by stochastic acceleration in the heliosheath. *Adv. Space Res.* 43, 1471–1478. <https://doi.org/10.1016/j.asr.2009.02.010>.

Fisk, L.A., Kozlovsky, B., Ramaty, R., 1974. An interpretation of the observed oxygen and nitrogen enhancements in low-energy cosmic rays. *Astrophys. J. Lett.* 190, L35–L37. <https://doi.org/10.1086/181498>.

Florinski, V., Zank, G.P., Pogorelov, N.V., 2003. Galactic cosmic ray transport in the global heliosphere. *J. Geophys. Res. Space Phys.* 108, 1228. <https://doi.org/10.1029/2002JA009695>.

Forbush, S.E., 1937. On the effects in cosmic-ray intensity observed during the recent magnetic storm. *Phys. Rev.* 51, 1108–1109. <https://doi.org/10.1103/PhysRev.51.1108.3>.

Forbush, S.E., 1946. Three unusual cosmic-ray increases possibly due to charged particles from the Sun. *Phys. Rev.* 70, 771–772. <https://doi.org/10.1103/PhysRev.70.771>.

Forbush, S.E., 1954. World-wide cosmic ray variations, 1937–1952. *J. Geophys. Res.* 59, 525–542. <https://doi.org/10.1029/JZ059i004p00525>.

Forbush, S.E., 1958. Cosmic-ray intensity variations during two solar cycles. *J. Geophys. Res.* 63, 651–669. <https://doi.org/10.1029/JZ063i004p00651>.

Freiherr von Forstner, J.L., Guo, J., Wimmer-Schweingruber, R.F., Hassler, D.M., Temmer, M., Dumbović, M., Jian, L.K., Appel, J.K., Čalogović, J., Ehresmann, B., Heber, B., Lohf, H., Posner, A., Steigies, C.T., Vršnak, B., Zeitlin, C.J., 2018. Using Forbush decreases to ferive the transit time of ICMEs propagating from 1 AU to Mars. *J. Geophys. Res. Space Phys.* 123, 39–56. <https://doi.org/10.1002/2017JA024700>.

Fox, N.J., Velli, M.C., Bale, S.D., Decker, R., Driesman, A., Howard, R.A., Kasper, J.C., Kinnison, J., Kusterer, M., Lario, D., Lockwood, M.K., McComas, D.J., Raouafi, N.E., Szabo, A., 2016. The Solar Probe Plus mission: humanity's first visit to our star. *Space Sci. Rev.* 204, 7–48. <https://doi.org/10.1007/s11214-015-0211-6>.

Freiherr von Forstner, J.L., Guo, J., Wimmer-Schweingruber, R.F., Dumbović, M., Janvier, M., Démoulin, P., Veronig, A., Temmer, M., Papaioannou, A., Dasso, S., Hassler, D.M., Zeitlin, C.J., 2020. Comparing the properties of ICME-induced Forbush decreases at Earth and Mars. *J. Geophys. Res. Space Phys.* 125, e27662. <https://doi.org/10.1029/2019JA027662>.

Fu, S., Ding, Z., Zhang, Y., Zhang, X., Li, C., Li, G., Tang, S., Zhang, H., Xu, Y., Wang, Y., et al., 2022. First report of a solar energetic particle event observed by China's Tianwen-1 mission in transit to Mars. *Astrophys. J. Lett.* 934, L15. <https://doi.org/10.3847/2041-8213/ac80f5>.

Fu, S., Zhao, L., Zhang, X., Luo, P., Li, Y., 2021. Comparison of anomalous and galactic cosmic-ray oxygen at 1 au during 1997–2020. *Astrophys. J. Lett.* 920, L12. <https://doi.org/10.3847/2041-8213/ac29b9>.

Garcia-Munoz, M., Mason, G.M., Simpson, J.A., 1973. A new test for solar modulation theory: the 1972 May-July low-energy galactic cosmic-ray proton and helium spectra. *Astrophys. J.* 182, L81. <https://doi.org/10.1086/181224>.

Giacalone, J., Drake, J.F., Jokipii, J.R., 2012. The acceleration mechanism of anomalous cosmic rays. *Space Sci. Rev.* 173, 283–307. <https://doi.org/10.1007/s11214-012-9915-z>.

Giacalone, J., Fahr, H., Fichtner, H., Florinski, V., Heber, B., Hill, M.E., Kóta, J., Leske, R.A., Potgieter, M.S., Rankin, J.S., 2022. Anomalous cosmic rays and heliospheric energetic particles. *Space Sci. Rev.* 218, 22. <https://doi.org/10.1007/s11214-022-00890-7>.

Giacalone, J., Nakano, M., Zank, G.P., Kóta, J., Opher, M., Richardson, J.D., 2021. Hybrid simulations of interstellar pickup protons accelerated at the solar-wind termination shock at multiple locations. *Astrophys. J.* 911, 27–34. <https://doi.org/10.3847/1538-4357/abe93a>.

Gieseler, J., Heber, B., Herbst, K., 2017. An empirical modification of the force field approach to describe the modulation of galactic cosmic rays close to Earth in a broad range of rigidities. *J. Geophys. Res. Space Phys.* 122, 10964–10979. <https://doi.org/10.1002/2017JA024763>.

Gil, A., Kovaltsov, G.A., Mikhailov, V.V., Mishev, A., Poluanov, S., Usoskin, I.G., 2018. An anisotropic cosmic-ray enhancement event on 07-June-2015: a possible origin. *Sol. Phys.* 293, 154. <https://doi.org/10.1007/s11207-018-1375-5>.

Gleeson, L.J., Axford, W.I., 1968. Solar modulation of galactic cosmic rays. *Astrophys. J.* 154, 1011–1026. <https://doi.org/10.1086/149822>.

Gloeckler, G., Fisk, L.A., 2014. A test for whether or not Voyager 1 has crossed the heliopause. *Geophys. Res. Lett.* 41, 5325–5330. <https://doi.org/10.1002/2014GL060781>.

Gómez-Herrero, R., Dresing, N., Klassen, A., Heber, B., Lario, D., Agueda, N., Malandraki, O.E., Blanco, J., Rodríguez-Pacheco, J., Banjac, S., 2015. Circumsolar energetic particle distribution on 2011 November 3. *Astrophys. J.* 799, 55–71. <https://doi.org/10.1088/0004-637X/799/1/55>.

Guo, F., Jokipii, J.R., Kóta, J., 2010. Particle acceleration by collisionless shocks containing large-scale magnetic-field variations. *Astrophys. J.* 725, 128–133. <https://doi.org/10.1088/0004-637X/725/1/128>.

Guo, J., Dumbović, M., Wimmer-Schweingruber, R.F., Temmer, M., Lohf, H., Wang, Y., Veronig, A., Hassler, D.M., Mays, L.M., Zeitlin, C., et al., 2018. Modeling the evolution and propagation of 10 September 2017 CMEs and SEPs arriving at Mars constrained by remote sensing and in situ measurement. *Space Weather* 16, 1156–1169. <https://doi.org/10.1029/2018SW001973>.

Guo, J., Li, X., Zhang, J., Dobynne, M.I., Wang, Y., Xu, Z., Berger, T., Semkova, J., Wimmer-Schweingruber, R.F., Hassler, D.M., et al., 2023. The first ground level enhancement seen on three planetary surfaces: Earth, Moon, and Mars. *Geophys. Res. Lett.* 50. <https://doi.org/10.1029/2023GL103069>, e2023GL103069.

Guo, J., Lillis, R., Wimmer-Schweingruber, R.F., Zeitlin, C., Simonson, P., Rahmati, A., Posner, A., Papaioannou, A., Lundt, N., Lee, C.O., et al., 2018. Measurements of Forbush decreases at Mars: both by MSL on ground and by MAVEN in orbit. *Astron. Astrophys.* 611, A79. <https://doi.org/10.1051/0004-6361/201732087>.

Guo, J., Zeitlin, C., Wimmer-Schweingruber, R.F., Hassler, D.M., Ehresmann, B., Rafkin, S., Freiherr von Forstner, J.L., Khaksarighiri, S., Liu, W., Wang, Y., 2021. Radiation environment for future human exploration on the surface of Mars: the current understanding based on MSL/RAD dose measurements. *Astron. Astrophys. Rev.* 29, 8. <https://doi.org/10.1007/s00159-021-00136-5>.

Hands, A., Lei, F., Davis, C., Clewer, B., Dyer, C., Ryden, K., 2022. A new model for nowcasting the aviation radiation environment with comparisons to in situ measurements during GLEs. *Space Weather* 20, <https://doi.org/10.1029/2022SW003155>, e2022SW003155.

Hassler, D.M., Zeitlin, C., Wimmer-Schweingruber, R.F., Böttcher, S.I., Martin, C., Andrews, J., Böhm, E., Brinza, D., Bullock, M., Burmeister, S., et al., 2012. The Radiation Assessment Detector (RAD) investigation. *Space Sci. Rev.* 170, 503–558. <https://doi.org/10.1007/s11214-012-9913-1>.

Heber, B., Fichtner, H., Scherer, K., 2006. Solar and heliospheric modulation of galactic cosmic rays. *Space Sci. Rev.* 125, 81–93. <https://doi.org/10.1007/s11214-006-9048-3>.

Herbst, K., Muscheler, R., Heber, B., 2017. The new local interstellar spectra and their influence on the production rates of the cosmogenic radionuclides ^{10}Be and ^{14}C . *J. Geophys. Res. Space Phys.* 122, 23–34. <https://doi.org/10.1002/2016JA023207>.

Hess, V.F., Demmelmair, A., 1937. World-wide effect in cosmic ray intensity, as observed during a recent magnetic storm. *Nature* 140, 316–317. <https://doi.org/10.1038/140316a0>.

Honig, T., Witasse, O.G., Evans, H., Nieminen, P., Kuulkers, E., Taylor, M.G.G.T., Heber, B., Guo, J., Sánchez-Cano, B., 2019. Multi-point galactic cosmic ray measurements between 1 and 4.5 AU over a full solar cycle. *Ann. Geophys.* 37, 903–918. <https://doi.org/10.5194/angeo-37-903-2019>.

Huovelin, J., Vainio, R., Kilpua, E., Lehtolainen, A., Korpela, S., Esko, E., Muinonen, K., Bunce, E., Martindale, A., Grande, M., Andersson, H., Nenonen, S., Lehti, J., Schmidt, W., Genzer, M., Viavainen, T., Saari, J., Peltonen, J., Valtonen, E., Talvioja, M., Portin, P., Narendranath, S., Jarvinen, R., Okada, T., Milillo, A., Laurenza, M., Heino, E., Oleynik, P., 2020. Solar intensity X-ray and particle spectrometer SIXS: instrument design and first results. *Space Sci. Rev.* 216, 94. <https://doi.org/10.1007/s11214-020-00717-3>.

Iancu, O.D., Boutros, S.W., Olsen, R.H., Davis, M.J., Stewart, B., Eiwaz, M., Marzulla, T., Belknap, J., Fallgren, C.M., Edmondson, E.F., et al., 2018. Space radiation alters genotype–phenotype correlations in fear learning and memory tests. *Front. Genet.* 9, 404. <https://doi.org/10.3389/fgene.2018.00404>.

Janvier, M., Démoulin, P., Guo, J., Dasso, S., Regnault, F., Topsi-Moutesidou, S., Gutierrez, C., Perri, B., 2021. The two-step Forbush decrease: a tale of two substructures modulating galactic cosmic rays within coronal mass ejections. *Astrophys. J.* 922, 216–230. <https://doi.org/10.3847/1538-4357/ac2b9b>.

Jokipii, J., Kóta, J., 1989. The polar heliospheric magnetic field. *Geophys. Res. Lett.* 16, 1–4. <https://doi.org/10.1029/GL016i001p0001>.

Jokipii, J.R., Giacalone, J., Kóta, J., 2004. Transverse streaming anisotropies of charged particles accelerated at the solar wind termination shock. *Astrophys. J. Lett.* 611, L141–L144. <https://doi.org/10.1086/423993>.

Jordan, A.P., Spence, H.E., Blake, J.B., Shaul, D.N.A., 2011. Revisiting two-step Forbush decreases. *J. Geophys. Res. Space Phys.* 116, A11103. <https://doi.org/10.1029/2011JA016791>.

Kahler, S., 1994. Injection profiles of solar energetic particles as functions of coronal mass ejection heights. *Astrophys. J.* 428, 837–842. <https://doi.org/10.1086/174292>.

Kahler, S.W., Cliver, E.W., Ling, A.G., 2007. Validating the proton prediction system (PPS). *J. Atmos. Sol. Terr. Phys.* 69, 43–49. <https://doi.org/10.1016/j.jastp.2006.06.009>.

Kahler, S.W., White, S.M., Ling, A.G., 2017. Forecasting $E > 50\text{-MeV}$ proton events with the proton prediction system (PPS). *J. Space Weather Space Clim.* 7, A27. <https://doi.org/10.1051/swsc/2017025>.

Kappl, R., 2016. SOLARPROP: charge-sign dependent solar modulation for everyone. *Comput. Phys. Commun.* 207, 386–399. <https://doi.org/10.1016/j.cpc.2016.05.025>.

Kennedy, A.R., 2014. Biological effects of space radiation and development of effective countermeasures. *Life Sci. Space Res.* 1, 10–43. <https://doi.org/10.1016/j.lssr.2014.02.004>.

Kilpua, E., Koskinen, H.E.J., Pulkkinen, T.I., 2017. Coronal mass ejections and their sheath regions in interplanetary space. *Living Rev. Sol. Phys.* 14, 5. <https://doi.org/10.1007/s41116-017-0009-6>.

Klecker, B., McNab, M.C., Blake, J.B., Hamilton, D.C., Hovestadt, D., Kaestle, H.,Looper, M.D., Mason, G.M., Mazur, J.E., Scholer, M., 1995. Charge state of anomalous cosmic-ray nitrogen, oxygen, and neon: SAMPEX observations. *Astrophys. J. Lett.* 442, L69–L72. <https://doi.org/10.1086/187818>.

Kleimann, J., Oughton, S., Fichtner, H., Scherer, K., 2023. A three-dimensional model for the evolution of magnetohydrodynamic turbulence in the outer heliosphere. *Astrophys. J.* 953, 133–148. <https://doi.org/10.3847/1538-4357/acd84e>.

Klein, K.L., Dalla, S., 2017. Acceleration and propagation of solar energetic particles. *Space Sci. Rev.* 212, 1107–1136. <https://doi.org/10.1007/s11214-017-0382-4>.

Klein, K.L., Musset, S., Vilmer, N., Briand, C., Krucker, S., Battaglia, A. F., Dresing, N., Palmroos, C., Gary, D.E., 2022. The relativistic solar particle event on 28 October 2021: evidence of particle acceleration within and escape from the solar corona. *Astron. Astrophys.* 663, A173. <https://doi.org/10.1051/0004-6361/202243903>.

Knutson, E.W., Witasse, O., Sanchez-Cano, B., Lester, M., Wimmer-Schweingruber, R.F., Denis, M., Godfrey, J., Johnstone, A., 2021. Galactic cosmic ray modulation at Mars and beyond measured with EDACs on Mars Express and Rosetta. *Astron. Astrophys.* 650, A165. <https://doi.org/10.1051/0004-6361/202140767>.

Kohl, J.L., Noci, G., Cranmer, S.R., Raymond, J.C., 2006. Ultraviolet spectroscopy of the extended solar corona. *Astron. Astrophys. Rev.* 13, 31–157. <https://doi.org/10.1007/s00159-005-0026-7>.

Koldobskiy, S.A., Kovaltsov, G.A., Usoskin, I.G., 2018. Effective rigidity of a polar neutron monitor for recording ground-level enhancements. *Sol. Phys.* 293, 110. <https://doi.org/10.1007/s11207-018-1326-1>.

Kollhoff, A., Kouloumvakos, A., Lario, D., Dresing, N., Gómez-Herrero, R., Rodríguez-García, L., Malandraki, O.E., Richardson, I.G., Posner, A., Klein, K.L., et al., 2021. The first widespread solar energetic particle event observed by Solar Orbiter on 2020 November 29. *Astron. Astrophys.* 656, A20. <https://doi.org/10.1051/0004-6361/202140937>.

Kóta, J., 2010. Particle acceleration at near-perpendicular shocks: the role of field-line topology. *Astrophys. J.* 723, 393–397. <https://doi.org/10.1088/0004-637X/723/1/393>.

Kóta, J., Jokipii, J.R., 2008. Anomalous cosmic rays in the heliosheath: simulation with a blunt termination shock, in: Li, G., Hu, Q., Verkhoglyadova, O., Zank, G.P., Lin, R.P., Luhmann, J. (Eds.), *Particle Acceleration and Transport in the Heliosphere and Beyond: 7th Annual International AstroPhysics Conference*, pp. 397–403. doi:10.1063/1.2982477.

Kouloumvakos, A., Nindos, A., Valtonen, E., Alissandrakis, C., Malandraki, O., Tsitsipis, P., Kontogeorgos, A., Moussas, X., Hillaris, A., 2015. Properties of solar energetic particle events inferred from their associated radio emission. *Astron. Astrophys.* 580. <https://doi.org/10.1051/0004-6361/201424397>.

Kounine, A., 2012. The Alpha Magnetic Spectrometer on the International Space Station. *Int. J. Mod. Phys. E* 21, 1230005. <https://doi.org/10.1142/S0218301312300056>.

Kress, B.T., Rodriguez, J.V., Onsager, T.G., 2020. Chapter 20 - The GOES-R Space Environment In Situ Suite (SEISS): measurement of energetic particles in geospace, in: Goodman, S.J., Schmit, T.J., Daniels, J., Redmon, R.J. (Eds.), *The GOES-R Series*. Elsevier, pp. 243–250. doi:10.1016/B978-0-12-814327-8.00020-2.

Krimigis, S.M., Decker, R.B., Roelof, E.C., Hill, M.E., Armstrong, T.P., Gloeckler, G., Hamilton, D.C., Lanzerotti, L.J., 2013. Search for the exit: Voyager 1 at heliosphere's border with the galaxy. *Science* 341, 144–147. <https://doi.org/10.1126/science.1235721>.

Krucker, S., Larson, D.E., Lin, R.P., Thompson, B.J., 1999. On the origin of impulsive electron events observed at 1 AU. *Astrophys. J.* 519, 864–875. <https://doi.org/10.1086/307415>.

Kühl, P., Dresing, N., Heber, B., Klassen, A., 2017. Solar energetic particle events with protons above 500 mev between 1995 and 2015 measured with SOHO/EPHIN. *Sol. Phys.* 292, 10. <https://doi.org/10.1007/s11207-016-1033-8>.

Laitinen, T., Huttunen-Heikinmaa, K., Valtonen, E., Dalla, S., 2015. Correcting for interplanetary scattering in velocity dispersion analysis of solar energetic particles. *Astrophys. J.* 806, 114–124. <https://doi.org/10.1088/0004-637X/806/1/114>.

Laitinen, T., Kopp, A., Effenberger, F., Dalla, S., Marsh, M.S., 2016. Solar energetic particle access to distant longitudes through turbulent field-line meandering. *Astron. Astrophys.* 591, A18. <https://doi.org/10.1051/0004-6361/201527801>.

Lario, D., Aran, A., Gómez-Herrero, R., Dresing, N., Heber, B., Ho, G., Decker, R., Roelof, E., 2013. Longitudinal and radial dependence of solar energetic particle peak intensities: STEREO, ACE, SOHO, GOES, and MESSENGER observations. *Astrophys. J.* 767, 41–58. <https://doi.org/10.1088/0004-637X/767/1/41>.

Lario, D., Kallenrode, M.B., Decker, R., Roelof, E., Krimigis, S., Aran, A., Sanahuja, B., 2006. Radial and longitudinal dependence of solar 4–13 MeV and 27–37 MeV proton peak intensities and fluences: Helios and IMP 8 observations. *Astrophys. J.* 653, 1531–1544. <https://doi.org/10.1086/508982>.

Lario, D., Kwon, R.Y., Vourlidas, A., Raouafi, N., Haggerty, D., Ho, G., Anderson, B., Papaioannou, A., Gómez-Herrero, R., Dresing, N., et al., 2016. Longitudinal properties of a widespread solar energetic particle event on 2014 February 25: evolution of the associated CME shock. *Astrophys. J.* 819, 72–94. <https://doi.org/10.3847/0004-637X/819/1/72>.

Lazarian, A., Opher, M., 2009. A model of acceleration of anomalous cosmic rays by reconnection in the heliosheath. *Astrophys. J.* 703, 8–21. <https://doi.org/10.1088/0004-637X/703/1/8>.

Lefèvre, L., Vennerstrøm, S., Dumbović, M., Vršnak, B., Sudar, D., Arlt, R., Clette, F., Crosby, N., 2016. Detailed analysis of solar data related to historical extreme geomagnetic storms: 1868–2010. *Sol. Phys.* 291, 1483–1531. <https://doi.org/10.1007/s11207-016-0892-3>.

Li, G., Lee, M.A., 2015. Scatter-dominated interplanetary transport of solar energetic particles in large gradual events and the formation of double power-law differential fluence spectra of ground-level events during solar cycle 23. *Astrophys. J.* 810, 82–96. <https://doi.org/10.1088/0004-637X/810/1/82>.

Li, G., Zank, G.P., 2006. Particle acceleration at a rippling termination shock, in: Heerikhuisen, J., Florinski, V., Zank, G.P., Pogorelov, N.V. (Eds.), *Physics of the Inner Heliosheath*, pp. 183–189. doi:10.1063/1.2359325.

Lin, R., Anderson, K., Ashford, S., Carlson, C., Curtis, D., Ergun, R., Larson, D., McFadden, J., McCarthy, M., Parks, G., et al., 1995. A three-dimensional plasma and energetic particle investigation for the wind spacecraft. *Space Sci. Rev.* 71, 125–153. <https://doi.org/10.1007/BF00751328>.

Lin, R., Szabo, A., Antiochos, S., Bale, S., Davila, J., et al., 2006. Solar Sentinels: Report of the Science and Technology Definition Team. NASA/TM 2006214137. URL: <https://ntrs.nasa.gov/api/citations/20090024212/downloads/20090024212.pdf>.

Liu, S., Petrosian, V., Mason, G.M., 2006. Stochastic acceleration of ^3He and ^4He in solar flares by parallel-propagating plasma waves: general results. *Astrophys. J.* 636, 462–474. <https://doi.org/10.1086/497883>.

Liu, W., Guo, J., Wang, Y., Slaba, T.C., 2024. A comprehensive comparison of various galactic cosmic-ray models to the state-of-the-art particle and radiation measurements. *Astrophys. J. Suppl. Ser.* 271, 18–47. <https://doi.org/10.3847/1538-4365/ad18ad>.

Luo, X., Zhang, M., Rassoul, H.K., Pogorelov, N.V., Heerikhuisen, J., 2013. Galactic cosmic-ray modulation in a realistic global magnetohydrodynamic heliosphere. *Astrophys. J.* 764, 85–100. <https://doi.org/10.1088/0004-637X/764/1/85>.

Maliniemi, V., Arsenovic, P., Seppälä, A., Nesse Tyssøy, H., 2022. The influence of energetic particle precipitation on Antarctic stratospheric chlorine and ozone over the 20th century. *Atmos. Chem. Phys.* 22, 8137–8149. <https://doi.org/10.5194/acp-22-8137-2022>.

Marsh, M.S., Dalla, S., Kelly, J., Laitinen, T., 2013. Drift-induced perpendicular transport of solar energetic particles. *Astrophys. J.* 774, 4–12. <https://doi.org/10.1088/0004-637X/774/1/4>.

Masías-Meza, J., Dasso, S., Démoulin, P., Rodriguez, L., Janvier, M., 2016. Superposed epoch study of icme sub-structures near Earth and their effects on galactic cosmic rays. *Astron. Astrophys.* 592, A118. <https://doi.org/10.1051/0004-6361/201628571>.

Mason, G., Cohen, C., Cummings, A., Dwyer, J., Gold, R., Krimigis, S., Leske, R., Mazur, J., Mewaldt, R., Möbius, E., et al., 1999. Particle acceleration and sources in the November 1997 solar energetic particle events. *Geophys. Res. Lett.* 26, 141–144. <https://doi.org/10.1029/1998GL900235>.

Mason, G., Li, G., Cohen, C., Desai, M., Haggerty, D., Leske, R., Mewaldt, R., Zank, G., 2012. Interplanetary propagation of solar energetic particle heavy ions observed at 1 AU and the role of energy scaling. *Astrophys. J.* 761, 104–130. <https://doi.org/10.1088/0004-637X/761/2/104>.

Mason, G.M., 2007. ^3He -rich solar energetic particle events. *Space Sci. Rev.* 130, 231–242. <https://doi.org/10.1007/s11214-007-9156-8>.

Mason, G.M., Gloeckler, G., 2012. Power law distributions of suprathermal ions in the quiet solar wind. *Space Sci. Rev.* 172, 241–251. <https://doi.org/10.1007/s11214-010-9741-0>.

Masson, S., Klein, K.L., Bütkofer, R., Flückiger, E., Kurt, V., Yushkov, B., Krucker, S., 2009. Acceleration of relativistic protons during the 20 January 2005 flare and CME. *Sol. Phys.* 257, 305–322. <https://doi.org/10.1007/s11207-009-9377-y>.

Matthaeus, W.H., Velli, M., 2011. Who needs turbulence? A review of turbulence effects in the heliosphere and on the fundamental process of reconnection. *Space Sci. Rev.* 160, 145–168. <https://doi.org/10.1007/s11214-011-9793-9>.

Mavromichalaki, H., Souvatzoglou, G., Sarlanis, C., Mariatos, G., Papaioannou, A., Belov, A., Eroshenko, E., Yanke, V., et al., 2010. Implementation of the ground level enhancement alert software at NMDB database. *New Astron.* 15, 744–748. <https://doi.org/10.1016/j.newast.2010.05.009>.

McComas, D., Alexander, N., Angold, N., Bale, S., Beebe, C., Birdwell, B., Boyle, M., Burgum, J., Burnham, J., Christian, E., et al., 2016. Integrated Science Investigation of the Sun (ISIS): design of the energetic particle investigation. *Space Sci. Rev.* 204, 187–256. <https://doi.org/10.1007/s11214-014-0059-1>.

McComas, D., Christian, E.R., Schwadron, N.A., Fox, N., Westlake, J., Allegrini, F., Baker, D., Biesecker, D., Bzowski, M., Clark, G., et al., 2018. Interstellar Mapping and Acceleration Probe (IMAP): a new NASA mission. *Space Sci. Rev.* 214, 116. <https://doi.org/10.1007/s11214-018-0550-1>.

McComas, D.J., Elliott, H.A., Gosling, J.T., Reisenfeld, D.B., Skoug, R.M., Goldstein, B.E., Neugebauer, M., Balogh, A., 2002. Ulysses' second fast-latitude scan: complexity near solar maximum and the reformation of polar coronal holes. *Geophys. Res. Lett.* 29, 1290. <https://doi.org/10.1029/2001GL014164>.

McComas, D.J., Schwadron, N.A., 2006. An explanation of the Voyager paradox: particle acceleration at a blunt termination shock. *Geophys. Res. Lett.* 33, L04102. <https://doi.org/10.1029/2005GL025437>.

McCracken, K., Shea, M., Smart, D., 2023. A high time-resolution analysis of the ground-level enhancement (GLE) of 23 February 1956 in terms of the CSHKP standard flare model. *Adv. Space Res.* 72, 3414–3427. <https://doi.org/10.1016/j.asr.2023.06.049>.

Meier, M.M., Copeland, K., Klöble, K.E., Matthiä, D., Plettenberg, M.C., Schennett, K., Wirtz, M., Hellweg, C.E., 2020. Radiation in the atmosphere—a hazard to aviation safety? *Atmosphere* 11, 1358. <https://doi.org/10.3390/atmos11121358>.

Mertens, C.J., Slaba, T.C., 2019. Characterization of solar energetic particle radiation dose to astronaut crew on deep-space exploration missions. *Space Weather* 17, 1650–1658. <https://doi.org/10.1029/2019SW002363>.

Mewaldt, R.A., Davis, A.J., Lave, K.A., Leske, R.A., Stone, E.C., Wiedenbeck, M.E., Binns, W.R., Christian, E.R., Cummings, A.C., de Nolfo, G.A., Israel, M.H., Labrador, A.W., von Rosenvinge, T.T., 2010. Record-setting cosmic-ray intensities in 2009 and 2010. *Astrophys. J. Lett.* 723, L1–L6. <https://doi.org/10.1088/2041-8205/723/1/L1>.

Mewaldt, R.A., Selesnick, R.S., Cummings, J.R., Stone, E.C., von Rosenvinge, T.T., 1996. Evidence for multiply charged anomalous cosmic rays. *Astrophys. J.* 466, L43–L46. <https://doi.org/10.1086/310169>.

Milillo, A., Fujimoto, M., Murakami, G., Benkhoff, J., Zender, J., Aizawa, S., Dósa, M., Griton, L., Heyner, D., Ho, G., et al., 2020. Investigating Mercury's environment with the two-spacecraft BepiColombo mission. *Space Sci. Rev.* 216, 1–78. <https://doi.org/10.1007/s11214-020-00712-8>.

Miroshnichenko, L., 2018. Retrospective analysis of GLEs and estimates of radiation risks. *J. Space Weather Space Clim.* 8, A52. <https://doi.org/10.1051/swsc/2018042>.

Miroshnichenko, L., Vashenyuk, E., Pérez-Peraza, J., 2013. Solar cosmic rays: 70 years of ground-based observations. *Geomagn. Aeronomy* 53, 541–560. <https://doi.org/10.1134/S0016793213050125>.

Mishev, A., Usoskin, I., 2016. Analysis of the ground-level enhancements on 14 July 2000 and 13 December 2006 using neutron monitor data. *Sol. Phys.* 291, 1225–1239. <https://doi.org/10.1007/s11207-016-0877-2>.

Mishev, A., Usoskin, I., 2020. Current status and possible extension of the global neutron monitor network. *J. Space Weather Space Clim.* 10, 17. <https://doi.org/10.1051/swsc/2020020>.

Mishev, A., Usoskin, I., Raukunen, O., Paassilta, M., Valtonen, E., Kocharov, L., Vainio, R., 2018. First analysis of ground-level enhancement (GLE) 72 on 10 September 2017: spectral and anisotropy characteristics. *Sol. Phys.* 293, 136. <https://doi.org/10.1007/s11207-018-1354-x>.

Mishev, A.L., Koldobskiy, S.A., Kovaltsov, G.A., Gil, A., Usoskin, I.G., 2020. Updated neutron-monitor yield function: bridging between in situ and ground-based cosmic ray measurements. *J. Geophys. Res. Space Phys.* 125. <https://doi.org/10.1029/2019JA027433>.

Mishev, A.L., Poluianov, S., 2021. About the altitude profile of the atmospheric cut-off of cosmic rays: new revised assessment. *Sol. Phys.* 296. <https://doi.org/10.1007/s11207-021-01875-5>.

Miyake, S., Kataoka, R., Sato, T., 2017. Cosmic ray modulation and radiation dose of aircrews during the solar cycle 24/25. *Space Weather* 15, 589–605. <https://doi.org/10.1002/2016SW001588>.

Modzelewska, R., Iskra, K., Wozniak, W., Siluszyk, M., Alania, M.V., 2019. Features of the galactic cosmic ray anisotropy in solar cycle 24 and solar minima 23/24 and 24/25. *Sol. Phys.* 294, 148. <https://doi.org/10.1007/s11207-019-1540-5>.

Moloto, K., Engelbrecht, N.E., 2020. A fully time-dependent ab initio cosmic-ray modulation model applied to historical cosmic-ray modulation. *Astrophys. J.* 894, 121–132. <https://doi.org/10.3847/1538-4357/ab87a2>.

Moloto, K.D., Engelbrecht, N.E., Burger, R.A., 2018. A simplified ab initio cosmic-ray modulation model with simulated time dependence and predictive capability. *Astrophys. J.* 859, 107–118. <https://doi.org/10.3847/1538-4357/aac174>.

Moraal, H., 2013. Cosmic-ray modulation equations. *Space Sci. Rev.* 176, 299–319. <https://doi.org/10.1007/s11214-011-9819-3>.

Möstl, C., Rollett, T., Frahm, R.A., Liu, Y.D., Long, D.M., Colaninno, R.C., Reiss, M.A., Temmer, M., Farrugia, C.J., Posner, A., Dumbović, M., Janvier, M., Démoulin, P., Boakes, P., Devos, A., Kraaijkamp, E., Mays, M.L., Vršnak, B., 2015. Strong coronal channelling and interplanetary evolution of a solar storm up to Earth and Mars. *Nat. Commun.* 6, 7135. <https://doi.org/10.1038/ncomms8135>.

Müller, D., Cyr, O.S., Zouganelis, I., Gilbert, H.R., Marsden, R., Nieves-Chinchilla, T., Antonucci, E., Auchère, F., Berghmans, D., Horbury, T., et al., 2020. The Solar Orbiter mission. Science overview. *Astron. Astrophys.* 642, A1. <https://doi.org/10.1051/0004-6361/202038467>.

Muraki, Y., Matsubara, Y., Masuda, S., Sakakibara, S., Sako, T., Watanabe, K., Bütkofer, R., Flückiger, E., Chilingarian, A., Hovsepyan, G., et al., 2008. Detection of high-energy solar neutrons and protons by ground level detectors on April 15, 2001. *Astropart. Phys.* 29, 229–242. <https://doi.org/10.1016/j.astropartphys.2007.12.007>.

National Research Council, 2006. Space Radiation Hazards and the Vision for Space Exploration: Report of a Workshop. The National Academies Press, Washington, DC. <https://doi.org/10.17226/11760>.

URL: <https://nap.nationalacademies.org/catalog/11760/space-radiation-hazards-and-the-vision-for-space-exploration-report>.

Ngobeni, M., Aslam, O., Bisschoff, D., Potgieter, M., Ndiiwani, D., Boezio, M., Marcelli, N., Munini, R., Mikhailov, V., Koldobskiy, S., 2020. The 3D numerical modeling of the solar modulation of galactic protons and helium nuclei related to observations by PAMELA between 2006 and 2009. *Astrophys. Space Sci.* 365, 182. <https://doi.org/10.1007/s10509-020-03896-1>.

Núñez, M., 2022. Evaluation of the UMASEP-10 version 2 tool for predicting all >10 MeV SEP events of solar cycles 22, 23 and 24. *Universe* 8, 35. <https://doi.org/10.3390/universe8010035>.

Onsager, T., Grubb, R., Kunches, J., Matheson, L., Speich, D., Zwickl, R. W., Sauer, H., 1996. Operational uses of the GOES energetic particle detectors, in: Washwell, E.R. (Ed.), GOES-8 and Beyond, pp. 281–290. doi:10.1111/12.254075.

Opher, M., Bibi, F.A., Toth, G., Richardson, J.D., Izmodenov, V.V., Gombosi, T.I., 2009. A strong, highly-tilted interstellar magnetic field near the Solar System. *Nature* 462, 1036–1038. <https://doi.org/10.1038/nature08567>.

Oughton, S., Engelbrecht, N.E., 2021. Solar wind turbulence: connections with energetic particles. *New Astron.* 83, 101507. <https://doi.org/10.1016/j.newast.2020.101507>.

Parker, E.N., 1965. The passage of energetic charged particles through interplanetary space. *Planet. Space Sci.* 13, 9–49. [https://doi.org/10.1016/0032-0633\(65\)90131-5](https://doi.org/10.1016/0032-0633(65)90131-5).

Pesses, M.E., Jokipii, J.R., Eichler, D., 1981. Cosmic ray drift, shock wave acceleration, and the anomalous component of cosmic rays. *Astrophys. J.* 246, L85–L88. <https://doi.org/10.1086/183559>.

Petukhova, A.S., Petukhov, I.S., Petukhov, S.I., 2019. Theory of the formation of Forbush decrease in a magnetic cloud: dependence of Forbush decrease characteristics on magnetic cloud parameters. *Astrophys. J.* 880, 17–28. <https://doi.org/10.3847/1538-4357/ab2889>.

Picozza, P., Galper, A.M., Castellini, G., Adriani, O., Altamura, F., Ambriola, M., Barbarino, G.C., Basili, A., Bazilevskaja, G.A., Bencardino, R., Boezio, M., Bogomolov, E.A., Bonechi, L., Bongi, M., Bongiorno, L., Bonvicini, V., Cafagna, F., Campana, D., Carlson, P., Casolino, M., de Marzo, C., de Pascale, M.P., de Rosa, G., Fedele, D., Hofverberg, P., Koldashov, S.V., Krutkov, S.Y., Kvashnin, A.N., Lund, J., Lundquist, J., Maksumov, O., Malvezzi, V., Marcelli, L., Menn, W., Mikhailov, V.V., Minor, M., Misin, S., Mocchiutti, E., Morselli, A., Nikonov, N.N., Orsi, S., Osteria, G., Papini, P., Pearce, M., Ricci, M., Ricciarini, S.B., Runtso, M.F., Russo, S., Simon, M., Sparvoli, R., Spillantini, P., Stozhkov, Y.I., Taddei, E., Vacchi, A., Vannuccini, E., Voronov, S.A., Yurkin, Y.T., Zampa, G., Zampa, N., Zverev, V.G., 2007. PAMELA – a payload for antimatter matter exploration and light-nuclei astrophysics. *Astropart. Phys.* 27, 296–315. <https://doi.org/10.1016/j.astropartphys.2006.12.002>.

Plainaki, C., Antonucci, M., Bemporad, A., Berrilli, F., Bertucci, B., Castronuovo, M., De Michelis, P., Giardino, M., Iuppa, R., Laurenza, M., et al., 2020. Current state and perspectives of space weather science in Italy. *J. Space Weather Space Clim.* 10, 6. <https://doi.org/10.1051/swsc/2020003>.

Plainaki, C., Belov, A., Eroshenko, E., Mavromichalaki, H., Yanke, V., 2007. Modeling ground level enhancements: event of 20 January 2005. *J. Geophys. Res. Space Phys.* 112, A04102. <https://doi.org/10.1029/2006JA011926>.

Plainaki, C., Mavromichalaki, H., Belov, A., Eroshenko, E., Yanke, V., 2009a. Modeling the solar cosmic ray event of 13 December 2006 using ground level neutron monitor data. *Adv. Space Res.* 43, 474–479. <https://doi.org/10.1016/j.asr.2008.07.011>.

Plainaki, C., Mavromichalaki, H., Belov, A., Eroshenko, E., Yanke, V., 2009b. Neutron monitor asymptotic directions of viewing during the event of 13 December 2006. *Adv. Space Res.* 43, 518–522. <https://doi.org/10.1016/j.asr.2008.09.007>.

Plainaki, C., Mavromichalaki, H., Laurenza, M., Gerontidou, M., Kanellakopoulos, A., Storini, M., 2014. The ground-level enhancement of 2012 May 17: derivation of solar proton event properties

through the application of the NMBANGLE PPOLA model. *Astrophys. J.* 785, 160–172. <https://doi.org/10.1088/0004-637X/785/2/160>.

Pogorelov, N.V., Heerikhuisen, J., Zank, G.P., Mitchell, J.J., Cairns, I.H., 2009. Heliospheric asymmetries due to the action of the interstellar magnetic field. *Adv. Space Res.* 44, 1337–1344. <https://doi.org/10.1016/j.asr.2009.07.019>.

Poluianov, S., Usoskin, I., Mishev, A., Shea, M., Smart, D., 2017. GLE and sub-GLE redefinition in the light of high-altitude polar neutron monitors. *Sol. Phys.* 292, 176. <https://doi.org/10.1007/s11207-017-1202-4>.

Posner, A., 2007. Up to 1-hour forecasting of radiation hazards from solar energetic ion events with relativistic electrons. *Space Weather* 5, S05001. <https://doi.org/10.1029/2006SW000268>.

Potgieter, M., 2014. Very local interstellar spectra for galactic electrons, protons and helium. *Braz. J. Phys.* 44, 581–588. <https://doi.org/10.1007/s13538-014-0238-2>.

Potgieter, M.S., 2013. Solar modulation of cosmic rays. *Living Rev. Sol. Phys.* 10, 3. <https://doi.org/10.12942/lrsp-2013-3>.

Potgieter, M.S., 2017. The global modulation of cosmic rays during a quiet heliosphere: a modeling perspective. *Adv. Space Res.* 60, 848–864. <https://doi.org/10.1016/j.asr.2016.09.003>.

Qin, G., 2007. Nonlinear parallel diffusion of charged particles: extension to the nonlinear guiding center theory. *Astrophys. J.* 656, 217–221. <https://doi.org/10.1086/510510>.

Rankin, J.S., Bindi, V., Bykov, A.M., Cummings, A.C., Della Torre, S., Florinski, V., Heber, B., Potgieter, M.S., Stone, E.C., Zhang, M., 2022. Galactic cosmic rays throughout the heliosphere and in the very local interstellar medium. *Space Sci. Rev.* 218, 42. <https://doi.org/10.1007/s11214-022-00912-4>.

Raukunen, O., Paassilta, M., Vainio, R., Rodriguez, J.V., Eronen, T., Crosby, N., Dierckxsens, M., Jiggens, P., Heynderickx, D., Sandberg, I., 2020. Very high energy proton peak flux model. *J. Space Weather Space Clim.* 10, 24. <https://doi.org/10.1051/swsc/2020024>.

Raukunen, O., Vainio, R., Tylka, A.J., Dietrich, W.F., Jiggens, P., Heynderickx, D., Dierckxsens, M., Crosby, N., Ganse, U., Siipola, R., 2018. Two solar proton fluence models based on ground level enhancement observations. *J. Space Weather Space Clim.* 8, A04. <https://doi.org/10.1051/swsc/2017031>.

Reames, D.V., 1999. Particle acceleration at the sun and in the heliosphere. *Space Sci. Rev.* 90, 413–491. <https://doi.org/10.1023/A:1005105831781>.

Reames, D.V., 2013. The two sources of solar energetic particles. *Space Sci. Rev.* 175, 53–92. <https://doi.org/10.1007/s11214-013-9958-9>.

Reames, D.V., 2015. What are the sources of solar energetic particles? Element abundances and source plasma temperatures. *Space Sci. Rev.* 194, 303–327. <https://doi.org/10.1007/s11214-015-0210-7>.

Reeves, G., Cayton, T., Gary, S., Belian, R., 1992. The great solar energetic particle events of 1989 observed from geosynchronous orbit. *J. Geophys. Res. Space Phys.* 97, 6219–6226. <https://doi.org/10.1029/91JA03102>.

Richardson, I., von Rosenvinge, T., Cane, H., Christian, E., Cohen, C., Labrador, A., Leske, R., Mewaldt, R., Wiedenbeck, M., Stone, E., 2014. > 25 mev proton events observed by the high energy telescopes on the STEREO A and B spacecraft and/or at Earth during the first seven years of the STEREO mission. *Sol. Phys.* 289, 3059–3107. https://doi.org/10.1007/978-1-4939-2038-9_27.

Richardson, I.G., 2004. Energetic particles and corotating interaction regions in the solar wind. *Space Sci. Rev.* 111, 267–376. <https://doi.org/10.1023/B:SPAC.0000032689.52830.3e>.

Richardson, I.G., 2018. Solar wind stream interaction regions throughout the heliosphere. *Living Rev. Sol. Phys.* 15, 1. <https://doi.org/10.1007/s41116-017-0011-z>.

Richardson, I.G., Cane, H.V., 2011. Galactic cosmic ray intensity response to interplanetary coronal mass ejections/magnetic clouds in 1995–2009. *Sol. Phys.* 270, 609–627. <https://doi.org/10.1007/s11207-011-9774-x>.

Rodriguez, J.V., Krosschell, J.C., Green, J.C., 2014. Intercalibration of GOES 8–15 solar proton detectors. *Space Weather* 12, 92–109. <https://doi.org/10.1002/2013SW000996>.

Rodríguez-Pacheco, J., Wimmer-Schweingruber, R., Mason, G., Ho, G., Sánchez-Prieto, S., Prieto, M., Martín, C., Seifert, H., Andrews, G., Kulkarni, S., et al., 2020. The energetic particle detector-energetic particle instrument suite for the solar orbiter mission. *Astron. Astrophys.* 642, A7. <https://doi.org/10.1051/0004-6361/201935287>.

Ross, E., Chaplin, W.J., 2019. The behaviour of galactic cosmic-ray intensity during solar activity cycle 24. *Sol. Phys.* 294, 8. <https://doi.org/10.1007/s11207-019-1397-7>.

Rouillard, A.P., Sheeley, N.R., Tylka, A., Vourlidas, A., Ng, C.K., Rakowski, C., Cohen, C.M.S., Mewaldt, R.A., Mason, G.M., Reames, D., Savani, N.P., StCyr, O.C., Szabo, A., 2012. The longitudinal properties of a solar energetic particle event investigated using modern solar imaging. *Astrophys. J.* 752, 44–63. <https://doi.org/10.1088/0004-637x/752/1/44>.

Roussos, E., Dialynas, K., Krupp, N., Kollmann, P., Paraniclas, C., Roelof, E.C., Yuan, C., Mitchell, D.G., Krimigis, S.M., 2020. Long- and short-term variability of galactic cosmic-ray radial intensity gradients between 1 and 9.5 au: observations by cassini, BESS, BESS-polar, PAMELA, and AMS-02. *Astrophys. J.* 904, 165–179. <https://doi.org/10.3847/1538-4357/abc346>.

Sandberg, I., Jiggens, P., Heynderickx, D., Daglis, I., 2014. Cross calibration of NOAA GOES solar proton detectors using corrected NASA IMP-8/GME data. *Geophys. Res. Lett.* 41, 4435–4441. <https://doi.org/10.1002/2014GL060469>.

Sauer, H.H., 1989. SEL monitoring of the Earth's energetic particle radiation environment, in: Rester, A.C., J., Trombka, J.I. (Eds.), *High-Energy Radiation Background in Space*, pp. 216–221. doi:10.1063/1.38171.

Schwadron, N.A., Lee, M.A., McComas, D.J., 2008. Diffusive acceleration at the blunt termination shock. *Astrophys. J.* 675, 1584–1600. <https://doi.org/10.1086/527026>.

Shalchi, A., 2020. Perpendicular transport of energetic particles in magnetic turbulence. *Space Sci. Rev.* 216, 23. <https://doi.org/10.1007/s11214-020-0644-4>.

Shea, M., Smart, D., 1993. History of energetic solar protons for the past three solar cycles including cycle 22 update. Springer. https://doi.org/10.1007/978-1-4615-2916-3_3.

Shen, Z., Qin, G., Zuo, P., Wei, F., Xu, X., 2020. A study of variations of galactic cosmic-ray intensity based on a hybrid data-processing method. *Astrophys. J.* 900, 143–156. <https://doi.org/10.3847/1538-4357/abac60>.

Shen, Z., Yang, H., Zuo, P., Qin, G., Wei, F., Xu, X., Xie, Y., 2021. Solar modulation of galactic cosmic-ray protons based on a modified force-field approach. *Astrophys. J.* 921, 109–115. <https://doi.org/10.3847/1538-4357/ac1fe8>.

Sihver, L., Ploc, O., Puchalska, M., Ambrožová, I., Kubančák, J., Kyselová, D., Shurshakov, V., 2015. Radiation environment at aviation altitudes and in space. *Radiat. Prot. Dosim.* 164, 477–483. <https://doi.org/10.1093/rpd/ncv330>.

Slaba, T.C., Blattnig, S.R., 2014. GCR environmental models I: sensitivity analysis for gcr environments. *Space Weather* 12, 217–224. <https://doi.org/10.1002/2013SW001025>.

Smart, D., Shea, M., 1989. Pps-87: A new event oriented solar proton prediction model. *Adv. Space Res.* 9, 281–284. [https://doi.org/10.1016/0273-1177\(89\)90450-X](https://doi.org/10.1016/0273-1177(89)90450-X).

Smart, D., Shea, M., 1992. Modeling the time-intensity profile of solar flare generated particle fluxes in the inner heliosphere. *Adv. Space Res.* 12, 303–312. [https://doi.org/10.1016/0273-1177\(92\)90120-M](https://doi.org/10.1016/0273-1177(92)90120-M).

Sokół, J.M., Bzowski, M., Tokumaru, M., Fujiki, K., McComas, D.J., 2013. Heliolatitude and time variations of solar wind structure from in situ measurements and interplanetary scintillation observations. *Sol. Phys.* 285, 167–200. <https://doi.org/10.1007/s11207-012-9993-9>.

Song, X., Luo, X., Potgieter, M.S., Liu, X., Geng, Z., 2021. A numerical study of the solar modulation of galactic protons and helium from

2006 to 2017. *Astrophys. J. Suppl. Ser.* 257, 48–60. <https://doi.org/10.3847/1538-4365/ac281c>.

Stassinopoulos, E., Raymond, J.P., 1988. The space radiation environment for electronics. *Proc. IEEE* 76, 1423–1442. <https://doi.org/10.1109/5.90113>.

Stone, E.C., Cummings, A.C., Heikkila, B.C., Lal, N., 2019. Cosmic ray measurements from Voyager 2 as it crossed into interstellar space. *Nat. Astron.* 3, 1013–1018. <https://doi.org/10.1038/s41550-019-0928-3>.

Stone, E.C., Cummings, A.C., McDonald, F.B., Heikkila, B.C., Lal, N., Webber, W.R., 2005. Voyager 1 explores the termination shock region and the heliosheath beyond. *Science* 309, 2017–2020. <https://doi.org/10.1126/science.1117684>.

Stone, E.C., Cummings, A.C., McDonald, F.B., Heikkila, B.C., Lal, N., Webber, W.R., 2008. An asymmetric solar wind termination shock. *Nature* 454, 71–74. <https://doi.org/10.1038/nature07022>.

Stone, E.C., Cummings, A.C., McDonald, F.B., Heikkila, B.C., Lal, N., Webber, W.R., 2013. Voyager 1 observes low-energy galactic cosmic rays in a region depleted of heliospheric ions. *Science* 341, 150–153. <https://doi.org/10.1126/science.1236408>.

Stone, E.C., Frandsen, A., Mewaldt, R., Christian, E., Margolies, D., Ormes, J., Snow, F., 1998. The Advanced Composition Explorer. *Space Sci. Rev.* 86, 1–22. <https://doi.org/10.1023/A:1005082526237>.

Strauss, R., Fichtner, H., 2015. On aspects pertaining to the perpendicular diffusion of solar energetic particles. *Astrophys. J.* 801, 29–37. <https://doi.org/10.1088/0004-637X/801/1/29>.

Strauss, R.D., le Roux, J.A., Engelbrecht, N.E., Ruffolo, D., Dunzlaff, P., 2016. Non-axisymmetric perpendicular diffusion of charged particles and their transport across tangential magnetic discontinuities. *Astrophys. J.* 825, 43–56. <https://doi.org/10.3847/0004-637X/825/1/43>.

Strauss, R.D.T., Effenberger, F., 2017. A hitch-hiker's guide to stochastic differential equations. Solution methods for energetic particle transport in space physics and astrophysics. *Space Sci. Rev.* 212, 151–192. <https://doi.org/10.1007/s11214-017-0351-y>.

Temmer, M., Scolini, C., Richardson, I.G., Heinemann, S.G., Paouris, E., Vourlidas, A., Bisi, M.M., Al-Haddad, N., Amerstorfer, T., et al., 2023. CME propagation through the heliosphere: status and future of observations and model development. *Adv. Space Res.* <https://doi.org/10.1016/j.asr.2023.07.003>, in press.

Teufel, A., Schlickeiser, R., 2003. Analytic calculation of the parallel mean free path of heliospheric cosmic rays. II. Dynamical magnetic slab turbulence and random sweeping slab turbulence with finite wave power at small wavenumbers. *Astron. Astrophys.* 397, 15–25. <https://doi.org/10.1051/0004-6361:20021471>.

Thomas, S.R., Owens, M.J., Lockwood, M., 2014. The 22-year Hale cycle in cosmic ray flux—evidence for direct heliospheric modulation. *Sol. Phys.* 289, 407–421. <https://doi.org/10.1007/s11207-013-0341-5>.

Tomassetti, N., Orcinha, M., Barão, F., Bertucci, B., 2017. Evidence for a time lag in solar modulation of galactic cosmic rays. *Astrophys. J. Lett.* 849, L32–L37. <https://doi.org/10.3847/2041-8213/aa9373>.

Townsend, L.W., Cucinotta, C.F., Wilson, J.W., Shinn, J.L., Badhwar, G., 1994. Solar modulation and nuclear fragmentation effects in galactic cosmic ray transport through shielding. *Adv. Space Res.* 14, 853–861. [https://doi.org/10.1016/0273-1177\(94\)90550-9](https://doi.org/10.1016/0273-1177(94)90550-9).

Tylka, A., Cohen, C., Dietrich, W., Lee, M., MacLennan, C., Mewaldt, R., Ng, C., Reames, D., 2005. Shock geometry, seed populations, and the origin of variable elemental composition at high energies in large gradual solar particle events. *Astrophys. J.* 625, 474–495. <https://doi.org/10.1086/429384>.

Tylka, A.J., Adams, J.H., Boberg, P.R., Brownstein, B., Dietrich, W.F., Flueckiger, E.O., Petersen, E.L., Shea, M.A., Smart, D.F., Smith, E.C., 1997. CREME96: a revision of the cosmic ray effects on microelectronics code. *IEEE Trans. Nucl. Sci.* 44, 2150–2160. <https://doi.org/10.1109/23.659030>.

Usoskin, I., Bazilevskaya, G., Kovaltsov, G., 2011. Solar modulation parameter for cosmic rays since 1936 reconstructed from ground-based neutron monitors and ionization chambers. *J. Geophys. Res. Space Phys.* 116, A02104. <https://doi.org/10.1029/2010JA016105>.

Usoskin, I., Kananen, H., Mursula, K., Tanskanen, P., Kovaltsov, G., 1998. Correlative study of solar activity and cosmic ray intensity. *J. Geophys. Res. Space Phys.* 103, 9567–9574. <https://doi.org/10.1029/97JA03782>.

Usoskin, I., Koldobskiy, S., Kovaltsov, G., Gil, A., Usoskina, I., Willamo, T., Ibragimov, A., 2020. Revised GLE database: fluences of solar energetic particles as measured by the neutron-monitor network since 1956. *Astron. Astrophys.* 640, A17. <https://doi.org/10.1051/0004-6361/202038272>.

Usoskin, I., Kovaltsov, G., Adriani, O., Barbarino, G., Bazilevskaya, G., Bellotti, R., Boezio, M., Bogomolov, E., Bongi, M., Bonvicini, V., et al., 2015. Force-field parameterization of the galactic cosmic ray spectrum: validation for forbush decreases. *Adv. Space Res.* 55, 2940–2945. <https://doi.org/10.1016/j.asr.2015.03.009>.

Usoskin, I.G., 2023. A history of solar activity over millennia. *Living Rev. Sol. Phys.* 20, 2. <https://doi.org/10.1007/s41116-023-00036-z>.

Usoskin, I.G., Gil, A., Kovaltsov, G.A., Mishev, A.L., Mikhailov, V.V., 2017. Heliospheric modulation of cosmic rays during the neutron monitor era: calibration using PAMELA data for 2006–2010. *J. Geophys. Res. Space Phys.* 122, 3875–3887. <https://doi.org/10.1002/2016JA023819>.

Vainio, R., Desorgher, L., Heynderickx, D., Storini, M., Flückiger, E., Horne, R.B., Kovaltsov, G.A., Kudela, K., Laurenza, M., McKenna-Lawlor, S., Rothkaehl, H., Usoskin, I.G., 2009. Dynamics of the Earth's particle radiation environment. *Space Sci. Rev.* 147, 187–231. <https://doi.org/10.1007/s11214-009-9496-7>.

Väistänen, P., Usoskin, I., Mursula, K., 2021. Seven decades of neutron monitors (1951–2019): Overview and evaluation of data sources. *J. Geophys. Res. Space Phys.* 126. <https://doi.org/10.1029/2020JA028941>, e2020JA028941.

Van Allen, J.A., 2000. On the modulation of galactic cosmic ray intensity during solar activity cycles 19, 20, 21, 22 and early 23. *Geophys. Res. Lett.* 27, 2453–2456. <https://doi.org/10.1029/2000GL003792>.

van den Berg, J., Strauss, D.T., Effenberger, F., 2020. A primer on focused solar energetic particle transport. *Space Sci. Rev.* 216, 146. <https://doi.org/10.1007/s11214-020-00771-x>.

Vennerstrom, S., Lefevre, L., Dumbović, M., Crosby, N., Malandraki, O., Patsou, I., Clette, F., Veronig, A., Vršnak, B., Leer, K., Moretto, T., 2016. Extreme geomagnetic storms – 1868–2010. *Sol. Phys.* 291, 1447–1481. <https://doi.org/10.1007/s11207-016-0897-y>.

Vos, E.E., Potgieter, M.S., 2016. Global gradients for cosmic-ray protons in the heliosphere during the solar minimum of cycle 23/24. *Sol. Phys.* 291, 2181–2195. <https://doi.org/10.1007/s11207-016-0945-7>.

Vourlidas, A., 2015. Mission to the Sun-Earth L5 Lagrangian point: an optimal platform for space weather research. *Space Weather* 13, 197–201. <https://doi.org/10.1002/2015SW001173>.

Vršnak, B., Dumbović, M., Heber, B., Kirin, A., 2022. Analytic modeling of recurrent Forbush decreases caused by corotating interaction regions. *Astron. Astrophys.* 658, A186. <https://doi.org/10.1051/0004-6361/202140846>.

Wang, B.B., Bi, X.J., Fang, K., Lin, S.J., Yin, P.F., 2019. Time-dependent solar modulation of cosmic rays from solar minimum to solar maximum. *Phys. Rev. D* 100, 063006. <https://doi.org/10.1103/PhysRevD.100.063006>.

Wang, B.B., Bi, X.J., Fang, K., Lin, S.J., Yin, P.F., 2022. Solar modulation of cosmic proton and helium with AMS-02. *Phys. Rev. D* 106, 063006. <https://doi.org/10.1103/PhysRevD.106.063006>.

Wang, B.B., Zank, G.P., Adhikari, L., Zhao, L.L., 2022. On the conservation of turbulence energy in turbulence transport models. *Astrophys. J.* 928, 176–185. <https://doi.org/10.3847/1538-4357/ac596e>.

Wang, L., Lin, R., Krucker, S., Mason, G.M., 2012. A statistical study of solar electron events over one solar cycle. *Astrophys. J.* 759, 69–80. <https://doi.org/10.1088/0004-637X/759/1/69>.

Wang, L., Yang, L., He, J., Tu, C., Pei, Z., Wimmer-Schweingruber, R.F., Bale, S.D., 2015. Solar wind ~20–200 keV superhalo electrons at quiet times. *Astrophys. J. Lett.* 803, L2. <https://doi.org/10.1088/2041-8205/803/1/L2>.

Wang, Y., Bai, X., Chen, C., Chen, L., Cheng, X., Deng, L., Deng, L., Deng, Y., Feng, L., Gou, T., Guo, J., Guo, Y., Hao, X., He, J., Hou, J., Huang, J., Huang, Z., Ji, H., Jiang, C., Jiang, J., Jin, C., Li, X., Li, Y., Liu, J., Liu, K., Liu, L., Liu, R., Liu, R., Qiu, C., Shen, C., Shen, F., Shen, Y., Shi, X., Su, J., Su, Y., Su, Y., Sun, M., Tan, B., Tian, H., Wang, Y., Xia, L., Xie, J., Xiong, M., Xu, M., Yan, X., Yan, Y., Yang, S., Yang, S., Zhang, S., Zhang, Q., Zhang, Y., Zhao, J., Zhou, G., Zou, H., 2023. Solar ring mission: building a panorama of the Sun and inner-heliosphere. *Adv. Space Res.* 71, 1146–1164. <https://doi.org/10.1016/j.asr.2022.10.045>.

Wang, Y., Guo, J., Li, G., Roussos, E., Zhao, J., 2022. Variation in cosmic-ray intensity lags sunspot number: implications of late opening of solar magnetic field. *Astrophys. J.* 928, 157–168. <https://doi.org/10.3847/1538-4357/ac5896>.

Waterfall, C.O.G., Dalla, S., Laitinen, T., Hutchinson, A., Marsh, M., 2022. Modeling the transport of relativistic solar protons along a heliospheric current sheet during historic GLE events. *Astrophys. J.* 934, 82–97. <https://doi.org/10.3847/1538-4357/ac795d>.

Whitman, K., Egeland, R., Richardson, I.G., Allison, C., Quinn, P., Barzilia, J., Kitiashvili, I., Sadykov, V., Bain, H.M., Dierckxsens, M., et al., 2023. Review of solar energetic particle prediction models. *Adv. Space Res.* 72, 5161–5242. <https://doi.org/10.1016/j.asr.2022.08.006>.

Wibberenz, G., Cane, H., 2006. Multi-spacecraft observations of solar flare particles in the inner heliosphere. *Astrophys. J.* 650, 1199–1207. <https://doi.org/10.1086/506598>.

Wiedenbeck, M.E., Mason, G.M., Cohen, C.M.S., Nitta, N.V., Gómez-Herrero, R., Haggerty, D.K., 2012. Observations of solar energetic particles from ^3He -rich events over a wide range of heliographic longitude. *Astrophys. J.* 762, 54–62. <https://doi.org/10.1088/0004-637x/762/1/54>.

Wiengarten, T., Oughton, S., Engelbrecht, N.E., Fichtner, H., Kleimann, J., Scherer, K., 2016. A generalized two-component model of solar wind turbulence and ab initio diffusion mean-free paths and drift lengthscales of cosmic rays. *Astrophys. J.* 833, 17–33. <https://doi.org/10.3847/0004-637X/833/1/17>.

Wijesen, N., Aran, A., Scolini, C., Lario, D., Afanasiev, A., Vainio, R., Sanahuja, B., Pomoell, J., Poedts, S., 2022. Observation-based modelling of the energetic storm particle event of 14 July 2012. *Astron. Astrophys.* 659, A187. <https://doi.org/10.1051/0004-6361/202142698>.

Wimmer-Schweingruber, R.F., Berger, L., Kollhoff, A., Kühl, P., Heber, B., Yang, L., Heidrich-Meisner, V., Klassen, A., Gomez-Herrero, R., Rodriguez-Pacheco, J., et al., 2023. Unusually long path length for a nearly scatter-free solar particle event observed by Solar Orbiter at 0.43 au. *Astron. Astrophys.* 678, A98. <https://doi.org/10.1051/0004-6361/202346319>.

Wimmer-Schweingruber, R.F., Yu, J., Böttcher, S.I., Zhang, S., Burmeister, S., Lohf, H., Guo, J., Xu, Z., Schuster, B., Seimetz, L., et al., 2020. The Lunar Lander Neutron and Dosimetry (LND) experiment on Chang'E 4. *Space Sci. Rev.* 216, 1–40. <https://doi.org/10.1007/s11214-020-00725-3>.

Winslow, R.M., Schwadron, N.A., Lugaz, N., Guo, J., Joyce, C.J., Jordan, A.P., Wilson, J.K., Spence, H.E., Lawrence, D.J., Wimmer-Schweingruber, R.F., Mays, M.L., 2018. Opening a window on ICME-driven GCR modulation in the inner solar system. *Astrophys. J.* 856, 139–147. <https://doi.org/10.3847/1538-4357/aab098>.

Witasse, O., Sánchez-Cano, B., Mays, M.L., Kajdič, P., Opgenoorth, H., Elliott, H.A., Richardson, I.G., Zouganelis, I., Zender, J., Wimmer-Schweingruber, R.F., Turc, L., Taylor, M.G.G.T., Roussos, E., Rouillard, A., Richter, I., Richardson, J.D., Ramstad, R., Provan, G., Posner, A., Plaut, J.J., Odstrcil, D., Nilsson, H., Niemenen, P., Milan, S.E., Mandt, K., Lohf, H., Lester, M., Lebreton, J.P., Kuulkers, E., Krupp, N., Koenders, C., James, M.K., Intzakara, D., Holmstrom, M., Hassler, D.M., Hall, B.E.S., Guo, J., Goldstein, R., Goetz, C., Glassmeier, K.H., Génot, V., Evans, H., Espley, J., Edberg, N.J.T., Dougherty, M., Cowley, S.W.H., Burch, J., Behar, E., Barabash, S., Andrews, D.J., Altobelli, N., 2017. Interplanetary coronal mass ejection observed at STEREO-A, Mars, comet 67P/Churyumov-Gerasimenko, Saturn, and New Horizons en route to Pluto: comparison of its Forbush decreases at 1.4, 3.1, and 9.9 AU. *J. Geophys. Res. Space Phys.* 122, 7865–7890. <https://doi.org/10.1002/2017JA023884>.

Wozniak, W., Iskra, K., Modzelewska, R., Siluszyk, M., 2023. Analysis of galactic cosmic ray anisotropy during the time period from 1996 to 2020. *Sol. Phys.* 298, 28. <https://doi.org/10.1007/s11207-023-02120-x>.

Xie, H., St. Cyr, O.C., Mäkelä, P., Gopalswamy, N., 2019. Statistical study on multospacecraft widespread solar energetic particle events during solar cycle 24. *J. Geophys. Res. Space Phys.* 124, 6384–6402. doi:10.1029/2019JA026832.

Xu, Z., Guo, J., Wimmer-Schweingruber, R.F., Freiherr von Forstner, J. L., Wang, Y., Dresing, N., Lohf, H., Zhang, S., Heber, B., Yang, M., 2020. First solar energetic particles measured on the lunar far-side. *Astrophys. J. Lett.* 902, L30. <https://doi.org/10.3847/2041-8213/abbccc>.

Zank, G.P., 1999. Interaction of the solar wind with the local interstellar medium: a theoretical perspective. *Space Sci. Rev.* 89, 413–688. <https://doi.org/10.1023/A:1005155601277>.

Zank, G.P., Adhikari, L., Hunana, P., Shiota, D., Bruno, R., Telloni, D., 2017. Theory and transport of nearly incompressible magnetohydrodynamic turbulence. *Astrophys. J.* 835, 147. <https://doi.org/10.3847/1538-4357/835/2/147>.

Zank, G.P., Dosch, A., Hunana, P., Florinski, V., Matthaeus, W.H., Webb, G.M., 2012. The transport of low-frequency turbulence in astrophysical flows. I. Governing equations. *Astrophys. J.* 745, 35–54. <https://doi.org/10.1088/0004-637X/745/1/35>.

Zank, G.P., Matthaeus, W.H., Bieber, J.W., Moraal, H., 1998. The radial and latitudinal dependence of the cosmic ray diffusion tensor in the heliosphere. *J. Geophys. Res. Space Phys.* 103, 2085–2098. <https://doi.org/10.1029/97JA03013>.

Zhao, L.L., Adhikari, L., Zank, G.P., Hu, Q., Feng, X.S., 2017. Cosmic ray diffusion tensor throughout the heliosphere derived from a nearly incompressible magnetohydrodynamic turbulence model. *Astrophys. J.* 849, 88–103. <https://doi.org/10.3847/1538-4357/aa932a>.

Zhao, L.L., Adhikari, L., Zank, G.P., Hu, Q., Feng, X.S., 2018. Influence of the solar cycle on turbulence properties and cosmic-ray diffusion. *Astrophys. J.* 856, 94–109. <https://doi.org/10.3847/1538-4357/aab362>.

Zhao, L.L., Zank, G.P., Hu, Q., Chen, Y., Adhikari, L., leRoux, J.A., Cummings, A., Stone, E., Burlaga, L.F., 2019. ACR proton acceleration associated with reconnection processes beyond the heliospheric termination shock. *Astrophys. J.* 886, 144–154. <https://doi.org/10.3847/1538-4357/ab4db4>.

Zhu, C.R., Yuan, Q., Wei, D.M., 2018. Studies on cosmic-ray nuclei with Voyager, ACE, and AMS-02. I. Local interstellar spectra and solar modulation. *Astrophys. J.* 863, 119–128. <https://doi.org/10.3847/1538-4357/aacf9>.

Zurbuchen, T.H., 2007. A new view of the coupling of the Sun and the heliosphere. *Annu. Rev. Astron. Astrophys.* 45, 297–338. <https://doi.org/10.1146/annurev.astro.45.010807.154030>.